

Aus der Neurologischen Klinik des Universitätsklinikums  
der Heinrich-Heine-Universität

Direktor: Prof. Dr. Hans-Peter Hartung

**Axonal Regeneration  
in Biohybrid Nerve Guidance Channels following  
Implantation into Rat Spinal Cord**

Dissertation

zur Erlangung des Grades eines Doktors der  
Medizin

Der Medizinischen Fakultät der Heinrich-Heine Universität  
Düsseldorf

vorgelegt von

**Caterina Schulte-Eversum**

**2007**

Als Inauguraldissertation gedruckt mit Genehmigung der Medizinischen Fakultät der  
Heinrich-Heine Universität Düsseldorf

gez.: Univ.-Prof. Dr. med. Dr. rer. nat. Bernd Nürnberg

Referent: Prof. Dr. Hans-Werner Müller

Korreferent: Prof. Dr. Guido Reifenberger

„Damit das Mögliche entsteht,  
muß immer wieder das  
Unmögliche versucht werden.“

*Hermann Hesse*

*für meine Großmutter*

# CONTENTS

Abbreviations .....	9
<b>1.0 Introduction .....</b>	<b>12</b>
1.1 History on Nerve Injury .....	12
1.2 Axonal Regeneration in the PNS versus CNS .....	12
1.3 Pathophysiology of Spinal Cord Injury .....	13
1.4 Human Spinal Cord Injury .....	14
1.4.1 Epidemiology .....	14
1.4.2 Classification .....	15
1.5 Therapies of Spinal Cord Injury .....	16
1.5.1 Current Standard Therapies .....	16
1.5.2 Therapies in Clinical Trial .....	17
1.6 Different Approaches in Spinal Cord Injury Research .....	18
1.7 Regeneration Inhibiting Barrier – the Lesion Site .....	20
1.7.1 Fibrous Scar .....	21
1.7.2 Glial Scar .....	22
1.7.3 Anti-Scarring Treatment .....	22
1.8 Entubulation .....	24
1.8.1 History of Entubulation .....	24
1.8.2 Qualities of a Guidance-Channel .....	27
1.9 Schwann Cells .....	28
1.10 Rodent Models in Spinal Cord Injury.....	29
1.11 Aim of this Thesis .....	31

<b>2.0</b>	<b>Material and Methods .....</b>	<b>32</b>
2.1	Cell Culture .....	32
2.1.1	Cell Culture .....	32
2.1.2	Retroviral Overexpression of eGFP <i>in vitro</i> .....	32
2.2	Buffers and Antibodies .....	33
2.2.1	Buffers and Other Solutions .....	33
2.2.2	Antibodies .....	35
2.2.2.1	Primary Antibodies .....	35
2.2.2.2	Secondary Antibodies .....	36
2.2.2.3	Reagents and Tracers .....	36
2.3	Guidance Channels .....	36
2.3.1	Tube Material .....	36
2.3.2	Improvement of the Guidance Channel Filling Procedure .....	37
2.4	Experimental Settings .....	39
2.5	Surgery .....	40
2.5.1	Optimisation of the Surgery .....	40
2.5.2	Protocol of the Optimised Operating Technique .....	41
2.5.3	Post-Operative Care .....	43
2.5.4	Animal Sacrifice .....	43
2.6	Tracing .....	43
2.6.1	Stereotaxic Methods .....	43
2.6.2	Injection of BDA into Layer V of the Somatosensory Cortex .....	44
2.6.3	Anterograde Tracing of the Dorsal Column at Th11 with BDA .....	44
2.7	Tissue Processing .....	45
2.7.1	Paraffin Sections .....	45
2.7.2	Freezing-Microtome Sections .....	46
2.8	Staining Protocols .....	46
2.8.1	Histological Stainings .....	46
2.8.2	Immunohistochemical Stainings .....	48
2.8.2.1	Paraffin Sections .....	48
2.8.2.2	Fluorescent Staining of Freezing-Microtome Sections .....	50
2.9	Analysis and Documentation .....	50

<b>3.0</b>	<b>Results .....</b>	<b>51</b>
3.1	Improvement of the Experimental Setting .....	51
3.1.1	Improvement of the Guidance Channel Filling Procedure .....	51
3.1.2	Optimisation of the Surgery .....	51
3.1.3	Histological Phenomena observed in Nissl-Stainings .....	52
3.1.3.1	Guidance Channel Placement .....	52
3.1.3.2	Guidance Channel Stability .....	53
3.1.3.3	Tissue Bridge .....	54
3.1.3.4	Guidance Channel Wall Presence .....	56
3.1.3.5	Bleeding Sites .....	56
3.1.3.6	Cyst-like Structures .....	57
3.1.3.7	Tearing apart of Tissue .....	59
3.2	Material Properties of the Implant .....	60
3.2.1	Tube Degradation .....	60
3.2.1.1	Quota of Luminal Sections .....	60
3.2.1.2	Tube Deformation .....	61
3.2.1.3	Cellular Infiltration of the Tube Wall .....	61
3.3	Characterisation of the Spinal Cord Lesion .....	63
3.3.1	Lesion Size .....	63
3.3.1.1	Role of Inbleeding on the Lesion Size .....	63
3.3.2	Cellular Reactions after Lesion .....	65
3.3.2.1	Astrogliosis .....	65
3.3.2.2	Inflammation .....	67
3.4	Visualisation, Localisation and Survival of Implanted Schwann Cells .....	68
3.4.1	Visualisation of Implanted Schwann Cells .....	68
3.4.2	eGFP/DAPI Double-Staining .....	69
3.4.3	Survival and Quantity of Implanted Schwann Cells .....	70
3.4.4	Schwann Cell Localisation .....	70
3.5	Cells Invading the Guidance Channel .....	72
3.5.1	Morphologically Schwann Cell-resembling Cells .....	72
3.5.2	Small Round Cells .....	73
3.6	Scar Formation .....	73
3.6.1	The Glial Scar .....	73
3.6.2	The Collagen IV containing Fibrous Scar .....	74
3.6.2.1	Description of the Fibrous Scar in this Injury Model .....	74
3.6.2.2	Effect of Schwann Cells on Scarring .....	76

3.6.2.3	Influence of the Anti-Scarring Treatment .....	76
3.6.2.4	Development of the Scar with Time .....	78
3.6.3	Phenomena observed in Collagen IV-immunopositive Sections .....	79
3.6.3.1	Classification of the Fibrous Scar .....	79
3.6.3.2	Cyst or Ripped Tissue? .....	81
3.6.3.3	Difficulties regarding the Application of Matrigel® .....	82
3.7	Axonal Degeneration and Regrowth .....	83
3.7.1	Axonal Degeneration .....	83
3.7.1.1	Description of Stainings with PAM in different Lesion Models ..	83
3.7.1.2	Axonal Retraction .....	84
3.7.1.3	Role of Inbleeding on Axon Stop .....	86
3.7.2	Axonal Regrowth into the Implant .....	88
3.7.2.1	Growth into Cell-free versus Schwann Cell-filled Tubes .....	88
3.7.2.2	Untreated Animals versus Anti-Scarring Treated Animals .....	91
3.7.2.3	Association of Schwann Cells with Regenerating Fibres .....	93
3.7.2.4	Observations in Immunohistochemical Stainings with PAM .....	94
3.7.3	Traced Fibre Tracts .....	95
3.7.3.1	Fibre Origin .....	95
3.7.3.2	CST Tracing with BDA .....	95
3.7.3.3	Dorsal Column Tracing with BDA .....	97
<b>4.0</b>	<b>Discussion .....</b>	<b>98</b>
4.1	Improvement of the Experimental Setting .....	98
4.1.1	Improvement of the Guidance Channel Filling Procedure .....	98
4.1.2	Optimisation of the Surgery .....	99
4.1.3	Histological Phenomena observed in Nissl-Stainings .....	99
4.2	Material Properties of the Implant .....	102
4.2.1	Material Properties .....	102
4.2.2	Tube Degradation .....	102
4.3	Characterisation of the Spinal Cord Lesion .....	103
4.3.1	Lesion Size .....	103
4.3.2	Cellular Reactions after Lesion .....	104
4.3.2.1	Astrogliosis .....	104
4.3.2.2	Inflammation .....	105
4.4	Visualisation, Localisation and Survival of Implanted Schwann Cells .....	106

4.5	Cells invading the Guidance Channel .....	109
4.6	Scar Formation .....	111
4.6.1	Glial Scar .....	111
4.6.2	The Collagen IV containing Fibrous Scar .....	111
4.7	Axonal Degeneration and Regrowth .....	116
4.7.1	Axonal Degeneration .....	116
4.7.2	Axonal Regrowth .....	117
4.7.3	Traced Fibre Tracts .....	121
<b>5.0</b>	<b>References .....</b>	<b>123</b>
	Danksagung.....	141
	Curriculum vitae.....	142
	Summary and Perspectives.....	143
	Zusammenfassung .....	144



## ABBREVIATIONS

8-Br-cAMP	8-Brome-cyclic Adenoside MonoPhosphate
AB	Antibody
ABC	Avidine-Biotine-Complex
AH	Anterior Horn
ASIA	American Spinal Cord Injury Association
AST	Anti-Scarring Treatment
	tube filled with Matrigel/Schwann Cell mélange plus AST
Avi-Alexa	Avidin-Alexa 488
BBB	Blood-Brain Barrier
BDA	Biotinylated Dextrane-Amine
BDNF	Brain derived Nerve Growth Factor
BM	Basal Membrane
BPY-DCA	2,2`- Bipyridine-5,5`-Dicarboxylic Acid (Iron Chelator)
BWSTT	Body-weight supported Treadmill Training
C3	C. botulinum
Ca <sup>2+</sup>	Calcium
CC	Central Canal
CNS	Central Nervous System
Coll IV	Collagen type IV
CSF	Cerebrospinal Fluid
CSPG	Chondroitinsulphate Proteoglycane
CST	Corticospinal Tract
DAB	Diaminobenzidine
DC	Dorsal Column
DMEM	Dulbecco's Modified Eagle's Medium
DPX	a Xylole-containing mounting fluid
DRG	Dorsal Root Ganglia
ECM	Extracellular Matrix
eGFP	Green Fluorescent Protein
Elvax	Ethylene Vinyle Acetate Copolymer
EtOH	Ethanol
FCS	Fetal Calf Serum
FES	Functional Electrical Stimulation
FF	Free-Floating (staining method)
Fig.	Figure
G	Gauge

G&R	Goat anti Rabbit
GAG	Glycosaminoglycane
GCW	Guidance Channel Wall
GDNF	Glial Cell-Line Derived Neurotrophic Factor
GFAP	Glial Fibrillary Acidic Protein
gt	Goat
H&M	Horse anti Mouse
HCl	Hydrochloric Acid
HE	Hematoxyline-Eosine staining
HEMA	Hydroxyethyl - Methylacrylat
hs	Horse
K <sup>+</sup>	Potassium
MAG	Myelin associated Glycoprotein
ME-008	Guidance Channel material
ME-021	Guidance Channel material
Med	Medium
MetOH	Methanol
MG	Matrigel®
MG/Med	Tube filled with Matrigel/Medium mélange
MG/SC	Tube filled with Matrigel/Schwann Cell mélange
n	Number
Na <sup>+</sup>	Sodium
Na <sub>2</sub> HPO <sub>4</sub>	Di-sodium Hydrogenphosphate Anhydrous
Na <sub>2</sub> HPO <sub>4</sub> x 2 H <sub>2</sub> O	Sodium di-Hydrogenphosphate
NaCl	Sodium Chloride
NaH <sub>2</sub> PO <sub>4</sub> x H <sub>2</sub> O	Sodium di-Hydrogenphosphate Monohydrate
NaOH	Sodium Hydroxide solution
NGF	Nerve Growth Factor
NGF, BDNF, NT-3, GDNF	Trophic Factors
NgR	Nogo Receptor
NTF	Neurotrophic Factor
OEC	Olfactory Ensheathing Cell
OMgp	Oligodendrocyte Myelin Glycoprotein
ORFs	Open Reading Frames
PAM	Pan-axonal Marker
PAN/PVC	Poly(acrylonitrile) poly(vinyl chloride)
PB	Phosphate Buffer
PBS	Phosphate Buffered Saline
PCR	Polymerase Chain Reaction

PEG	Polyethylene glycol
PFA	Paraformaldehyde
PG	Proteoglycane
PGA	Polyglycolic Acid
PGA	Poly ( $\alpha$ -hydroxy) acids
PH	Proly-4-Hydroxylase
PH	Posterior Horn
PHB	Poly- $\beta$ -Hydroxybutane
PKA	Protein Kinase A
PLA	Poly ( $\alpha$ -hydroxy) acids
PLGA	Poly ( $\alpha$ -hydroxy) acids
PLLA	Poly(L-lactic acid)
PN	Peripheral Nerve
PNS	Peripheral Nervous System
rb	Rabbit
ROCK	Rho associated Kinase
ROTI	Roti-Histol (Roth, Germany)
RT	Room Temperature
SC	Schwann Cell
SCI	Spinal Cord Injury
Tab.	Table
TGF $\beta$	Transforming Growth Factor $\beta$
Th	Thoracic Level
TMC-CL	Trimethylene Carbonate-Caprolactone Copolymer
TRIS	Tris(hydroxymethyle)-aminomethane

## 1.0 Introduction

### 1.1 History on Nerve Injury

Tello and colleagues in 1911 first demonstrated the ability of central nervous system (CNS) fibres to regenerate into a peripheral nerve (PN) graft (Tello, 1911). Ramón y Cajal in 1928 noticed the scar formation, always following a spinal cord injury (SCI), postulating a role in axonal regeneration. He implied that the deficit in CNS axonal regeneration was not an inability of the central axons themselves to regrow but that it was due to an environment lacking in nutritive substances and a barrier encountered like the scar forming after SCI (Ramon y Cajal, 1928). In the early eighties, the approach of PN transplantation was rediscovered in spinal cord research. David and Aguayo (David and Aguayo, 1981) showed evidence for long PN bridges circumventing the spinal cord carrying CNS axonal processes for remarkable distances, e.g. from the lower medulla to the thoracic cord. In a follow-up study, Richardson et al. (1984) demonstrated that the distance of injury to the cell body was a crucial determinant of regeneration (Richardson et al., 1984). In all these experiments, no fibres could be observed to leave the graft to re-enter the distal spinal cord. The above mentioned is still valid. In contrast to the PNS with its high restitutive capacity, regeneration in the CNS is deficient.

### 1.2 Axonal Regeneration in the Peripheral and Central Nervous System

Traumatic injuries can lead to axotomy in the peripheral as well as in the central nervous system. There are differences, however, in the body's response to axotomy. *In the PNS*, the distal stump, the part separated from the cell body, undergoes complete Wallerian Degeneration (for a better understanding of the underlying mechanisms and the exact local reaction see (Stoll and Muller, 1999;Stoll et al., 2002;2001a). A high number of rapidly invading macrophages clear up the cell and myelin debris to facilitate regeneration by providing a suitable environment. The macrophages not only secrete proteases but also a number of growth promoting factors as well as stimulants for Schwann cell proliferation (Perry, 1987;Perry, 1992). While the axon degrades, the Schwann cells de-differentiate and longitudinally align to form the Bands of Büngner. These "bands" provide a guiding structure for regrowing fibres (Lee and Wolfe, 2000). Within one day axons begin to form bulbous swellings at their proximal ending as a sign for the accumulation of newly arrived axoplasm containing cytoskeletal components, mitochondria, sER etc. These "clublike structures", as described by Ramón y Cajal in 1928, give rise to growth cones leading the axon's

regeneration at a rate of 1-2mm/day, the growth cone following guidance signals (Johnsen et al., 2003). In transection lesion, regeneration and target innervation occur only in injuries with a maximum gap of 1cm and a performed re-anastomosis of the cut ends. Following a crush lesion to the peripheral nerve, even longer distances can be overcome (Schaumburg, 1992). *In the CNS*, the distal stump degenerates at the same rate as in the PNS. CNS cells, however, respond in a completely different way to that degradation. Microglia (resident macrophages) are activated and some blood-born macrophages invade the lesion site around the third day, but the number of phagocytising cells remains lower than it would be in the PNS. Therefore, the removal of debris occurs much slower in CNS than in PNS lesions (George and Griffin, 1994; Nacimiento and Noth, 1997). The proximal stump, after having retracted a little, does sprout for some millimeters to stop right at the lesion site (Ramon y Cajal, 1928; Stichel and Muller, 1998b). Corresponding to this, central neurons seem to have the intrinsic capacity of regeneration. This has been proven by Aguayo et al. in his experiments of transplanting a peripheral nerve as a “linkage” between medulla and spinal cord (David and Aguayo, 1981). Nonetheless, until today, the reason for the growth arrest at the lesion site remains unknown. There are several hypotheses to explain the nature of this insurmountable barrier and experimental settings working on each of the mechanisms.

### **1.3 Pathophysiology of Spinal Cord Injury**

Spinal cord injury most often results in a direct mechanical trauma with the common feature of contusion secondary to a fracture accompanied with the dislocation of adjacent bony structures. Due to the pathophysiology of the trauma, a proportion of white matter in the lesion's periphery usually remains preserved (Kromer and Cornbrooks, 1987; Kakulas, 1999a). Within the lesion core, nerve cells, axons and blood vessels are damaged at the moment of injury. Normal blood flow is disrupted leading to ischemia, oxygen deprivation at the lesion site, and instantaneous cell death, necrosis. The axonal membranes are damaged, causing electrolytic shifts at the site of injury. A spinal shock lasting for about 24 hours is the equivalent of a generalised failure of the spinal network. Hemorrhages and disturbed microcirculation, loss of nerve conduction, localised edema, loss of vascular autoregulation and mechanical damage due to the injury's impact as well as further spinal cord compression are some important consequences of the acute phase SCI. This *primary injury* initiates a cascade of events leading to *secondary injury*. Ischemia, electrolytic shifts and edema continue. Within the first 30 minutes, extracellular glutamate concentration reaches a cytotoxic level due to cell lysis from the mechanical injury. Lipid peroxidation and free radical production occur as a result of glutamate-activated pathways, further enlarging the lesion area (Harkey, III et al., 2003; Hulsebosch, 2002). Apoptosis is activated, lasting for weeks. By penetrating the disrupted blood brain barrier (BBB), neutrophils invade the lesion

site within 12 hours after injury, followed by T-cells with a peak level at 2 days post-injury. By secretion of cytokines and chemokines, these intruding T-cells increase the inflammatory reaction taking place (Raivich and Kreutzberg, 2000; Dusart and Schwab, 1994; Blight, 1992). Blood-born macrophages and CNS-resident microglia transformed into macrophages arrive around day 3, remaining over days to gradually remove dead tissue. In contrast to the PNS, this is happening much slower in the CNS (George and Griffin, 1994; Ramer et al., 2000; Leskovaar et al., 2000; Mueller et al., 2003). Glial cells are activated, visible by an increased expression of glial fibrillary acidic protein (GFAP). Extracellular matrix (ECM) molecules are produced by migrating fibroblasts, endothelial cells, and activated astrocytes mainly. Semaphorin III A, which has been shown to be present in the core region of the lesion scar (Pasterkamp et al., 1999), leads to growth cone collapse, TGF $\beta$  secretion results in an increased fibroblast proliferation with, in consequence, even more ECM molecule production. This results in restructuring of the ECM. In the *subacute and chronic phase of SCI*, scarring and tethering of the cord, demyelination resulting in nerve conduction deficits and the development of syringomyelia, a cyst formation gradually worsening over time are the main complications. Chronic pain syndromes might develop due to permanent hyperexcitability of some cell types. For further details on the pathophysiology of SCI refer to (2006a; Bethea, 2000; Kakulas, 1999b; Kakulas, 1999a; Nacimiento and Noth, 1997; Raivich and Kreutzberg, 2000; Ramer et al., 2000; Sandvig et al., 2004; Schwab and Bartholdi, 1996; Stoll and Muller, 1999; www.bio.davidson.edu, 2003).

## 1.4 Human Spinal Cord Injury

### 1.4.1 Epidemiology

In Germany, there are about 20 new cases of SCI per million per year, that is about 1600 patients per year, to treat in one of our SCI centres (21 centres in 1997) (Exner and Meinecke, 1997). To compare, in the USA there are 8000-10000 new cases per year (2006b). 70-80% of the SCI are of a *traumatic* cause, mainly traffic accidents (35%), workplace related (14%) or recreational activity related injuries (4%). The other 20-30% are *non-traumatic*, main reasons being primary and secondary tumours (15-20%) or disturbance in blood circulation with different underlying mechanisms (Dietz and Boos, 2001; Exner and Meinecke, 1997; Sekhon and Fehlings, 2001). Most traumatic SCI patients are young males (70%). 62% of the traumatic SCI patients become paraplegic, 38% tetraplegic (Dietz and Boos, 2001; Exner and Meinecke, 1997; Masanneck, 2003; Sekhon and Fehlings, 2001). Mortality at the time of the accident or on arrival at the hospital is very high (50-79%). Morbidity is also elevated. Many patients require re-admission to the hospital for various complications like soft tissue disorders, urinary tract complications or spine and extremity

disorders (Exner and Meinecke, 1997). *Vegetative dysfunctions* accompanying SCI are mainly due to a deficit in the sympathetic part (Th1-L2) with, in consequence, a predomination of parasympathetic functions. Thermoregulation is disturbed following a parasympathetic vasodilatation, heart frequency and blood pressure decrease. An intestinal malfunction within 24 hours causes a paralytic ileus, bladder and sexual function are troubled (Dietz and Boos, 2001). *Late complications* of SCI are recurrent cord compression, neuropathic pain, cord tethering or the development of a syringomyelia. Minor pain or even signals unappreciated from below the lesion site (e.g. a bladder infection or a rectal fissure) may induce spasms or dysautonomia associated with sympathetic reactions like sweating, hypertension etc. In a chronic state, the initial flaccid paralysis will be superseded by spasticity, further on leading to spasms, hyperreflexia and contractures as well as dystonic postures interfering with hygiene and the self-image. These consequences, not the SCI and the locomotor deficit alone, render the patients' lives so difficult (el Masry and Short, 1997).

#### **1.4.2 Classification of Spinal Cord Injury**

Spinal cord injury, a challenging clinical diagnosis. Few conditions are as devastating or disabling as SCI imposing a sudden paralysis. SCI goes along with deficits in motor, sensible and/or vegetative functions. There are different ways to classify SCI. One could categorise SCI according to whether the patient is para- (thoracic, lumbar or sacral spinal segment involved) or tetraplegic (cervical segment involved) (Harkey, III et al., 2003), whether it is a primary or a secondary spinal cord lesion, an upper or lower motoneuron lesion, traumatic (direct) or non-traumatic (indirect), an open or a closed lesion. The ASIA (American Spinal Cord Injury Association) grades SCI in 5 levels, also classified according to complete versus incomplete injury. A complete injury leads to a functional transection without any function left (neither sensation nor motor activity) below the lesion level. Both sides are equally affected. In incomplete lesions, there is some function preserved, covering a spectrum from minimal functional preservation to almost normal utility (Becker et al., 2003; Ghirnikar et al., 2001; Harkey, III et al., 2003). Other than the "classic" para- or tetraplegia following trauma, bleeding, tumour or cord ischemia showing spastic (if lesion above L1) or flaccid (if lesion below L1, cauda) symptoms, different spinal cord dysfunction - syndromes can be described in incomplete SCI (see Fig. 1.1 for the most current examples). For further information see (Young, 2006).

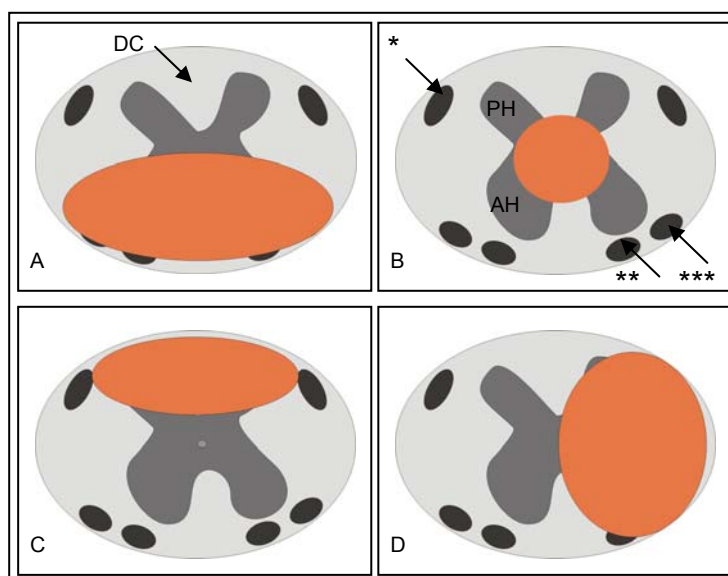


Fig. 1.1: The most important Spinal cord dysfunction syndromes are represented in this scheme. (A) Anterior cord syndrome (B) Central cord syndrome (C) Posterior cord syndrome and (D) Brown-Séquard syndrome. Arrows indicate the different fibre tracts. \* CST, \*\* Anterior spinothalamic tract, \*\*\* Lateral spinothalamic tract, DC Dorsal column. AH Anterior horn, PH Posterior horn, orange areas represent the site of cord injury.

## 1.5 Therapies of Spinal Cord Injury

### 1.5.1 Current Standard Therapies of Spinal Cord Injury

Confronted with a patient suffering SCI, several therapeutical options are in common use. One could divide the different therapies in pharmacological, surgical and rehabilitative strategies. None of the current standard therapies “goes down to the roots”, though. All are symptomatic therapies. For further information on the standards applied see (Hulsebosch, 2002; Gunnarsson and Fehlings, 2003; Dobkin and Havton, 2004; Young, 1995; Dietz and Boos, 2001; Hadley, 2002; Dobkin, 2003). *Rehabilitation* plays a crucial role in the treatment of spinal cord injured patients. Physio- and Ergotherapy go hand in hand in prevention of muscle atrophy and contractures, daily-life skills, wheelchair use and management of skin, bowel and bladder care as some examples. Biofeedback-training can be applied. Various stimulators for Functional Electrical Stimulation (FES), the application of electrical current to a muscle via a varying number of electrodes to induce contractions of paralysed muscles, are in use. Diaphragmatic pacers, bladder stimulators, walking devices (e.g. Parastep) or hand stimulators (Mulcahey et al., 2004), robotic devices (Reinkensmeyer et al., 2002) or BIONs™ (Loeb et al., 2001) are some examples (Young, 1995). Application leads to a decrease of secondary medical complications (Scremin et al., 2000; Dobkin and Havton, 2004). The BWSTT (Body-weight supported treadmill training) locomotor training is based on experiments by Barbeau and Rossignol (Barbeau and Rossignol, 1987) who showed,



that in spinalised cats stepping over a treadmill can be triggered and trained under conditions of body weight support with only the hind limbs on the treadmill. Among the *pharmacological therapies* applied in SCI, the acute administration of methylprednisolone has been studied in extent (Bracken and Holford, 2002). Desired effects were the acute anti-inflammatory and immunosuppressive actions of the glucocorticosteroids. Today, the usage of methylprednisolone is controversially discussed (Vellman et al., 2003;Hurlbert, 2000;Hugenholtz, 2003). There are no significant positive effects proven for SCI (Sayer et al., 2006) nor is the administration of methylprednisolone mentioned in the guidelines for SCI treatment. It remains an option. Prevention of deep venous thrombosis is very important since pulmonary embolism is the 3<sup>rd</sup> leading cause of death following SCI (Gunnarsson and Fehlings, 2003). Baclofene or botulinum-toxine as anti-spasticity treatment and the therapy of potentially developing neuropathic pain syndromes are currently administered (Young, 1995). Depending on the type of injury, several *surgical therapies* like stabilisation, untethering of the spinal cord or decompression (Gunnarsson and Fehlings, 2003;Guest et al., 2002) are an option non of which has been clinically evaluated yet. Urological catheters and artificial bladder or bowel sphincters may be introduced into the patient. In the chronic state of SCI, adhesions can be removed and the CSF flow restored using a dural graft.

### **1.5.2 Therapies in Clinical Trial**

There are quite a number of potential therapies in clinical trial for acute, subacute or chronic SCI at the moment. The product Sygen® (GM-1) by FIDIA may accelerate recovery in acute SCI as shown in a finished phase III study. Methylprednisolone (NASCIS-studies) remains controversially discussed after finished phase III. Cethrin® (Rho-inhibition through C3) by Bioaxone induces compensatory sprouting. No results of the phase IIa dose escalation have been published yet. Procord®, the activated macrophages of Proneuron for application in subacute SCI are in IIb multicenter studies since 2004. The finished phase III multicenter-study in chronic SCI on Fampridine®, a K<sup>+</sup>-channel blocker, produced by Acorda Therapeutics, was not significant in its outcome. Other compassionate use applications are in progress without valid studies. For further information see (Hulsebosch, 2002;Schwab et al., 2004;Hermanns, 2004;Dobkin and Havton, 2004;Young, 1995) and the internet homepages of the given companies.

## 1.6 Different Approaches in Spinal Cord Injury Research

Many groups around the world are trying to develop therapeutical strategies to achieve spinal cord regeneration. Their above goal is to “make people walk again”. But for patients by far more important is to achieve functional recovery in all their other deficits like bladder and bowel function or sexual dysfunction for example. Often, functional deficits are not apparent until 90% axonal loss. The regeneration of only a few axons can equally lead to a return of some respectable function (Fawcett, 1998). Yet, description of recovery is no evidence for real axonal regeneration. Plasticity of the nervous system, compensational mechanisms or collateral sprouting can also play an important role in some functional improvement. To achieve real long-distance axonal regeneration in the former pathways through the lesion site, several steps have to be fulfilled. The induction of regrowth, the regenerative sprouting, has to be followed by the elongation of fibres through the scar tissue at the lesion site. Appropriate target finding and then, re-synaptogenesis has to occur as well as remyelination to approve for real functional recovery (Stichel and Muller, 1998a). Until today, it remains unclear why regeneration in the mammalian CNS is not successful. There are several hypotheses to explain the failure of CNS restitution. Since Aguayo’s proof of principle of the CNS neurons’ intrinsic capacity of regrowth, it is obvious that it is not the neurons themselves that are unable to regenerate (David and Aguayo, 1981). There might be a *lack of trophic support* for the regrowing axons or the expression of regeneration-promoting genes following injury is insufficient. Neurotrophic factors, regulators during development and in the adult CNS, modulate and support survival, growth and differentiation of neurons. Administration of NTFs by various mechanisms has widely been studied. Their effect is not acute but functioning via signalling pathways inducing gene transcription and protein synthesis (Bradbury et al., 1999; Cheng et al., 2004). In most studies, the NTFs were applied in combination with other regeneration supporting strategies (Bamber et al., 2001; Boyd and Gordon, 2003; Bregman et al., 2002; Bunge and Pearse, 2003; Coumans et al., 2001; Grill et al., 1997; Iannotti et al., 2003; Xu et al., 1995a). For review see (Bunge and Kleitman, 1999; Hempstead and Salzer, 2002; Tuszynski, 1999). *Growth inhibiting substances* may well accumulate after upregulation of their expression following SC lesion. Several proteins are said to be associated with myelin (Qiu et al., 2000; Silver and Miller, 2004; Sandvig et al., 2004; Fouad et al., 2001; GrandPre and Strittmatter, 2001). The most important are the three Nogo-isoforms (Hunt et al., 2002; Huber and Schwab, 2000; McKerracher and Winton, 2002), the MAG (myelin associated protein) (Bartsch, 1996; Filbin, 1995; Liu et al., 2002), and OMgp (oligodendrocyte myelin associated glycoprotein) (Wang et al., 2002). Nogo, MAG and OMgp signal through a common receptor, the NgR. A specific antibody against NgR would be interesting to combine the effect against inactivating myelin-associated inhibitory molecules (Qiu et al., 2000; Fournier and Strittmatter, 2001) since inactivation only of Nogo merely resulted in collateral sprouting

of uninjured axons (Li and Strittmatter, 2003; Schwab and Brosamle, 1997). *Modulation of signal transduction* is possible by modification of the Rho/Rock pathway. Rho GTPases are intracellular regulators of growth cone collapse. Direct activation of Rho by growth inhibitory molecules, e.g. Nogo-66, leads to growth cone collapse and neurite outgrowth inhibition. Rho can be inactivated by C3 toxin (C. botulinum) (McKerracher, 2001; Dergham et al., 2002), ROCK II directly by Y-27632, a specific antibody (Fournier et al., 2003a). Another way of Rho inactivation is due to intracellular elevation of cAMP. High levels of cAMP lead to a phosphorylation of Rho via the PKA (protein kinase A).

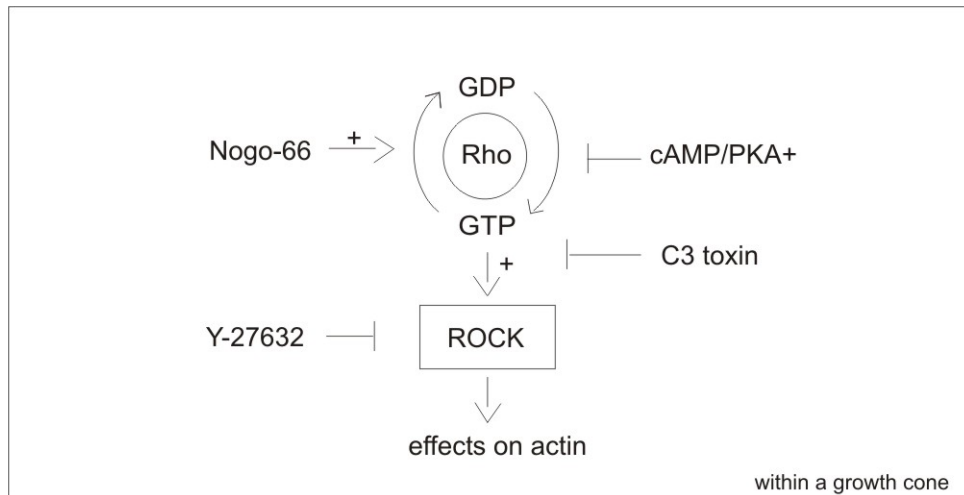


Fig. 1.2: The Rho pathway within a growth cone, taken from (Kwon et al., 2002a) and slightly modified.

The *developing scar* might prove to be a physical as well as a molecular barrier for the regrowing fibres implicating the need for scar modulation or bridging the lesion site. *Cell grafting* has emerged as a powerful and promising tool for enhancing restitution of the lost function following SCI. Main objectives are growth facilitation, the graft serving as a bridge for regrowing axons, administration of new neurons and neurotrophic factor secretion. Tissue sources for transplantation have been diverse. *Peripheral nerve grafts* (David and Aguayo, 1981; Levi et al., 2002; So and Yip, 2000), *Schwann cells* (Bunge, 2002; Martin et al., 1996; Paino and Bunge, 1991; Raisman, 1997; Keyvan-Fouladi et al., 2005), *Olfactory Ensheathing Glia (OECs)* (Franklin, 2003; Garcia-Alias et al., 2004; Jones, 2003; Keyvan-Fouladi et al., 2003; Li et al., 2003; Ramer et al., 2004; Ramon-Cueto et al., 2000; Santos-Benito and Ramon-Cueto, 2003), *fetal CNS tissue* (Coumans et al., 2001; McDonald et al., 1999), *neural stem cells* (2001b; Cao et al., 2002; Teng et al., 2002), *bone marrow stromal cells* (Mezey et al., 2003; Ohta et al., 2004; Zhang et al., 2005), blood-born *autologous macrophages* (Franzen et al., 1998; Prewitt et al., 1997; Rapalino et al., 1998), *astrocytes* (Fawcett and Asher, 1999) or *fibroblasts*, genetically modified to produce one of the common NTFs (Murray et al., 2002; Franzen et al., 1999; Grill et al., 1997) have widely been studied. None of the above stated therapies has proven evidence for successful regeneration when applied alone. A combination of strategies is therefore indispensable. To get an overview over the various approaches see (Sandvig et al., 2004; Fry, 2001; Jones et

al., 2001;Christie and Mendez, 2001;Lakatos and Franklin, 2002;Hulsebosch, 2002;Schwab and Bartholdi, 1996;Nacimiento and Noth, 1997;Blakemore and Franklin, 1991;Murray and Fischer, 2001;Sagen et al., 2000;Barami and Diaz, 2000;Dobkin and Havton, 2004;Young, 2002;Kwon et al., 2002a;Stichel and Muller, 1998a;Schwab et al., 2004;Ribotta et al., 2002;Jones et al., 2003;Reier, 2004;Zhang et al., 2005;Plant et al., 2000;Fernandez et al., 2006).

## 1.7 Regeneration-inhibitory Barrier – the Lesion Site

Following central nervous system lesion a scar formation comparable to scarring succeeding other tissue injury is taking place. Local intercellular and extracellular modifications to restrict damage occur. CNS integrity is re-established by sealing it off from the external environment. The BBB is re-sealed to prevent infections. Scar tissue has some contractile properties to approach the wound margins. Nutrition is provided by an invasion of epithelial cells leading to a neovascularisation (Stichel and Muller, 1998b). Activated glial-cells secrete many different factors functioning as regulators for regeneration, activators of immuno-competent cells or the reconstruction of the ECM (Yurchenco and Schittny, 1990;Yurchenco and O'Rear, 1994). In the 1970s, Russian scientists described the development of a BM at the lesion site after SCI. Windle, convinced of a multilayered scar composed of glial and connective tissue, in his Piromen® - studies concluded that the connective tissue scar seemed to be the more important impediment for regeneration (Reier and Guth, 1983). Experiments to remove the BM-scar by enzymatic digestion (Matinian and Andreasian, 1973) were unsuccessful since the BM around blood-vessels also got destroyed leading to further bleedings (Guth et al., 1980). After those failed experiments, the BM as a potentially regeneration inhibiting structure fell into oblivion until the late 1990s. Stichel (Stichel and Muller, 1998b;Stichel et al., 1999b;Stichel and Müller, 1998) could show that regenerating fibres stop abruptly at the lesion site, coinciding with depositions of Coll IV. Detailed studies by Klapka et al. showed that the scar is composed of two main constituents (Klapka et al., 2002): the fibrous part in the lesion centre surrounded by astrogliosis, the glial part.

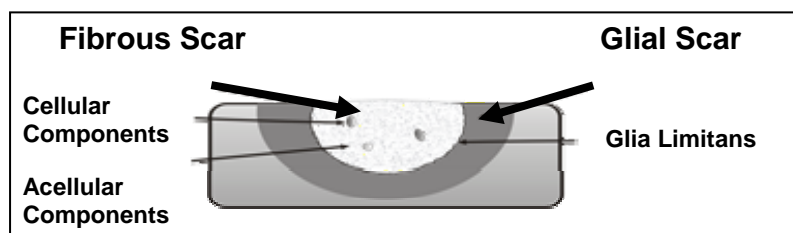


Fig. 1.3: Scar constitution as described by Klapka (Klapka et al., 2002). The fibrous scar (Collagen IV positive) in the lesion centre is separated from the surrounding GFAP positive glial part, the astrogliosis, by the glia limitans (Klapka, 2003).

### 1.7.1 Fibrous Scar

Acellular ECM is intermingled with cellular components like blood cells, macrophages, fibroblasts, meningeal cells, Schwann cells (from the DRGs) and microglia. One of the main molecules found in the fibrous scar is collagen IV. It is one of 19 known collagen types, situated in BM only and builds sheet-like networks. For further information see (Hermanns, 2001; Brown and Timpl, 1995; Aumailley and Gayraud, 1998). Other basement membrane components like laminin or entactin could also be immunostained. This led to the conclusion that the CNS scar in its core is mainly composed of BM visible five days post-lesion by an anti-collagen IV antibody (Hermanns et al., 2005). Being comprised of the forementioned collagen IV network linked to a laminin network via nidogen/entactin, the BM serves as a supporting structure during development, in tissue repair and as a scaffold for anchorage of many constituents via integrins (Yurchenco and Schittny, 1990; Yurchenco and O'Rear, 1994; Berry et al., 1987). BM-associated molecules are mainly secreted by reactive astrocytes, oligodendrocytes and fibroblasts (Fawcett and Asher, 1999; Davies et al., 1997). Some of these molecules have been shown to be inhibitory for axonal regeneration like Tenascin, Semaphorin III A or CSPGs (Klapka et al., 2002; Venstrom and Reichardt, 1993; Silver and Miller, 2004; Eckes et al., 2000). Following SCI, an upregulation of these molecules can be stated. Davies demonstrates a correlation between CSPG increase around CNS injuries and an axonal growth arrest where CSPGs are located (Davies et al., 1997) and *in vitro* studies showed their inhibitory effects. Application of an enzyme digesting the GAG chains from the protein core or disturbance of PG synthesis reduces the inhibitory effects. Bradbury et al. showed that Chondroitinase ABC degrades the CS-GAG chains, even restores post-synaptic activity (Bradbury et al., 2002). Yick (Yick et al., 2003) and Krekoski (Krekoski et al., 2001) demonstrated the same in studies with acellular nerve grafts, Chau 2004 in combination with Schwann cell filled mini-channels.

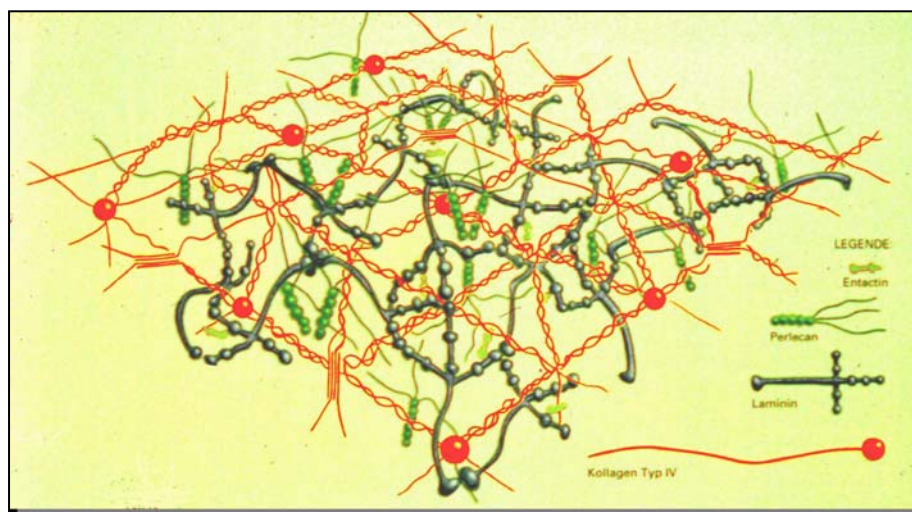


Fig. 1.4: Schema of the Basal Membrane, comprised of a Collagen IV and Laminin network as the main constituents, interconnected via entactin [modified according to (Yurchenco and Schittny, 1990)].

### 1.7.2 Glial Scar

Over the past decades, glial cells have been recognised as important functional components of the CNS in addition to their structural role. Oligodendrocytes are essential for myelination (Fitch and Silver, 1999), astrocytes participate in many functions like BBB maintenance (Pekny and Nilsson, 2005), ECM production (Bernstein et al., 1985; Heck et al., 2003) and neurotransmitter transport (Pekny and Nilsson, 2005) as well as in the maintenance of ion homeostasis (Fitch and Silver, 1999). Microglia act as the CNS resident phagocytic cells (Leme and Chadi, 2001). Within a few hours after injury, astroglia undergo structural changes, proliferate and build a dense network with their processes. This reaction is referred to as “reactive astrogliosis” (Pekny and Nilsson, 2005; Hadley, 1997). Astrocytes become hypertrophic, hyperplastic and increase their production of intermediate filaments (IFs), the major IF protein in unlesioned spinal cord astrocytes being GFAP (Pekny and Nilsson, 2005). In the acute post-injury phase, the prevalence of astrogliosis appears positive and necessary to restore function as soon as possible. The disrupted BBB is reconstituted and the astrocytic antioxidative and neurotransmissive role might be useful (Reier and Guth, 1983). In experiments with mice ablated of dividing astrocytes, healing processes were delayed (Faulkner et al., 2004). In the subacute phase, astrogliosis might rather have negative effects on axonal regeneration. Suggested theories for astrocytic contribution to regeneration failure are numerous (Fawcett and Asher, 1999; Pekny and Nilsson, 2005; Silver and Miller, 2004). The hypothesis originally arose from histological observations of transected fibres stopping at the site of injury, often within a glial matrix. Collagenous connective tissue, however, frequently coincided with the gliosis (Reier and Guth, 1983). The accumulation of the secreted molecules within the glial network, though, rests pure speculation. It is highly probable that the inhibitory proteins attach to the BM within the fibrous core of the scar (Reier and Guth, 1983; Klapka et al., 2002; Stichel et al., 1999b).

### 1.7.3 Anti-Scarring Treatment

Stichel’s observation of regenerating fibres stopping in front of Coll IV depositions at the lesion site (Stichel and Müller, 1998) led to the taking-up of the long forgotten hypothesis of BM as the regeneration inhibiting structure within the lesion site. A substance had to be developed that only inhibits the BM expression at the lesion site, leaving untouched the blood vessel BM. This was achieved by applying the collagen-biosynthesis inhibitor BPY (prolyl-4-hydroxylase inhibitor 2,2’-bipyridine) in a postcommissural fornix model. Prolyl-4-hydroxylase (PH) belongs to a family of  $\text{Fe}^{2+}$  dependant di-oxygenases using  $\text{O}_2$  as a substrate and requiring ascorbate as a cofactor (Franklin, 1991). There are several possible mechanisms to inhibit de PH-enzyme’s activity. The  $\text{Fe}^{2+}$  chelation deprives the PH of its

cofactor and therefore leads to a decreased protocollagen triplehelix stability. The new deposition of BM was reduced by prevention of Coll IV formation for 12d.

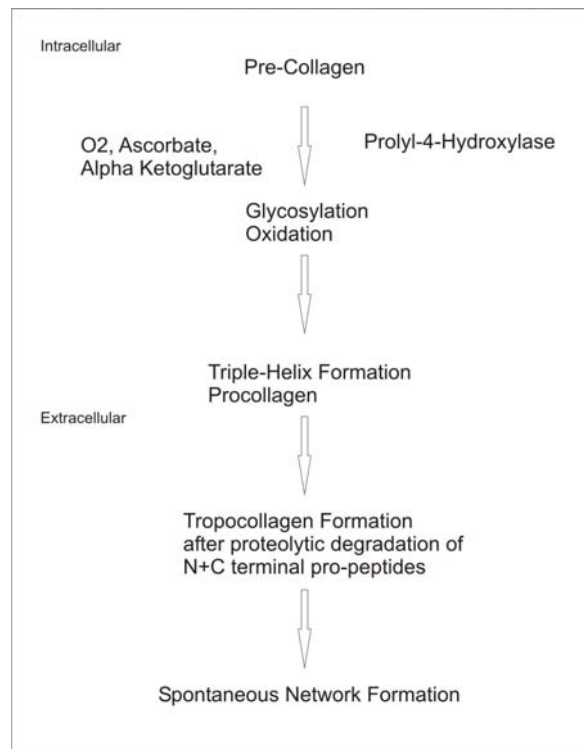


Fig. 1.5: Collagen IV synthesis shown in a slightly modified flow-diagram. Key enzymes PH is indicated. For further detail on Collagen IV synthesis see (Hermanns, 2001).

Short distance regeneration of transected fibres along former pathways as well as re-innervation of the target area (mamillary body) were possible within this "time window". Such regenerated fibres were found to be re-myelinated and re-established almost normal conduction properties (Stichel et al., 1999a). Inhibition of the collagenous BM of the lesion scar leads to regrowth of transected axons in the postcommissural fornix. In the spinal cord, the developing BM is of greater extent as compared to the fornix model. Meningeal cells are localised in close proximity. Mainly fibroblasts - the major source of collagen in wound healing processes - invade the lesion site, secreting large amounts of collagen (Halfter et al., 1990). This could explain the difficulties to reduce BM expression in the lesioned spinal cord. The iron chelator DPY was shown to be not potent enough to reduce the developing collagen scar in such a model. Modifications had to be made in order to prove an equivalent scar-delaying effect in the Th8 transection lesion (Hermanns and Muller, 2001; Hermanns et al., 2001b). Additional studies could demonstrate axonal long-distance regeneration as well as functional improvement in the follow-ups of SWK-transections (Hermanns, 2001; Klapka, 2003).

The modified AST is composed of

- (A) 6 injections of Prolyl-4-hydroxylase inhibitor BPY-DCA (2,2'-bipyridine-5,5'-dicarboxylic acid), 180x more potent than BPY (Hales and Beattie, 1993) into the lesion site.
- (B) Inhibition of fibroblast proliferation and, in consequence, ECM production, by 8-Br-cAMP [according to (Duncan et al., 1999)].
- (C) Continuous application of BPY-DCA via Elvax-copolymers [prepared according to the protocol in (Hermanns, 2001)].

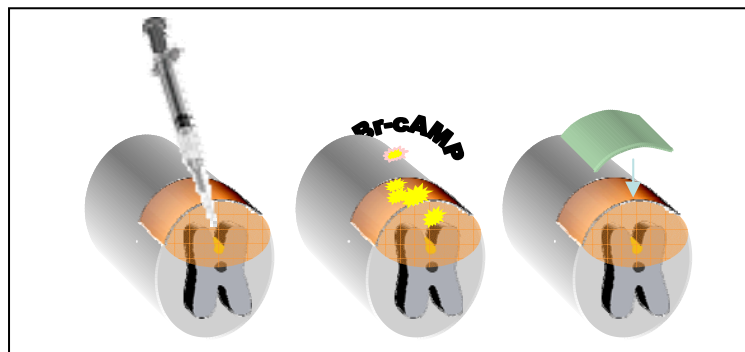


Fig. 1.6: AST application combining the administration of the iron chelator BPY-DCA into the lesion site (A) as well as for continuous application through an Elvax-copolymer (C) and the fibroblast proliferation inhibitor 8-Br-cAMP (B).

The described treatment, however, is mainly applicable to acute spinal cord lesions without gap due to tissue loss. In chronic SCI, the anatomic situation found is rather different. Tumour-, metastases-, scar- or cyst-resection creates a cavity that has to be overcome to achieve regeneration. In such cases, the nature of the injury probably requires combinations of treatment technologies: one to bridge the gap and one to prevent scarring of the tissue/graft interfaces in order to enable axonal regeneration.

## 1.8 Entubulation

### 1.8.1 History of Entubulation

The idea of entubulation for the repair of severed peripheral nerve is not new. Glück (Glück, 1880) was the first to describe the use of tubes to bridge injury-resulting gaps between nerve stumps. In the PNS, donor nerve number is *limited*, they are of *restricted length* and harvesting leads to a *denervation* of the donor area. In case of allogeneic grafts, immune rejection represents an additional difficulty (Doolabh and Mackinnon, 1999; Evans et al., 1994; Lassner, 1444; Schaller et al., 1991). Entubulation appears to be a potential alternative to autograft repair. The implanted materials are supposed to serve as scaffolds to facilitate nerve regrowth and guide the regrowing fibres. Many groups are working on entubulation



studies of diverse materials alone or in combination with other regeneration promoting therapies in PNS. Tube material can be classified by its characteristics in biological or synthetic, biodegradable or non-degradable or the material is combined with other substances to form a composite. For a review in PN regeneration see (Fields et al., 1989; Fine et al., 2000).

Tab. 1.1: Selection of materials studied for guidance channel application in the PNS.

<b>Biological Material</b>	<b>Synthetic Polymers</b>	<b>Composite Implants</b>
<b>Degradable Conduit Material</b>		
Acellular Nerve Grafts (Kim et al., 2004)	Poly ( $\alpha$ -hydroxy) acids (PLA (Maquet et al., 2000), PGA (Rosen et al., 1990), PLGA)	PLGA + SCs (Hadlock et al., 2000)
Veins (Chiu, 1999; Tang, 1995)	Poly(L-lactic acid) (PLLA) (Evans et al., 2002)	Poly-D,L-Lactide , Poly-DL-lactide- $\epsilon$ -caprolactone (Giardino et al., 1999; Meek et al., 1999; den Dunnen et al., 1996)
Collagen I (Anselin et al., 1997; Archibald et al., 1991; Kim et al., 1994; Yu and Bellamkonda, 2003)	Poly-caprolactone (Nicoli et al., 2000)	Trimethylenecarbonate-co-epsilon-caprolactone (TMC/CL) + SCs (Lietz et al., 2005; Sinis et al., 2005)
Alginate (Sufan et al., 2001)	Polyphosphoester (Wang et al., 2001)	Poly- $\beta$ -Hydroxybutane (PHB ) (Ljungberg et al., 1999)  PHB + poly (glycolode-co ( $\epsilon$ -caprolactone)-diol (Borkenhagen et al., 1998)
<b>Non-Degradable Conduit Material</b>		
	Hydroxyethyl - Methylacrylat (HEMA) Hydrogels	Poly(acrylonitrile) poly(vinyl chloride) (PAN/PVC) (Guenard et al., 1992; Aebischer et al., 1988; Aebischer et al., 1989b; Aebischer et al., 1989a)

In CNS however, the mere implantation of guidance channels of any material, with or without cells, did not show any good results in long-distance regeneration. "A bridge containing supportive substrates for axonal elongation in combination with other successful

strategies seems necessary” (Plant et al., 2000). A number of different scaffolds has been studied (see Tab. 1.2). For review see (Friedman et al., 2002;Novikova et al., 2003;Pachence and Kohn, 2000). Since the early 1990s, a group around Mary and Richard Bunge, the Miami Project to Cure Paralysis, in Miami, Florida, USA is working on Schwann cell-filled guidance channels to be implanted into the mammalian CNS. They found out that axons are only present in Schwann cell filled tubes (Paino and Bunge, 1991;Xu et al., 1995b;Paino et al., 1994), SCs facilitating the axonal ingrowth of fibres into the channel. Furthermore, the ability of regrowth depends on the Schwann cell distribution. Autologous SCs appear to be a better substrate than syngeneic SCs [shown for PNS (Rodriguez et al., 2000) and CNS (Guenard et al., 1992)]. Axonal outgrowth into the host tissue, on the other hand, hardly occurs (Xu et al., 1997;Christie and Mendez, 2001;Tresco, 2000;Sagen et al., 2000). Only in a hemisection model with SC-filled mini-channels (Xu et al., 1999), not in complete transection models (Xu et al., 1997), some fibres actually did cross the distal implant / host tissue border. Cell-filled channels alone were not sufficient to enhance fibre outgrowth. Combination strategies either with NTFs (Xu et al., 1995a) or with OECs proximally and distally injected into the graft (Fouad et al., 2005;Ramon-Cueto et al., 2000) seem crucial to stimulate some axonal regeneration back into the host tissue. In most studies, Miami Project worked with PAN/PVC tubes, a synthetic non-degradable material provided by Patrick Aebischer. Within those tubes, the SCs seem well aligned (Guest et al., 1997b), the material, however, poses some problems of tissue irritation due to its stiffness and non-degradability.

Tab. 1.2: Selection of materials studied for guidance channel application in the CNS.

<b>Biological Material</b>	<b>Synthetic Polymers</b>	<b>Composite Implants</b>
<b>Degradable Conduit Material</b>		
Carbon filaments (Khan et al., 1991)	Poly(lactic-co-glycolic acid) (PLGA) (Fournier et al., 2003b)	PLGA with Neural Stem Cells (Teng et al., 2002)
Collagen type I (Joosten et al., 1995;Kuhlengel et al., 1990a;Kuhlengel et al., 1990b;Paino and Bunge, 1991)	Poly-β-Hydroxybutane (PHB ) (Novikov et al., 2002)	Poly (D-L-lactide) + FGF (Maquet et al., 2001), + SC (Oudega et al., 2001)
Alginate hydrogel (Novikova et al., 2005;Suzuki et al., 2002)	Polyethylene glycol (PEG) (Borgens et al., 2002)	PHB + SC + alginate hydrogel (Novikov et al., 2002)
	Matrigel (Xu et al., 1995b;Novikova et al., 2005)	Nitrocellulose + fetal SC tissue +/- NTFs (Houle and Ziegler, 1994)
	Fibronectin	

<b>Non-Degradable Conduit Material</b>		
	NeuroGel (pHPMA) (Woerly, 2000) and pHEMA (Tsai et al., 2006;Plant et al., 1998;Plant et al., 1995)	PAN/PVC + SC, + NTFs (Kleitman, 2001;Xu et al., 1995b;Iannotti et al., 2003;Bamber et al., 2001;Pinzon et al., 2001)
	Silicone (Borgens, 1999)	Silicone + PNgraft + microchips (Lundborg et al., 1998)
		Agarose + BDNF (Jain et al., 2005)

### 1.8.2 Qualities of a Guidance Channel

The aim of combining cellular and biomaterial transplantation is to bridge a gap, guide axons to avoid misrouting and to create a controlled, growth permissive environment by introducing cells for self-sustained, permanent neurotrophic support (NTF-production) and excluding invasion of interfering cells like fibroblasts. Implantable guidance channels should be re-absorbable, first, to prevent repetitive irritations and microtrauma at the interface area and second, to avoid a second operation. The conduit material is to be flexible, easy to handle, though stable enough. Dimensions are to be variable for differing sizes of nerve or spinal cord diameters. Micropores are needed to provide sufficient nutrition for cells and fibres inside the conduit. Degradation products are to be biocompatible, that is, the components are to be hydrolyzed and degraded after regeneration has taken place. The degradation period shall be adjustable. In human peripheral nerve repair, the optimal case would be a degradation starting at the proximal end, gradually prolonging the guidance channel with nerve fibre regrowth. In the spinal cord the situation is somehow different since there is no "proximal" nor "distal" in repair. There are motor fibres growing from cranial to caudal but as well sensory fibres running in the opposite direction, from caudal to cranial.

## 1.9 Schwann Cells

Schwann Cells (SC) are remarkably supportive for the regrowth of axonal processes (for review see (Bunge, 1993;Bunge, 1994;Oudega et al., 2005;Plant et al., 2000;Martin et al., 1996;Montgomery et al., 1996). They survive transplantation (Baron-Van Evercooren et al., 1991), migrate (Franklin and Blakemore, 1993), form myelin (Blakemore, 1977;Duncan et al., 1981;Baron-Van Evercooren et al., 1997) and foster regeneration of CNS axons (Guenard et al., 1993;Dr.Robin Franklin, 2002). Characteristics important for the induction of axonal regrowth are for example the production of NTF like NGF (Bandtlow et al., 1987) or BDNF (Acheson et al., 1991), the synthesis and secretion of ECM molecules (Bunge, 1993;Mirsky and Jessen, 1999) as well as the expression of cell adhesion molecules (Bixby et al., 1988;Kleitman et al., 1988). In PNS, where SCs play an important role, axonal regeneration following injury is taking place. This fact led to experiments in CNS injury. The ability of PNS transplants into the CNS to induce axonal regrowth may largely be due to and dependent on the presence of Schwann Cells (Berry et al., 1988;Bunge, 2002;Montgomery and Robson, 1993;Paino et al., 1994;Ard et al., 1987). Schwann cell-free PN fails to support axonal regeneration (Guenard et al., 1993;Kleitman et al., 1988). Studies have shown that purified suspensions only of *living* SCs are able to promote regeneration and limit tissue loss in the CNS (Guenard et al., 1993;Kleitman et al., 1988;Martin et al., 1996;Montgomery et al., 1996;Paino and Bunge, 1991). Over 30 years ago, Richard Bunge developed techniques for isolation and culture of SCs from a patient's peripheral nerve for autologous transplantation. Today, the generation of large numbers of SCs is possible in rat (Morrissey et al., 1991) and humans (Levi et al., 1994). A major advantage of Schwann cells over other cell types is their easy acquisition and way of multiplication *in vitro*. Transplantation of such autologous SCs into the spinal cord will therefore not go along with a graft-host immune-reaction and be of minimal risk. In the past years, several SC implantation studies have been carried out. The implantation of cellular bridges into the spinal cord provides a permissive substrate for axonal growth across the site of injury. Repair of cord circuitry and, in consequence, restoration of function are the objective. Grafting SCs alone, though, does not result in considerable fibre outgrowth from the implant back into the host tissue (Bunge, 1993;Guest et al., 1997a). Combinations with other growth promoting strategies are imposed. Li and Raisman (1994) showed that CST fibres sprouted at contact with SC graft and regenerated into the distal fibre tract after transplantation of OECs (Li and Raisman, 1994). In combination with NTFs, the number of regrowing fibres is enhanced. Entubulation studies as discussed earlier in 1.8 have been worked on. Empty channels did not show any fibre ingrowth. In channel / SC composite transplantation, SCs are to be injected into the tubes before implantation to best support axonal regeneration. SC immigration from the nerve stumps would take time but axons appear to grow 8x faster than SC migration is taking place (Schlosshauer et al., 2003). Various studies combining SC transplantation with other

strategies have been carried out in the past years (Bamber et al., 2001;Bunge, 2002;Garcia-Alias et al., 2004;Guest et al., 1997b;Martin et al., 1993;Montgomery et al., 1996;Oudega et al., 2001;Paino et al., 1994;Pinzon et al., 2001;Plant et al., 2000;Ramon-Cueto et al., 2000;Tuszynski et al., 1998;Xu et al., 1995b). Until today, SCs remain one of the most promising cell type for spinal cord injury research and future clinical use for their myelinative, neuroprotective and regenerative capacities (Oudega et al., 2005). They are easily attainable from the patient, that is, no immunosuppression is needed and a large number of cells quickly can be generated *in vitro* without any ethical problem. Research on combination therapies will be continued in the future since SCs alone are inefficient.

## 1.10 Rodent Models of Spinal Cord Injury

In SCI research, there are three “classic” experimental rodent models performed in rat. The *contusion model*, the *compression model* and the *transection model*. For further detail on the applied rodent models see (Kwon et al., 2002b;Rosenzweig and McDonald, 2004;Talac et al., 2004). None of these models seemed appropriate for this study.

An injury model combining a partial cut and aspiration lesion as described in Materials and Methods 2.5.2 (rough schematic overview in Fig. 1.7) instead of one of the above mentioned models was chosen for this study for several reasons. *First*, the partial lesion in the new model leaves the animals in a better status and health with a smaller risk of complications than in a complete lesion. *Second*, in regard of human SCI mechanisms and pathophysiology, a complete transection did not seem appropriate. Human SCI hardly ever is a complete lesion. Even in completely paraplegic patients, the cord rarely is completely transected but there is some residual parenchyma in the lesion’s periphery (Kromer and Cornbrooks, 1987;Kakulas, 1999a). In chronic SCI other than in acute SCI, a lesion cavity or a gap of a certain distance often is resulting that has to be overcome. Resection of a fibrous scar, a tumour, a metastase or syringomyelia for example create such a gap within in spinal cord tissue. In many cases, this “resection” is performed by sharp preparation combined with an aspiration to leave the above mentioned cavity.

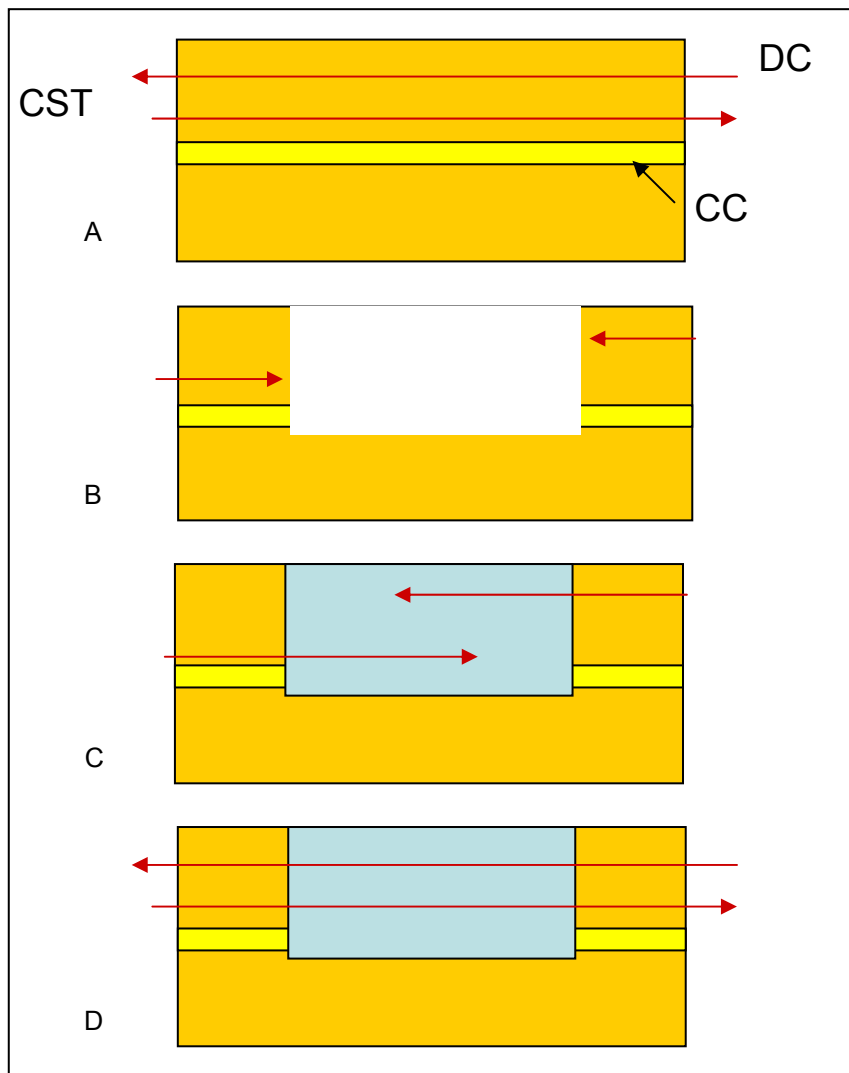


Fig 1.7: Schematic demonstration of the applied injury model. (A) The Central Canal (CC) can be seen as a landmark in rat spinal cord to determine fibre tract position. The CST fibres (corticospinal tract) located closely dorsal to the CC are directed from rostral to caudal whereas the dorsal column (DC) fibres run in the opposite direction. (B) Partial cut and aspiration lesion creates a gap, fibres stop close to the lesion site. (C) Implantation of a gap-bridging guidance channel shall lead to fibre-entrance from both sides. (D) AST application shall facilitate fibre re-entry into host spinal cord at the opposite graft end.

## 1.11 Aim of this Thesis

Peripheral nervous system axons are able to regenerate after a lesion. In the Central nervous system, this is not the case; after the initial sprouting response, the axons stop growing at the lesion site. A gap resulting of SCI due to necrotising tissue, cyst formation or for other reasons in subacute and chronic stages has to be overcome to provide a basic step in promoting regeneration. Furthermore, the lesion environment and the scar have to be modified to be rendered more regeneration supporting. Most researchers in the field agree that different regeneration enhancing strategies have to be combined to achieve better regenerative results.

The purpose of this study was to establish a model for bridging a gap in rat SC with a combined strategy of the implantation of a biodegradable guidance channel, the introduction of Schwann cells as a living factory for NTFs and the application of the anti-scarring treatment developed in our laboratory. The permeable guiding tubes with micropores serve as an orientation for the axons, preventing cell invasion from outside the tube but providing good nutrition. The Schwann cells, also serving as guidance structures, continuously secreting NTFs, are thought to direct the CNS fibres into and then along the channel. Until now, the main problem is that certain axons do enter the guidance channels but do not re-enter the host SC tissue distal to the lesion site. To achieve this as well as a higher number of axons traversing the channel, a combination with our AST seems attractive.

The following problems and questions have to be addressed:

1. Establishment of an appropriate injury model
2. Implantation of guidance channels
3. Tube filling-procedure with labelled Schwann Cells
  - Schwann Cell behaviour
4. Characterisation of the lesion
5. Definition of the scar formation in proximity of the implanted tube
  - Are there differences in scar formation in control or Schwann Cell filled tubes?
6. Axon behaviour
  - Do axons enter the guidance channels?
  - Are there any differences in control or Schwann cell filled tubes?
  - Do fibres grow in close proximity of the implanted Schwann Cells or are they even co-localised?
7. Application of the AST
  - Does it suppress scar formation in such a lesion model?
  - Are more axons found inside the tube in treated animals?
  - Do axons re-enter the distal host-tissue?

## 2.0 Material and Methods

### 2.1 Cell Culture

Cell culture and Schwann Cell transduction with eGFP (see below) have kindly been provided by Dr. Frank Bosse, Molecular Neurobiology Laboratory, HHU Düsseldorf.

#### 2.1.1 Cell Culture

Schwann cells were prepared from sciatic nerves of neonatal Wistar rats (P1-P2) and purified by complement lysis as described by (Brockes et al., 1979). Purity of approximately 99% was obtained under these conditions as confirmed by anti-Thy1.1 and anti-S100 immunostaining (data not shown). Purified Schwann cell cultures were expanded in Dulbecco's modified Eagle's medium (DMEM, Gibco) supplemented with 10% (v/v) fetal calf serum (FCS), 100 µg / ml crude glial growth factor protein preparation and 2 µM forskolin (Sigma) for 4-6 weeks (Porter et al., 1986). After growing to subconfluent cell layers, the cells would be transduced with the infectious "S11EGIN"-supernatant.

#### 2.1.2 Retroviral Overexpression of eGFP in vitro

To allow selection of transduced Schwann cells the eGFP-coding region of the IRES-EGFP cassette (of the retroviral plasmid S11IEG3) was replaced by the open reading frame (ORFs) of the neomycin phosphotransferase gene. The ORF of the enhanced fluorescent green protein (eGFP) was directionally inserted in front of the IRES-EGFP cassette in the 5' multi-cloning site of the retroviral plasmid S11IEG3 (data not shown). The PCR amplification products and all relevant cloning sites of the resulting retroviral "S11EGIN" plasmid were sequenced using an ABI310 sequencer (Applied Biosystems, Weiterstadt, Germany).

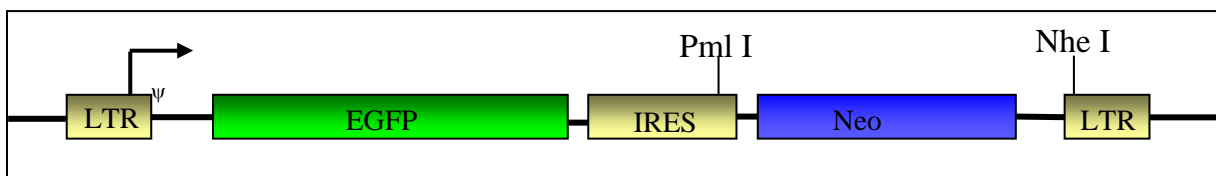


Fig. 2.1: S11EGIN-Plasmid (S11-EGFP-IRES-Neomycin<sup>R</sup>):

For generation of stable packaging cell lines ecotropic enveloped-pseudotyped retroviral supernatants were generated by transient transfection of subconfluent ecotropic Phoenix packaging (Nolan Lab, Stanford; Schulze et al, 2002) with 15 µg of plasmid DNA and 45 µg of Fugene (Roche, Mannheim, Germany) in 100 mm culture dishes. The next day DMEM



culture medium was replaced by IMEM medium and two days after transfection retrovirus containing medium collected and filtered through 0.45 µm filters (Sartorius, Göttingen, Germany). These ecotropically pseudotyped retroviruses were used to infect PG13-packaging cells (Miller et al., 1991) for three days in the presence of 7.5 µg/ml of protaminsulfate (Sigma, Deisenhofen, Germany) /ml medium (Hanenberg et al., 2002). Culture supernatants from transduced PG13 cells containing GALV-pseudotyped retroviral vectors were harvested from confluent dishes every 24 h for 4 days, purified by filtration through 0.45 µm and stored at -80 °C until use.

Retroviral transductions of subconfluent Schwann cells (40-60 %) with the infectious PG13-supernatant were performed in the presence of 7.5 µg protaminsulfate two times for 24 h. In order to generate stably EGFP-overexpressing Schwann cell populations, the cells were replated the next day and cultured in the presence of 0.8 mg/ml Geneticin (Sigma, Deisenhofen, Germany) for at least 10 days. EGFP- overexpression of the generated cell pools was confirmed by fluorescent microscopy and immunohistochemistry, respectively.

## 2.2 Buffers and Antibodies

### 2.2.1 Buffers and Other Solutions

Tab. 2.1: Buffers and solutions applied in this study

PBS (Phosphate-buffered saline) pH 7.4	100ml 18g ad 2000ml	0.2M PB NaCl Aqua dest.
0,2M PB (Phosphate buffer) pH 7.4	45.6g 12g ad 2000ml	Di-sodium hydrogenphosphate anhydrous Sodium di-hydrogenphosphate monohydrate Aqua dest.
TRIS buffer, 20mM pH 8.1	2.24g ad 1000ml	TRIS Aqua dest. with HCl: titrate pH 7.9
2,2'-bipyridine-5,5'-dicarboxylic acid (BPY-DCA, 30mM)	14,7mg ad 2ml	BPY-DCA (synthesized by M. Wehner, Institute for Organic Chemistry II, Heinrich Heine University Düsseldorf) TRIS
NHS 3% (Normal Horse Serum)	300µl ad 10ml	NHS PBS
NGS 3%	300µl	NGS

(Normal Goat Serum)	ad 10ml	PBS
Protease XXIV (Sigma)	2,5mg ad 5ml	Protease XXIV (Sigma) TRIS
DAB (Diaminobenzidine, Sigma)	140 mg ad 200 ml	PB
Sodium - Citrate Buffer pH 4.5	21g ad 1000ml 35.6g ad 1000ml	Citric Acid Monohydrate Aqua dest. Di-sodium hydrogenphosphate dihydrate Aqua dest.  50% from final volume of citric acid solution to mix with Na <sub>2</sub> HPO <sub>4</sub> -solution to pH 4.5 Final titration with NaOH
PFA (Paraformaldehyde) pH 7.4, 4%	20g ad 500ml	PFA 0.1M PB pH-titration with NaOH
Nissl-Solution	1.6326g 2.88ml ad 300ml 100mg	Na Acetate anhydrous Acetic Acid (glacial) Aqua dest. Cresyl Violet → mix 15'/60°C, then filtrate
Gelatine storage at 4°C	1g ad 200ml  0.1g	Gelatine Aqua dest. → heat 37-42°C (max) Chrome III KSO <sub>4</sub>
Matrigel™		Basement Membrane Matrix (BD Bioscience N° 356324)
Paraffine	100g 5g	Paraffine Cera Alba → heat 57°C
Succrose 10%	10g ad 100ml	Succrose PBS
Succrose 30%	30g ad 100ml	Succrose PBS
Elvax Preparation		according to the protocol in (Hermanns et al., 2001b;Hermanns, 2001)
Rotihistol (Roth, Karlsruhe)		
DPX (mounting fluid, Fluka)		

Triton-X 100, 0.4%		
FCS (Fetal Calf Serum)		
DMEM (Gibco)		
Hepes-Buffer		

## 2.2.2 Antibodies

### 2.2.2.1 Primary Antibodies

Tab. 2.2: Primary Antibodies applied in this study

Antibody	Class	Antigen	Localization of Antigen	Manufacture	Dilution	Demasking treatment
anti-Coll IV	rb IgG	Collagen type IV	BM and ECM	Progen	1:750	Citrat-Puffer. Protease
anti-Coll IV	gt IgG			Biodesign	1:500	Protease
anti-Pan Axonal Marker (PAM)	ms IgG	210 kd Neurofilament	Axons	Biotrend	1:100	--
anti-Pan Axonal Marker (PAM)	ms IgG			Affiniti	1:800	--
anti-Glial Fibrillary Acidic Protein (GFAP)	ms IgG	GFAP (astrocyte intermediate filament)	Astrocytes	Boehringer	1:40	--
anti-Glial Fibrillary Acidic Protein (GFAP)	ms IgG			Chemicon	1:350	--
anti-ED-1	ms IgG1	ED1 protein of the lysosomes	Phagocytizing cells (macrophages microglia)	Serotec	1:2000	--
anti-S100		S 100 calcium binding protein	Cytoplasmatic	Sigma	1:10000	Citrat-Puffer, Protease

anti-E-Green Fluorescent Protein (GFP) 11122	rb IgG	Green Fluorescent Protein (from Aequorea Victoria jellyfish)	Transduced Schwann cells	Molecular Probes	1:800	Triton 0,4%
---	--------	---	-----------------------------	---------------------	-------	-------------

### 2.2.2.2 Secondary Antibodies

Tab. 2.3: Secondary Antibodies applied in this study

Antibody	Class	Manufacture	Dilution
anti-mouse	hs IgG (biotinylated)	Vector Laboratories	1:150
anti-rabbit	gt IgG (biotinylated)	Vector Laboratories	1:150
anti-goat	hs IgG (biotinylated)	Vector Laboratories	1:150
Avidin-Alexa 488		MoBiTec	1:1000

### 2.2.2.3 Reagents and Tracers

Tab. 2.4: Reagents and Tracers applied in this study

Reagent/Tracer	Manufacture	Dilution
Avidin-Biotine-Peroxidase Complex (ABC-Elite Kit)	Vector	1:100
BDA (Biotinylated Dextrane Amine)	Molecular Probes	10%

## 2.3 Guidance Channel

### 2.3.1 Tube Material

The guidance channels used in this study were made of a Trimethylene carbonate-caprolactone copolymer (TMC-CL), produced using melt polymerization and freeze drying techniques, then  $\gamma$ -irradiated for sterilisation and provided by ITV Denkendorf (Lietz et al., 2005; Schlosshauer, 2003; Sinis et al., 2005). The first tube series, ME-008, was followed by ME-021 for irreproducibility of the first. Both presented an inner diameter of 1mm with an approximate wall thickness of 100  $\mu$ m. Micropores of 20.000kDa (around 20nm) integrated into the channel wall structure were big enough to provide nutrition and small enough to

prevent cellular infiltration. The application of similar material has already proven rather sufficient in PN regeneration (den Dunnen et al., 1996; Giardino et al., 1999).

### 2.3.2 Improvement of the Guidance Channel Filling Procedure

The day of implantation, MG, stored at  $-20^{\circ}\text{C}$ , was defrosted and warmed up to  $4^{\circ}\text{C}$  on dry ice for 2 hours. The Schwann cells (in case of MG/SC or AST group) were trypsinised and prepared for usage, dispersed into medium, to achieve a cell number of about  $1,56 \times 10^6/\text{ml}$ . Schwann cells and medium were mixed again shortly before mounting in a plastic pipette to be blended with the MG in a 2:1 (SC/Med:MG) dilution. The water inside the short tube pieces was dried on a filter. Now, the SC/MG mixture, again intermingled before usage, was introduced into the guidance channel. To optimise the filling technique several improvements were necessary.

#### A *In vitro*, lateral with a Hamilton syringe, refill *in vivo*, laterally, ME-008 tube

A several millimeter long tube was filled *in vitro* by injecting the MG/Med mixture laterally using a  $10\mu\text{l}$  Hamilton syringe. Guidance channel pieces of the needed length were prepared right before implantation. One tube end introduced into the lesion, a refill from the other, not yet implanted tube end, was performed to prevent MG/Med loss due to “drying” and handling. The second tube end was placed.

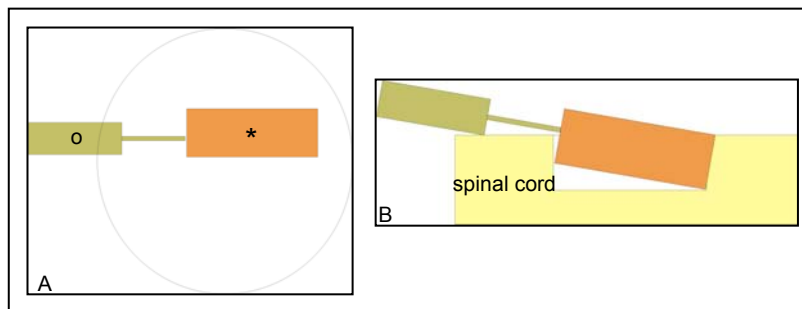


Fig. 2.2: First guidance channel filling technique. (A) The tube (star) was filled by injection using a Hamilton syringe (o). (B) Implantation of the guidance channel piece of needed length was performed one end first. Before introduction of the second tube end, a refill was performed.

#### B *In vitro* by capillary force, then 35-40 minutes at $37^{\circ}\text{C}$ , ME-021/PGA tube

The guidance channels, stored at  $4^{\circ}\text{C}$  in aqua bidest. and darkness were pre-cut into differently sized pieces (B). These pre-cut pieces were filled *in vitro* by placing a pipette just in front of one tube end (A). Filling was performed by capillary force. The filling could be verified macroscopically by the MG's pinkish colour filling the tube piece from end to end. Incubation at  $37^{\circ}\text{C}$  for 35-40 minutes before implantation (C) followed.

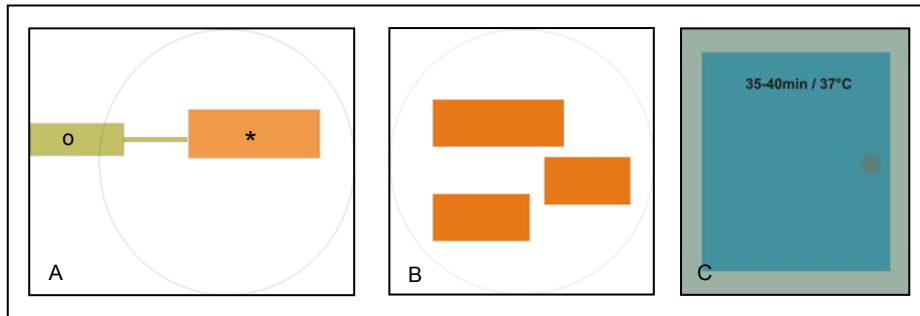


Fig. 2.3: Second guidance channel filling technique. (A) and (B) Pre-cut tube pieces (star) were filled by capillary force using a pipette (o). (C) Incubation of 35-40 min. at 37°C before implantation.

**C As B, then incubated in a humid chamber, 1-5h at 37°C and optimized OP-technique, ME-021/PGA tube**

Guidance channel pieces of 3mm, 4mm and >4mm (B) were prepared and immersed in medium 24 hours before usage. Tube filling was performed as described above in technique B (A). In addition, another drop of MG/Med mixture was placed on top of the just filled tube to prevent drying. The whole filling procedure took place in a humid chamber (B). This humid chamber was constructed of an agar plate, a humid piece of filter paper positioned inside and a small piece of parafilm® placed on top of the filter, right in the centre of the chamber. On top of the parafilm, the tube pieces were positioned and filled. Once all tube pieces filled, the cover of the chamber was replaced and the whole humid chamber was incubated at 37°C for at least one hour (C) before implanting the first tube.

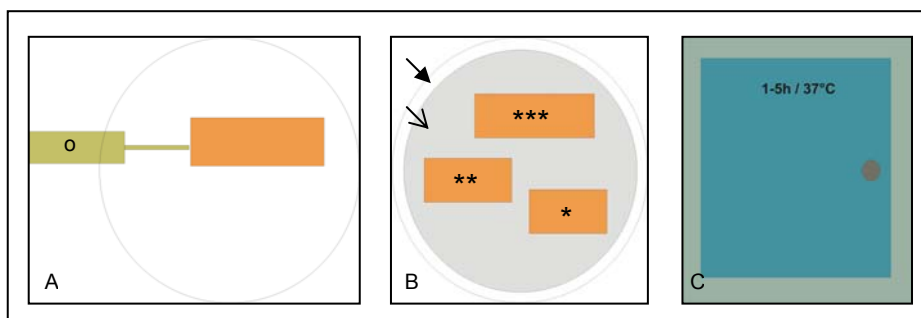


Fig. 2.4: Schematic demonstration of the final guidance-channel filling-technique. Pre-cut guidance channel pieces of different length (3mm \*, 4mm \*\*, >4mm \*\*\*) are filled by approaching the pipette (o) and using capillary force (A). The humid chamber is made up of the agar dish, a humid filter and a piece of parafilm® (B). Incubation for 1-5h at 37°C followed (C).

## 2.4 Experimental Settings

81 female adult Wistar rats (outbred) of 200-250g were sacrificed for the experiments. The animals were housed in accordance with the German Animal Protection Law, under specified pathogen-free conditions at a temperature of 21°C and a relative humidity of 50% +/- 5%. They received dry food pellets and soured, germ-free water (pH3) ad libitum.

The structure of the experimental setting demonstrates the continuous amelioration of the operating technique and the guidance channel filling-procedure, optimized in group III C, detailed in chapter 2.3.2 and 2.5.1. This group is made up of three different subgroups depending on the filling and treatment with AST at varying time points to visualise the scar, fibres and potential axonal regeneration.

### I Empty Tubes

Material	7d	--	1mo
ME-008 tube, empty	n=2	--	n=2

### II Pre-filled Tubes

Nerve guiding tubes were filled with MG/SC by the NMI, Reutlingen.

Material	4d	7d	14d
ME-008 tube, Lewis SC	n=2	n=2	n=2

### III Filled Tubes

#### A *in vitro*, lateral with a Hamilton syringe, refill *in vitro*, laterally, ME-008 tube

Material	--	14d	1mo
MG/SC (transduction efficacy 100% GFP)	--	n=3	n=3

**B *in vitro* by capillary force, then 35-40 minutes at 37°C, ME-021/PGA tube**

	Material	7d	14d	1mo
1	MG/Med	n=2	--	n=2
2	MG/SC GFP +/- TRIS injections	n=8	n=8	--
3	MG/SC/test BPY-DCA	n=4	--	--

**C as B, then incubation in a humid chamber, 1-5h at 37°C and optimized OP-technique, ME-021/PGA tube**

	Material	7d	14d	1mo	3mo	6mo
1	MG/Med	n=5	n=2	n=4	--	--
2	MG/SC GFP	n=4	n=4	n=4	n=4	n=1
3	AST	n=5	n=3	n=5	--	--

## 2.5 Surgery

### 2.5.1 Optimisation of the Surgery

The first experimental injury models applied revealed several problems. The guidance channel tended to move, to glide back out of the aspirated lesion (Fig. 2.5).

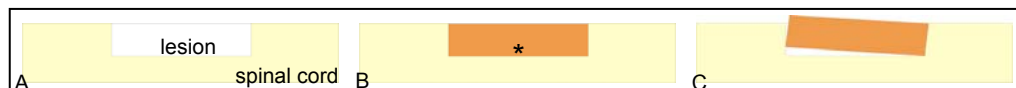


Fig. 2.5: Schematic view on the first operating protocol. (A) The aspiration lesion presents itself as a gap within in the spinal cord tissue. (B) Implanted guidance channel (star). (C) In histology, guidance channel movements were found as shown here.



For stabilisation of the tube within the lesion site, the implanted pieces were left a little longer than the lesion they were placed in. Host tissue stumps at both tube ends entered the tubes, thereby improving the positioning (Fig. 2.6). In histology, however, filling revealed less efficient in the centre of the tube than before.

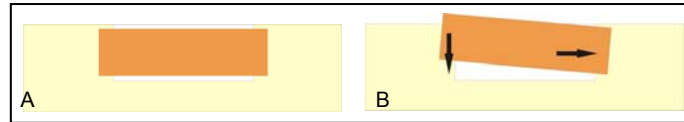


Fig. 2.6: Schema of an amelioration of the implantation protocol. (A) The implanted guidance channel is longer than the aspired lesion (Fig. 2.5 A). Host tissue stumps at both ends reach into the tube for stabilisation. (B) Introduction of this longer tube needed to be “one end first” before the other end could be integrated.

Another improvement of the operating protocol led to the final injury model. The implant has to exactly fit in the aspiration-lesion so that positioning is possible without any handling difficulty. To ensure the good placement, the dura is closed with 10/0 Ethilon – in contrast to the foregoing models. Lesion size is enlarged to propose a dura-opening longer than the aspiration site for AST injections (see below, 2.5.2)

## 2.5.2 Protocol of the Optimised Operating Technique

A dorsal cut was performed to open the skin on a thoracic level, the muscles were exposed and the tissue was prepared to have a good view on the spinal processes and vertebrae Th6-Th9. Spines and vertebral arches of Th7 and Th8 were removed using a Friedman-Pearsons micro-rongeur (FST 16020-14) to expose the dura over a distance of about 8-9mm (Fig. 2.8 A). Then, the dura was opened longitudinally in the midline for about 6mm using a dura-hook with the consequence that the spinal cord tissue prolapsed (Fig. 2.8 B). Now, two coronal cuts were made with microscissors, one proximal, the other one distal, each at a distance of about 1mm from the dura-opening to achieve a pre-cut region of about 3.5-5mm (Fig. 2.8 C). Subsequently, this pre-cut region was aspirated using a fine tipped Pasteur’s pipette connected to a vacuum pump (Titertek Vacuum Pump, Germany). A rectangular gap with a depth “at sight”, extending below the central canal and depending on the diameter of the nerve guiding tube to be implanted (see 4.1.3) - was attained (Fig. 2.8 D). Following this, the nerve guide was implanted by gently inserting it into the gap without pressure, squeezing or twincing it (Fig. 2.8 E). Ideally, the tube ends reach exactly the host tissue stumps.

The treated group (AST) received 6x0,2µl injections of BPY-DCA at each graft/host-tissue interface at a depth of 1mm, applied using a glass capillary. To assure a good view and easy access on the graft/host tissue interfaces and thereby facilitate the injections, the dura opening has to be larger than the tube length. This was followed by application of 4mg of the fibroblast proliferation inhibitor 8-Br-cAMP, inserted into the lesion site at each graft/host

interface using a small spatula. Third, each interface area was covered by a little square of BPY-DCA-loaded Elvax-copolymer sheet. Dura for all groups was sutured with 3-4 microsurgical nuds (Ethilon 10/0) followed by suture of muscles (inverted) and skin.

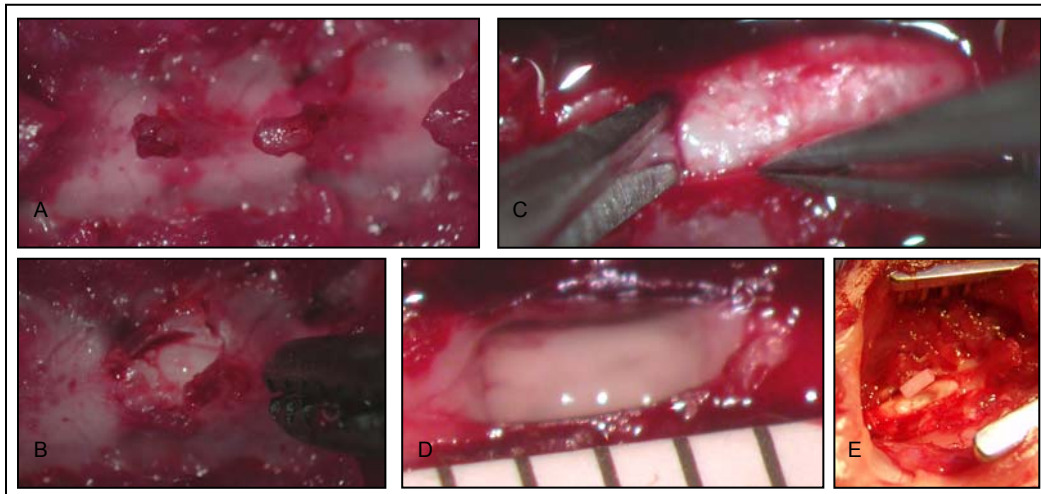


Fig. 2.7: Intra-operative pictures of the optimised operating technique. (A) View on the vertebral arches and spines, muscles tissue has been removed. (B) Opening of the vertebral arches using a FST micro-rongeur. (C) Microscissor pre-cuts of the rostral and caudal (not shown) limit for the aspiration lesion. (D) Rectangular gap following the spinal cord aspiration. (E) Implantation of the guidance channel.

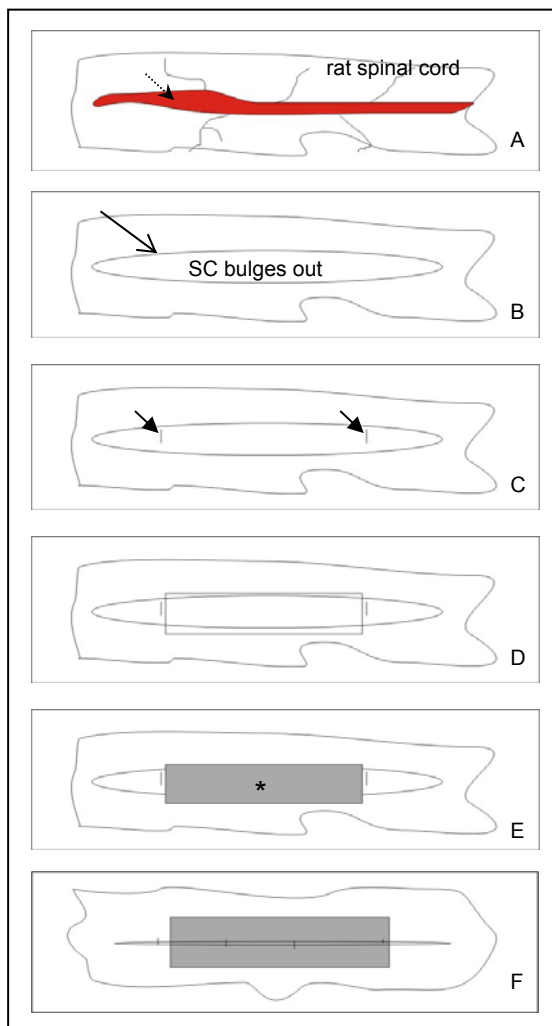


Fig. 2.8: Schema of the optimised operating technique. (A) Following Th7+Th8 laminectomy, the rat spinal cord is visible with a central artery rather in the spinal cord midline. (B) Longitudinal opening of the dura for 8-9mm length leads to a protrusion of the spinal cord through the aperture. (C) Microscissor pre-cuts of the spinal cord tissue to define the proximal and distal lesion borders. (D) Aspiration of the rectangular lesion producing a gap of about 3.5-5mm length with a variable depth depending on the tube dimensions. (E) Guidance channel implantation. (F) Re-closure of the dura with 3-4 nuds 10/0 Ethilon.

### 2.5.3 Post-Operative Care

Immediately after operation, the rats were returned into their cages. A subcutaneous injection of 5ml NaCl was administered to compensate for blood volume and electrolyte loss. For one week Baytril® antibiotic was injected or orally administered once a day, until spontaneous bladder function recovered. Bladder expression was performed twice a day until spontaneous recovery

### 2.5.4 Animal Sacrifice

The animals were deeply anesthetized with enflurane and chloralhydrate i.p.. The thorax and the left ventricle of the heart were opened. A canula connected to a perfusion pump (505S, Watson-Marlowe) was inserted into the left ventricle, advanced to be finally placed in the aorta and, there, fixed by clamp forceps. Subsequently, the right ventricle was opened. With a pump rate of 20ml/min, PBS (4°C) circulated in the rat's blood circulatory system for 2 minutes followed by another 15 minutes of perfusion with 4% PFA to fix the tissue.

## 2.6 Tracing

### 2.6.1 Stereotaxic Methods

In deep narcosis, the animal head was fixed in a Small Animal Adaptor (David Kopf Instruments) at both external acoustical meatus and the front teeth. The coordinates for injection into layer V of the sensomotoric cortex and marking of the corticospinal cellular bodies were determined with the aid of Paxinos and Watson (1982) Stereotaxic Atlas of the Rat Brain and have been established by Susanne Hermanns in modification of a lab protocol of Dr. Ray Grill, University of Texas, Houston, TX (Hermanns, 2001).

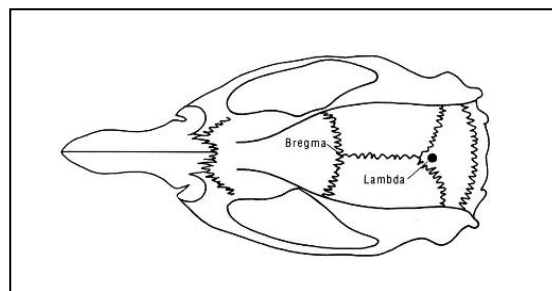


Fig. 2.9: Rat skull showing Bregma, Lambda and the cranial fissures between the skull bones important for orientation in tracing.

Tab. 2.5: Coordinates for BDA injections into layer V of the somatosensory cortex in regard to Bregma. A/P anterior/posterior, L lateral

<b>Bregma A/P</b>	<b>L left</b>	<b>L left</b>	<b>L right</b>	<b>L right</b>
-0,08	+0,20		-0,20	
-0,13	+0,22		-0,22	
-0,18	+0,24	+0,29	-0,24	-0,29
-0,23	+0,24	+0,29	-0,24	-0,29
-0,28	+0,24		-0,24	
-0,33	+0,24		-0,24	

### 2.6.2 Injection of BDA into Layer V of the Somatosensory Cortex

After an initial narcosis with enflurane, the animals were injected with chloralhydrate i.p. to achieve a deep anaesthesia. The skull was shaved under precaution not to cut the whiskers and locked into the stereotaxic device. Now, the cranium was exposed, the periosteum removed. Both cranial regions to be opened were marked and two little „windows“ along the sagittal and coronal suture were cut with a dental drill to expose the brain. Bregma was determined according to Fig. 2.9. Coordinates for injection were measured with regard to Bregma. BDA was then injected into the corticospinal pyramidal cell bodies in layer V of the somatosensory cortex at 8 spots per hemisphere. For injection, a glass capillary (40-60 µm diameter) had been fixed with sealing wax onto a Hamilton microliter-syringe (10 µl). The Hamilton-Syringe was filled with paraffin oil to prevent the occurrence of dead volume, then emptied a little and refilled with BDA. After adjusting the right coordinates, 0.2 µl BDA were pressure-injected at each target spot.

### 2.6.3 Anterograde Th 11 BDA Tracing of the Dorsal Column

After narcosis (see above) and a dorsal shave at Th11, the vertebral body Th11 was exposed (see 2.5.2), the distal portion was removed using a Friedman-Pearsons micro-rongeur (FST 16020-14). The dura was opened by a dura-hook. A sagittal cut of the spinal cord was performed using microscissors. Into this aperture, a small piece of gelfoam soaked with BDA was integrated. Then, a suture of muscles, subcutaneous fat and skin was carried out.

## 2.7 Tissue Processing

### 2.7.1 Paraffin Sections

#### *Processing for Paraffin Sections*

Immediately after perfusion (see 2.5.4), the Th4 - Th11 part of the spinal column was removed and post-fixed ON/4°C in the same fixative (4% PFA). The next day, the grafted area including several millimeters proximally and distally (A schematic, B *in vivo*) was dissected by fine bone scissors (FST 16109-14) and transferred into PBS ON/4°C.

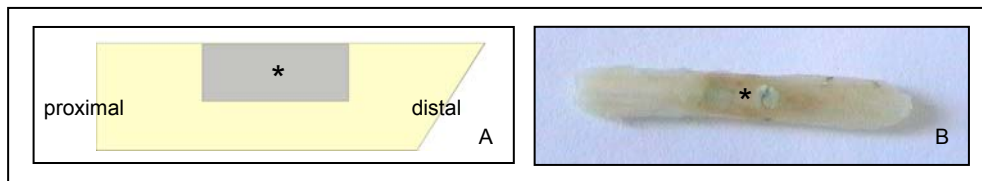


Fig. 2.10: Schematic (A) and *in vivo* (B) view of the dissected spinal cord segment around the grafted area (\*). Proximal ends of the segments always oriented to the left, distal side inclined. Schema lateral view, *in vivo* dorsal view.

#### *Paraffin-Embedding*

The tissue was dehydrated in an ascending ethanol line: 70% (30 min), 90% (60 min), 2 x 100% (60 min each) and in Methyl-benzoate ON/4°C. After an incubation in benzene for 15 minutes, the specimen were incubated in a benzene/paraffin mixture (1:10 v/v) for 30 minutes/57°C followed by three more incubations in freshly changed pure paraffin (1h/57°C each) with the final incubation ON/57°C. The next day, the specimen were embedded using fluid paraffin and a caoutchouc mould and formed into squares.

#### *Paraffin Sections*

The specimen in paraffin blocks were cut parasagittally on a paraffin-microtome (RM 2035, Jung) at 10µm thickness per section. To mount the sections on SuperFrost® Plus slides, the paraffin-specimen sections were collected in a 47°C water-tub. Finally, they were baked at 57°C in an oven.

## 2.7.2 Freezing-Microtome Sections

### *Processing for Freezing-Microtome Sections*

The tissue preparation was carried out as mentioned above. Two to three days before sectioning, the specimen were transferred from PBS into 10% Sucrose/4°C for one day followed by another day (or more, until tissue completely sunken in the Falcon tube) of incubation in 30% Succrose/4°C.

### *Freezing-Microtome Sections*

The areas distal to the lesion were cut on a freezing-microtome (Frigomobil) at 50 µm to better visualise the potentially regenerated fibres. The specimen were freeze-mounted sagittally onto the microtome using 30% Succrose.

## 2.8 Staining Protocols

### 2.8.1 Histological Stainings

#### ***Nissl***

- Deparaffinization (ROTI Histol 3x 10', EtOH 100% 3x 5', 90% 5', 70% 5', 50% 5')
- PBS 5'
- 5-7'/60°C Nissl-solution
- dip 3x in each: Aqua dest, ascending EtOH line (50%, 70%, 90%, 2x 100%), ROTI Histol 2x
- mount with DPX

#### ***Haemalaun-Eosin (HE)***

- Deparaffinization as before until 100% 2x, then 96% 1', 70% 1'
- Aqua dest. 3'
- Nucleus-staining: Mayer's hemalum solution 1'
- rinse in cold water for some seconds
- Differentiation in HCl-EtOH 1''
- "Blue-ing" under cold water 1'
- 0.1% liquid Eosin y (yellowish) with 1 drop acetic acid (glacial)
- ascending EtOH line (beginning at 70% - 96%...) each 1'
- ROTI Histol 2x 5'
- mount with DPX

### **van Gieson**

- Deparaffinization as in HE-staining
- Resorcinfuchsin-staining (Weigert) 15'
- rinse in cold water for 10'
- Weigert iron hematoxylin 2'
- "Darkening" under cold water 1'
- Aqua dest. 1'
- Pikrofuchsin (van Gieson) 1'
- Aqua dest. 1'
- ascending EtOH line and ROTI Histol as in HE
- mount with DPX

### **Resorcin-Pikrofuchsin** (modified Trichrom-Staining von Gieson → "bichrome")

- Deparaffinization as in HE
- Resorcinfuchsin (Weigert) 15'
- rinse under cold water 10'
- Aqua dest. 1'
- Pikrofuchsin (van Gieson) 1'
- Aqua dest. 1'
- ascending EtOH line and ROTI Histol as in HE
- mount with DPX

## 2.8.2 Immunohistochemical Stainings

### 2.8.2.1 Paraffin Sections

#### **Deparaffinisation**

ROTI Histol 3x 10', EtOH 100% 3x 5',  
inactivation of endogenous proteases: MetOH/H<sub>2</sub>O<sub>2</sub> 10',  
continuation of the EtOH line 90% 5', 70% 5', 50% 5',  
PBS 2x 5'

#### **Antigen-Demasking**

Protease XXIV in Tris 8'/37°C  
PBS 2x 5'

#### **Blocking (Pre-incubation)**

Normal Serum 3% 15'/RT

#### **Primary Antibody**

ON/4°C, dilution depends on AB  
PBS 2x 5'

#### **Secondary Antibody**

45'/RT  
PBS 2x 5'

#### **Detection**

ABC 45'/RT  
PBS 5'  
0.1M PB 5'

DAB reaction 1', then + 0.01% H<sub>2</sub>O<sub>2</sub> (incubation time depending on AB)  
Aqua dest. 5x change

#### **Dehydration**

EtOH 50%, 70%, 90%, 100% 2x 5', ROTI Histol 2x 10'

#### **Embedding**

DPX

Fig. 2.11: General protocol of Immunohistological Stainings on paraffin sections. Depending on the antibody applied, modifications of the above mentioned protocol are necessary (see below).



### ***Collagen IV***

The protocol in Fig. 2.11 was followed exactly for the finally used Collagen IV antibody (Bioscience). Only for the first Collagen IV antibody applied (Progen), a second antigen-demasking procedure was added: Right after the deparaffinisation and 2x PBS, the slices were placed in 200ml Citrate-buffer, pH 4,5, and incubated in a microwave for 8' at 600 watt. Before continuation of the general protocol, a 30' period of cooling down at room temperature and 2x 5' PBS were practiced. For the first used Collagen IV antibody (Progen), the secondary antibody was a goat anti-rabbit antibody (Vector Laboratories), a horse anti-goat antibody (Vector Laboratories) for the newly utilized Collagen IV (Bioscience). DAB/H<sub>2</sub>O<sub>2</sub> incubation time of 6' for the first Coll IV (Progen), 5' for the second Coll IV (Bioscience).

### ***PAM***

The PAM antibody (Pan-axonal marker) was applied according to the protocol above with two alterations: No Protease-demasking procedure. As secondary antibody, a horse anti-mouse antibody (Vector Laboratories) was utilized. DAB/H<sub>2</sub>O<sub>2</sub> incubation time of 5'.

### ***GFAP***

As for the PAM staining, the protocol above was minimally altered. No Protease-demasking procedure. As secondary antibody: horse anti-mouse (Vector Laboratories). DAB/H<sub>2</sub>O<sub>2</sub> incubation time of 6' for the first utilized GFAP antibody (Boehringer), 5' for the finally used antibody (Chemicon):

### ***ABC***

For this staining, the above protocol was abridged. Deparaffinisation and antigen-demasking were directly followed by incubation with ABC 1:100 ON/4°C without blocking nor primary or secondary antibody application. The next day, the detection was continued at the step of PBS with an incubation time in DAB/H<sub>2</sub>O<sub>2</sub> of 8' and the protocol was followed.

### ***GFP/DAPI***

The above protocol was again slightly altered for this eGFP staining (finally utilized: MP 11122, 1:1000). After deparaffinisation as above, another demasking procedure was applied: incubation in a 0,4% Triton solution for 10' followed by several steps of washing the sections in PBS. DAB/H<sub>2</sub>O<sub>2</sub> incubation time of 5-6'. After washing as described above, an incubation of 1' with DAPI 1:10 was practiced, the sections were rinsed again. Once dried, sections were cover-slipped with Vectashield to better preserve the DAPI fluorescence.

## 2.8.2.2 Fluorescent Staining of BDA-traced Fibres in Freezing-Microtome Sections

### *Avi-Alexa 488*

To ensure diffusion of the staining substance through the complete tissue of 50  $\mu\text{m}$ , a free-floating staining technique using 12-whole-microtiterplates on a shaker was chosen. First, the sections were washed in PBS (3x briefly, 4x 10'), followed by an ON incubation with Avidin-Alexa 488 (1:1000) at 4°C. The next day, the sections were washed as described above before mounting with gelatine. Once dried, the sections are cover-slipped with Vectashield and stored at  $-20^{\circ}\text{C}$ .

## 2.9 Analysis and Documentation

All sections were analysed using an Axioskop microscope (Zeiss) and a Nikon eclipse TE 200 fluorescent microscope with filters for green and red fluorescence. All pictures shown in this work with one exception were taken with an AxioCam MRc camera on an Olympus BH-2 microscope, Axiovision software Version 3.1. The pictures of the eGFP/DAPI stainings were shot with a Nikon FDX-35 camera. For assessment of lesion dimensions (see 3.3.1), an ocular with a framework has been used. Different measures can be taken. The primary lesion is defined as length A in Fig. 2.12 being composed of guidance channel length and a small margin around. B and C in Fig. 2.12 define the possible extent of inbleedings enlarging the primary lesion proximal and distal, respectively, to the implantation site (see 3.3.1.2).

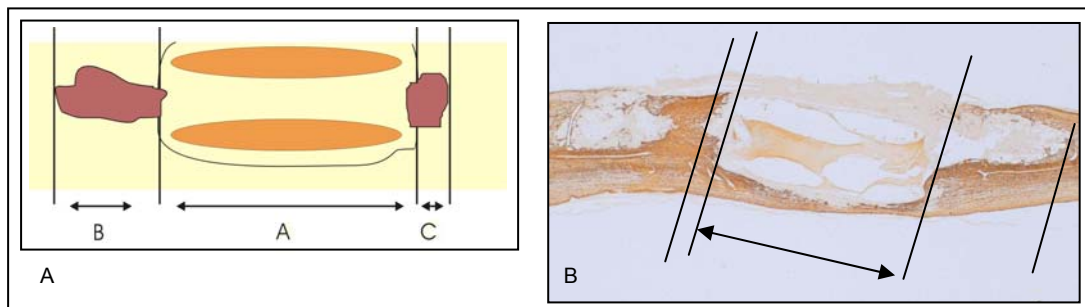


Fig. 2.12: Measurement of the lesion size. (A) Schematic description of the measures taken to describe the lesion's dimensions. (B) *In vivo* example (N486-82) regarding the measures described in the scheme A. The double-sided flash indicates the guidance channel length A.

## **3.0 Results**

### **3.1 Improvement of the Experimental Setting**

#### **3.1.1 Improvement of the Guidance Channel Filling Procedure**

Method A (Fig. 2.2) revealed itself as being irreproducible, the number of introduced Schwann cells cannot even be guessed on. The lateral *in vivo* refill was necessary since the filled tube seemed to “dry out”, the tube being less filled within ten minutes. Furthermore, the “one-side-first” tube implantation technique going hand in hand with this filling proves to be prone to channel dislocation (see 2.3.2 and 3.1.3.1) and handling difficulties as tube squeezing. In Filling method B (Fig. 2.3), the “drying” of the MG filling was reduced but still prevalent in some tube pieces. Filling of a pool of differently sized prepared tube pieces *in vitro* excluded loss of filling due to tube cutting and prevented tube end squeezing. In combination with the not yet optimised operating technique, however, handling difficulties led to channel compression while implantation. In consequence, filling technique as well as surgery were again improved (see 2.3.2 and 2.5.2). Guidance channel filling is rather reproducible with method C. No reduction in filling could be observed in any tube piece at the time of implantation.

#### **3.1.2 Optimisation of the Surgery**

In the first model, the guidance channel tended to move and glide out of the aspired lesion (see Fig. 2.5, Fig. 3.1 and Fig. 3.2). For stabilisation of the tube within the lesion site, the implanted pieces were left a little longer than the lesion they were placed in. Host tissue stumps at both tube ends entered the tubes, thereby improving the positioning (Fig. 2.6). In histology, however, filling seemed to be less efficient in the centre of the tube than before (data not shown). Another improvement of the operating protocol led to the final injury model (Fig. 2.7, Fig. 2.8). The implant has to exactly fit in the aspiration-lesion so that positioning is possible without any handling difficulty. To ensure the good placement, the dura is closed with 10/0 Ethilon – in contrast to the foregoing models. Lesion size is enlarged to propose a dura-opening longer than the aspiration site for AST injections (see 2.5.2).

### 3.1.3 Histological Phenomena observed in Nissl Stainings

Regarding the Nissl overviews of all animals, several observations are made some of which can be regrouped.

#### 3.1.3.1 Guidance Channel Placement

To verify whether the guidance channel has been well implanted quite in the middle of the spinal cord tissue, the course of the central canal can be followed (Fig. 3.1). Central canal in front of a luminal section standing for good placement (A), its facing against a closed tube end (B), a wall (C) or even its course below the implant (D) reveals less good positioning. Another important factor in tube placement is the channel integration into the host tissue (Fig. 3.2). The guidance channel's complete implantation into the host tissue (A) and deviations of incomplete integration as visible in various forms of the tube "sticking out" of the spinal cord tissue (B) can be described. Examples of such „sticking out“ mostly are combined with inclined positioning. This can take obvious dimensions (C) as well as it can seem rather well placed (D), the central canal's facing the tube wall at one end being an index for real functionality (see Fig. 3.1). Comparing animals of different groups, a net amelioration in positioning can be stated. Through the various animals operated according to the early protocols (n=32), thirteen animals presented rather important inclinations of the guidance channel as pictured in Fig. 3.2 B and C. In six cases, an obvious incomplete integration was found. The course of the CC in twelve animals revealed important discrepancies to the tube openings – not counted lateral deviations as Fig. 3.1 B. In the optimised groups IIIC 1-3 (n=40), only 4 guidance channels in a slightly inclined position were found. Two tubes appeared incompletely integrated. Twelve animals, however, showed a course of the CC as described in Fig. 3.1 C or D, among these, all four three months animals.

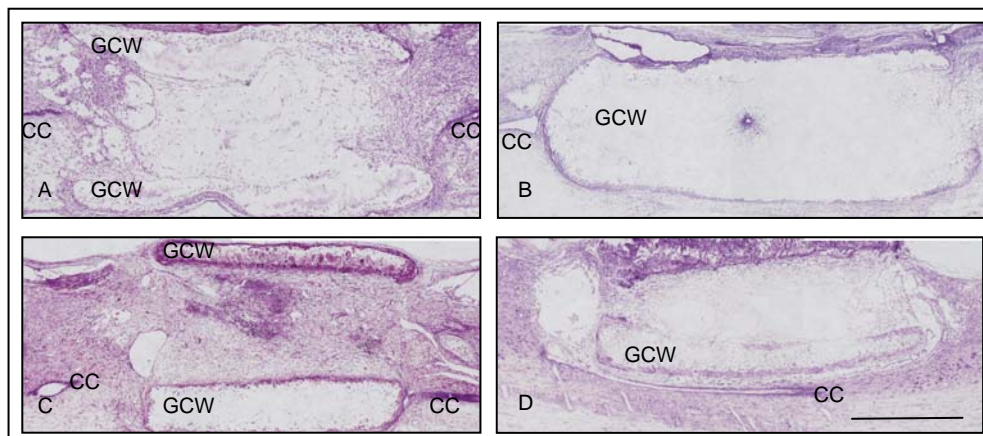


Fig. 3.1: The course of the central canal (CC) in regard to the implanted guidance channel wall (GCW) gives an idea of tube positioning. (A) Proximal and distal good placement (B) Proximal CC facing the already closed tube end, distal CC okay (C) Proximal CC probably okay, distal CC facing the tube wall (D) CC's course below the guidance channel. Scale bar: 1mm.

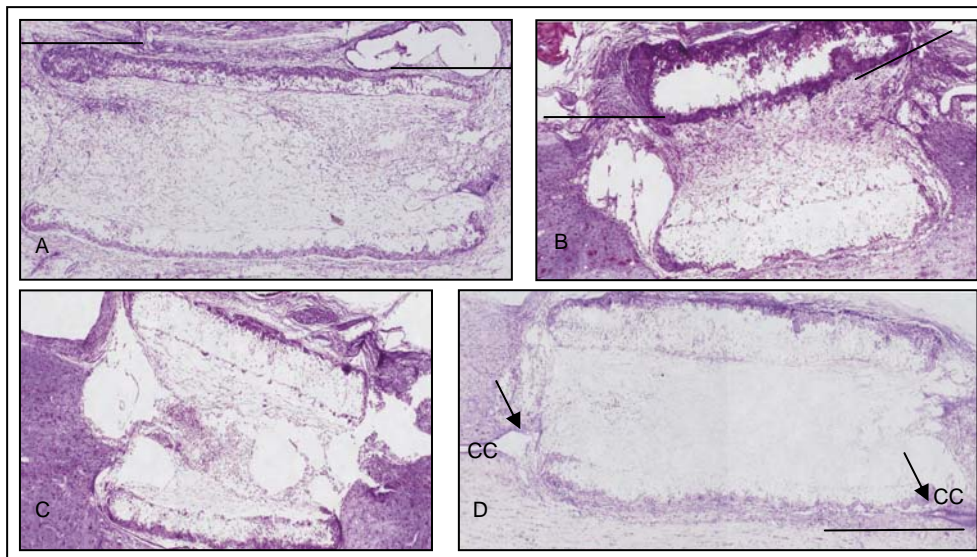


Fig. 3.2: Guidance channel integration into the host tissue. (A) Complete integration into the spinal cord tissue. (B) Incomplete integration of the guidance channel into the host tissue at the dorsal tube wall. (C) Combination of an inclined tube position with incomplete integration at the rostral end. (D) The guidance channel might seem well placed but regarding the course of the central canal (CC) indicated by arrows a slight inclination is visible. Rostrally, the tube is well placed whereas caudally, the course of the CC is ventral to the channel. Scale bar: 1mm.

### 3.1.3.2 Guidance Channel Stability

Both tube ends open, walls straight without any kinking or compression, an implanted guidance channel seems well in form (Fig. 3.3 D). Alterations of this „ideal“ tube image appearing squeezed at the channel ends (Fig. 3.3 A-C) or in the middle (Fig. 3.3 E) are found, potentially leading to a closure of the concerned tube end. Similar kinking can also be seen at later time points (Fig. 3.3 F). At this stage, heavy cellular infiltration of the tube walls also is visible. No obvious differences are found examining the various animal groups.

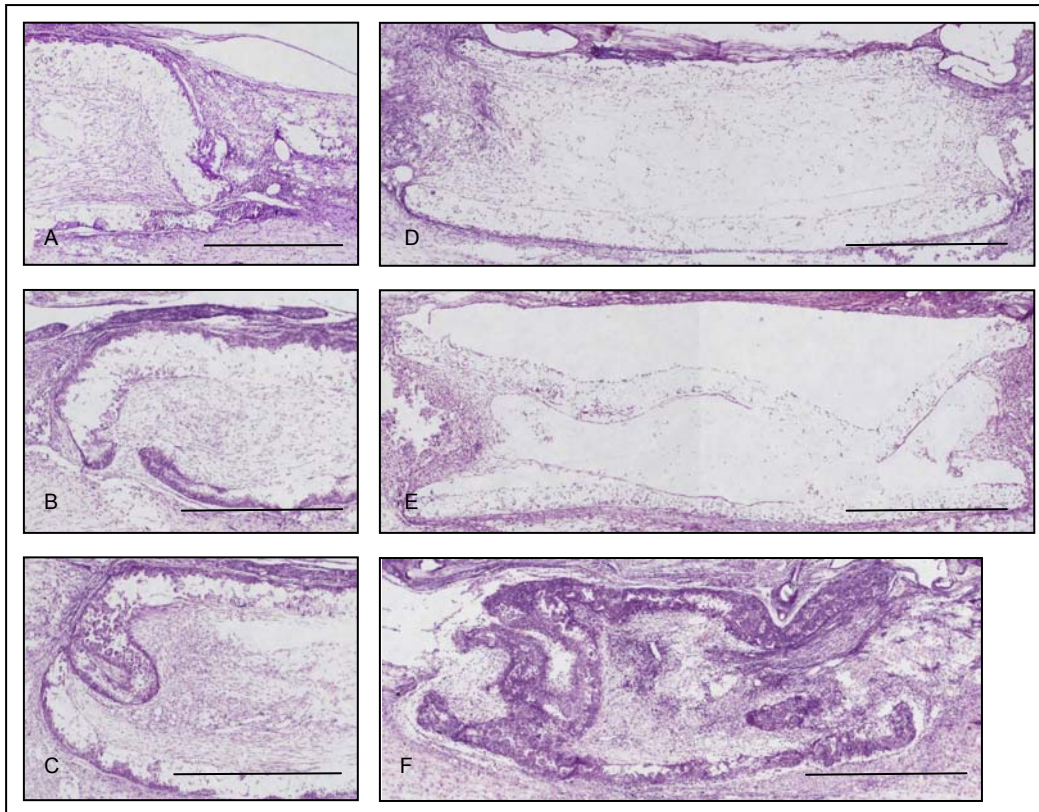


Fig. 3.3: Nissl stainings give an overview over guidance channel form and thus stability. (D) Example of good form stability (7d). In (A) – (C) bend down tube ends are shown with the consequence of a closure of the concerned guidance channel end. (A) 7d (B) 14d (C) 14d (E) The guidance channel is deformed, seems squeezed in the middle, both ends remain open (7d). (F) Heavy tube deformation is shown in a 1mo animal. Cellular infiltration of the GCW is visible. Scale bars: 1mm.

### 3.1.3.3 Tissue Bridge

The guidance channel entering host tissue stumps have to be distinguished from the tube filling of MG/Med or MG/SC in medium (Fig. 3.4 A). Heavy dorsally located tube filling over the entire guidance channel length can be seen in one of two group I (empty) one month animals. Cells are longitudinally oriented (Fig. 3.4 B,C). Nissl stainings of some animals throughout this study present the aspect of the filling having shrunk within the tube lumen (Fig. 3.4 D). The tissue bridge appears detached from the guidance channel walls leaving a margin visible in between (flashes). No differences are stated between the former and the optimised protocols. Decision whether a tissue bridge throughout the entire guidance channel has formed presents difficulties. Occurring bleedings (see below 3.1.3.5) disturb the tissue bridge at the tube openings or within the lumen. Even in cases where a complete tissue bridge seems to exist, classifications might pose some difficulties. Fig. 3.4 D exemplifies such a - in this case shrunken-looking - bridge. Often, luminal sections of filled tubes present a rarefied matrix in the middle of the lumen. In some cases, both spinal cord stumps are visible, the lumen seems empty, other sections show the tube wall's side wall.

For classification as tissue bridge positive, the tube centre was examined for blood vessels. In case of blood vessel presence, a tissue bridge was accorded. Sections showing wall-like structures in the lumen centre without any blood vessels visible were classified as “no central tissue bridge”. Another positive factor for tissue bridge presence even in case of indistinguishable vessels was accorded if a certain bridge “evolution” was observable throughout the sections of one animal: bridge disruption in the tube centre, an empty margin around the filling succeeded by GCW structures (data not shown). In general, a more continuous filling is found at later time points. The optimisation of the guidance channel filling and the surgery show effectiveness. More animals presenting complete tissue bridges are found than in the former groups.

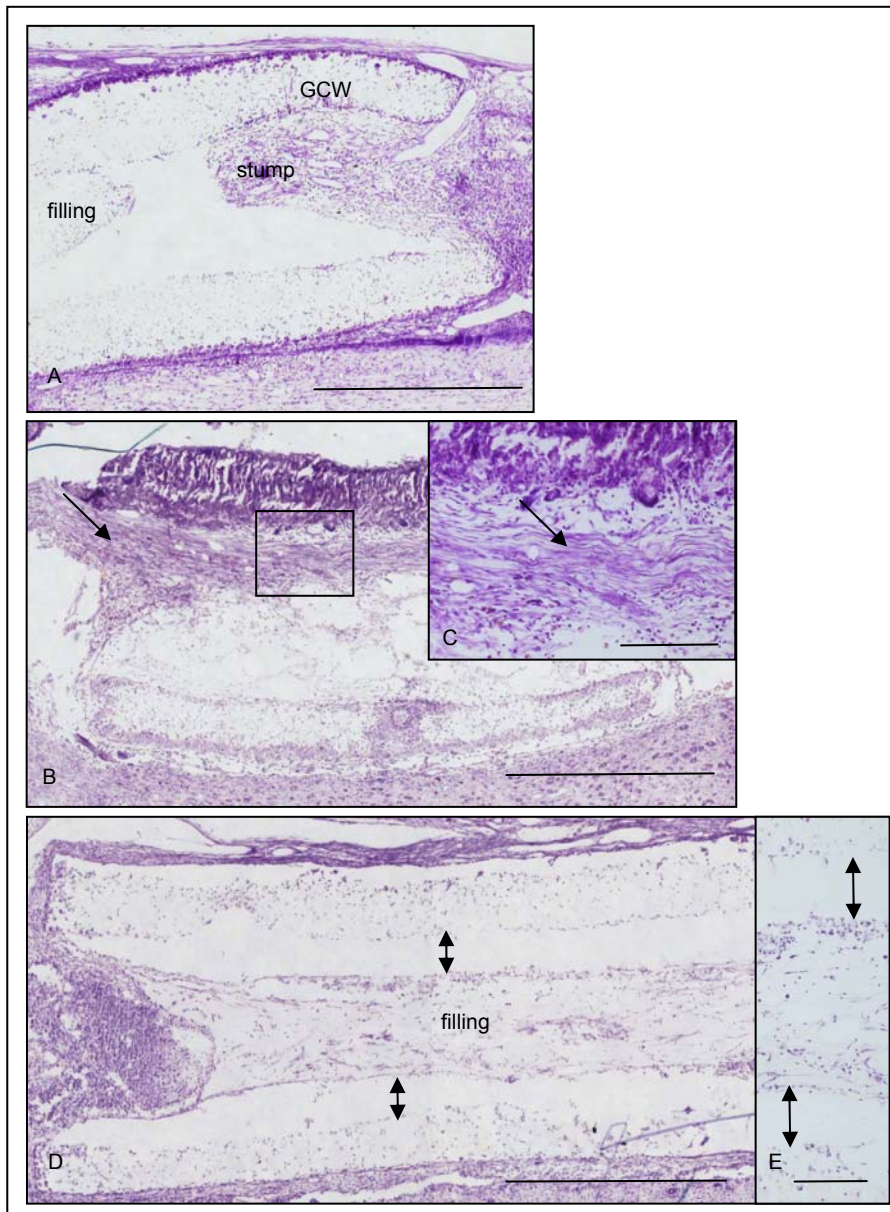


Fig. 3.4: (A) Differentiation of host tissue stumps from guidance channel filling. (B) and (C) Observed guidance channel filling at 1month in a formerly empty tube. Arrows indicate dorsal location of the numerous cells found within the tube lumen. (B) Overview of the guidance channel lumen. (C) Close-up of distally located cells. (D) and (E) Shrinkage of the guidance channel filling. The filling is detached from both guidance channel walls leaving a margin in between as indicated by double-pointing arrows. Scale bars: A,B,D: 1mm. C,E: 200  $\mu$ m.

### 3.1.3.4 Guidance Channel Wall Presence

Entire tube walls or segments of the wall structure seem “dissolved” in several animals throughout the whole study (Fig. 3.5). No evident differences can be stated in between the various animal groups.

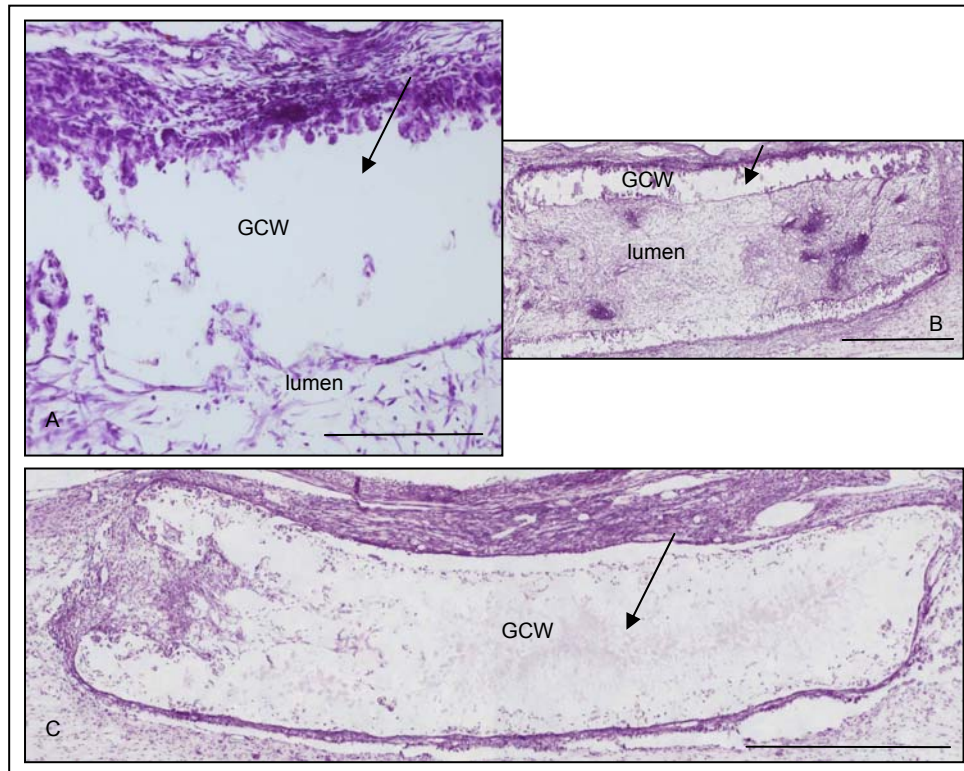


Fig. 3.5: “Dissolution” of the GCW as observed in Nissl stainings. (A) The GCW does not seem to have any matrix at locations as indicated by the arrow. Scale bar: 200  $\mu$ m. In (B) this effect is present over the length of the dorsal GCW. Scale bar: 1mm. (C) Bizarre purple Nissl background staining found where usually a matrix of the GCW is found. Scale bar: 1mm.

### 3.1.3.5 Bleeding Sites

Bleeding sites can be found at different locations (Fig. 3.6). Sites within the tube lumen (A), proximal (B) or distal (C) to the guidance channel ends are demonstrated as being the most current examples. The optimisation of the operating protocol does not seem to diminish neither the occurrence as such nor the dimensions of inbleeding. One might have the impression that the AST group more often shows slightly more important sites of inbleeding. This cannot be proven, though.



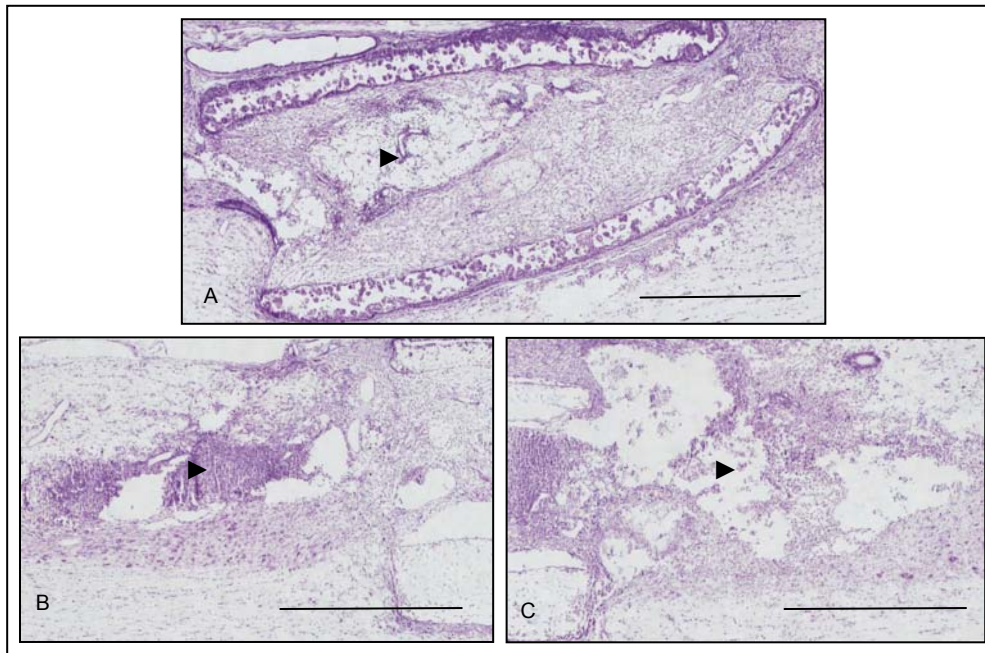


Fig. 3.6: Main location of bleeding sites indicated by arrowheads in this injury model. (A) Inbleeding within the guidance channel lumen. Bleeding site rostral (B) and caudal (C) to the implanted tube. Scale bars: 1mm.

### 3.1.3.6 Cyst-like Structures

Examples of cyst-like structures can be observed at various locations (Fig. 3.8) comparable to the sites of inbleeding (see 3.1.3.5 above). To decide whether real cysts are present, a staining with a Collagen IV antibody would be helpful (see 3.6.3.2 Fig. 3.38). Cysts have a Collagen IV positive rim by definition. Comparing the various animal groups, no obvious differences are found. In the course of time, more cyst-like structures are found at one month than at an early 7d time point. Not to confound with a site of inbleeding or a cyst formation is the in some cases observable dilatation of the central canal in front of an implant (Fig. 3.7).

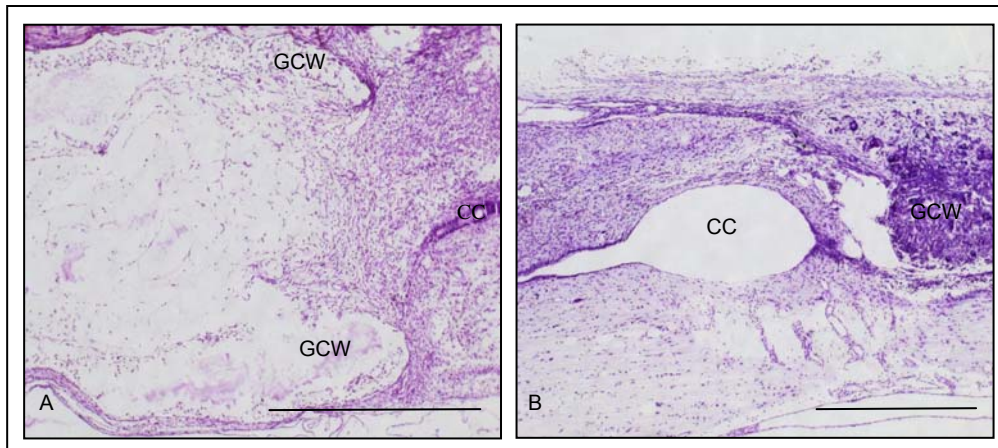


Fig. 3.7: Illustration of cyst-like central canal (CC) dilatation close to the guidance channel implant (GCW). (A) Central canal without dilatation facing the distal site of implantation. Scale bar: 1mm. (B) Cyst-like aspect of the central canal in front of the implant. Scale bar: 200  $\mu$ m.

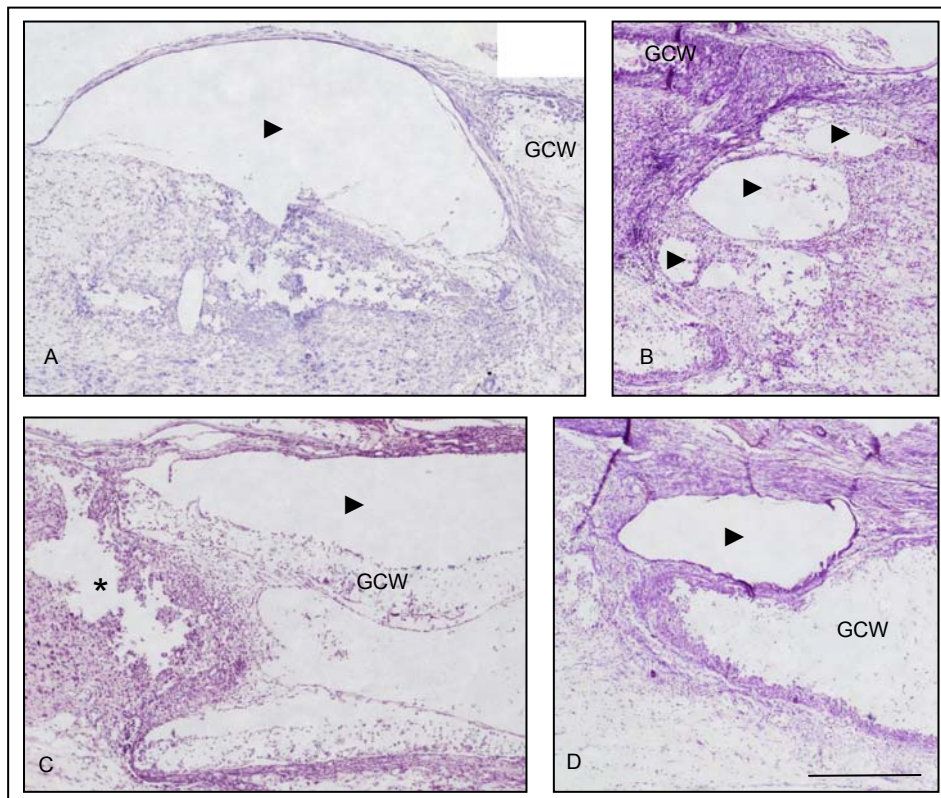


Fig. 3.8: Examples of cyst-like structures found in Nissl stainings as indicated by arrowheads. (A) Enormous cyst proximal to a guidance channel opening. (B) Cyst-like structures at the distal tube opening. (C) Cyst-like structure on top of the dorsal GCW. The wall seems squeezed. Indicated by a star at the proximal tube end an example of tissue tearing (see below, 3.1.3.7). (D) Cyst at a proximo-dorsal location of a guidance channel. The tube end is still closed in this far lateral section. Scale bar: 500  $\mu$ m

### 3.1.3.7 Tearing apart of Tissue

Potentially torn tissue is found in several animals (Fig. 3.9 A), mainly in proximity to bleeding sites. Differentiation of bleeding, cysts and ripped tissue is rather delicate. An example of cyst-like structures showing some remaining cell debris or other tissue in the centre is given in Fig. 3.9 B, suggesting a possible bleeding site. Another section in 200 $\mu$ m proximity demonstrates rather ripped-looking tissue (Fig. 3.9 C). In cases of torn tissue, no tissue loss is found.

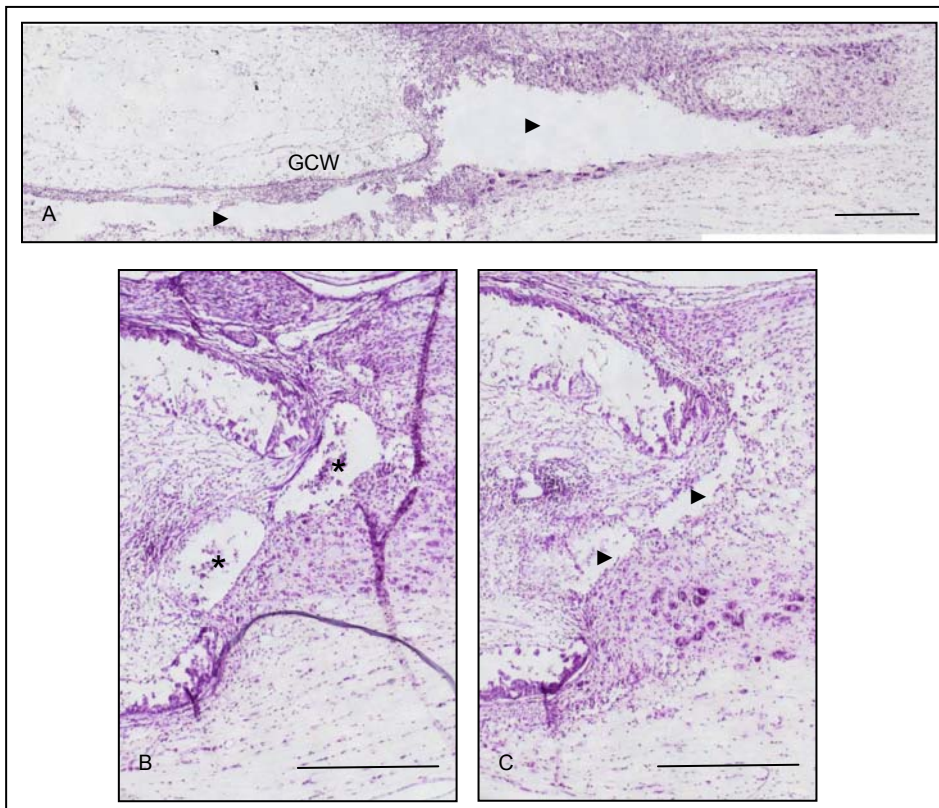


Fig. 3.9: Differentiation of cyst-like structures (stars) from tissue torn apart (arrowheads). (A) An example of torn tissue. (B,C) Comparison of cyst-like structures in (B) with torn tissue in (C) in sections of 200 $\mu$ m distance. Scale bars: 500  $\mu$ m.

## 3.2 Material Properties of the Implant ME-021/PEG

### 3.2.1 Tube Degradation

The tube material degenerates with time. Exact time point definition, though, is not possible. For estimation of the temporal progression of the tube degeneration, Nissl stainings in 59 animals were evaluated (Tab. 3.1). Three different aspects of tube degeneration were found: 1. Quota of luminal sections, 2. Tube deformation and 3. Cellular infiltration of the tube walls.

Tab. 3.1: Number of evaluated animals for estimation of a tube degeneration in regard to animal group (see experimental setting 2.4) and time point.

	7d	14d	1Mo	3Mo	6Mo	in total
IIIB1	2	-	-	-	-	2
IIIB2	8	8	-	-	-	16
IIIC1	5	2	4	-	-	11
IIIC2	4	4	4	4	1	17
IIIC3	5	3	5	-	-	13
<b>in total</b>	<b>24</b>	<b>17</b>	<b>13</b>	<b>4</b>	<b>1</b>	<b>59</b>

#### 3.2.1.1 Quota of Luminal Sections

Sections showing the lumen of implanted guidance channels were counted for each animal and taken as an indicator for well-preserved tubes. Results are shown in Fig. 3.10. It can be noted that the number of sections showing the tube lumen is decreasing comparing 7d and 3 months animals, giving a hint for a temporal degeneration of the guidance channels.

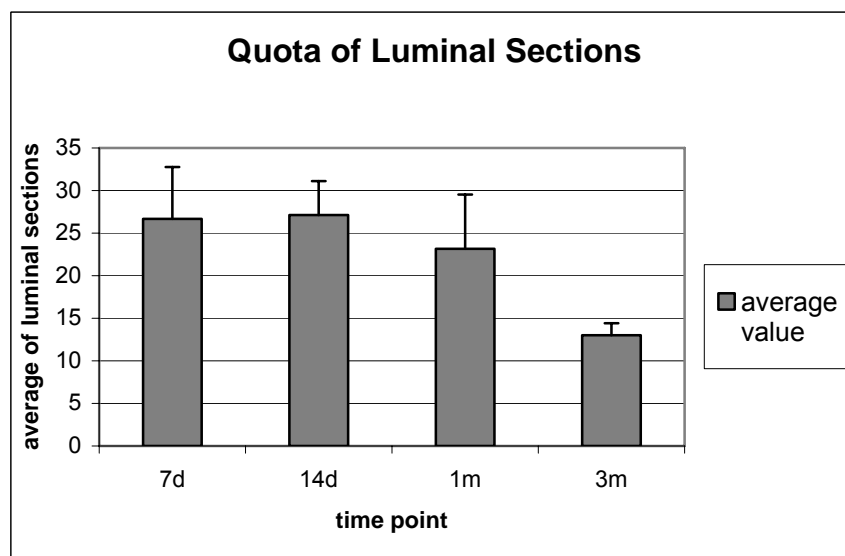


Fig. 3.10: Comparison of the number of luminal sections at different time points from 7d to 3 months. The bars represent mean group values +/- standard deviation.

### 3.2.1.2 Tube Deformation

Another marker for tube degeneration could be the observable deformation of the tube over time (Fig. 3.11). At 7d (A) and 14d (B) time points, almost all guidance channels seem fully in place and “intact”. Deformation of the tube walls can be suspected at one month (C) and clearly be illustrated at three (D) and six months (E).

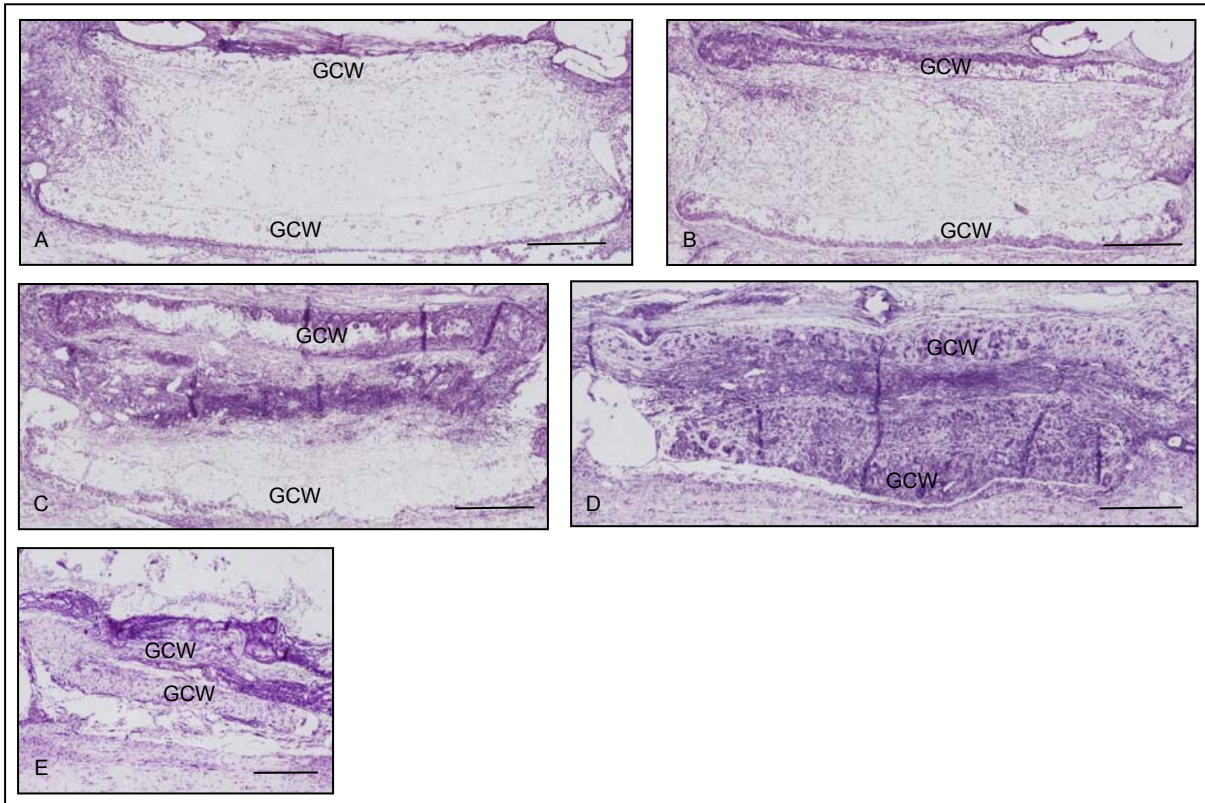


Fig. 3.11: Examples of observable guidance channel deformation at different time points. (A) 7d (B) 14d (C) 1mo (D) 3mo (E) 6mo. Scale bars: 500  $\mu$ m.

### 3.2.1.3 Cellular Infiltration of the Tube Wall

Once the guidance channels are implanted, the tube walls become infiltrated by unknown cells (see 3.5). This infiltration can be described in different ways – quantity (see Fig. 3.13, classified into four groups) and development over time (not shown). It can be stated that cellular invasion seems to correlate with the evolution of time (see Fig. 3.12) - the longer the implantation time, the more cells are invading the tube walls. At early time points (7d), the dorsal wall is becoming infiltrated. Invasion depth increases with time (14d). At one month, the ventral wall also is getting more and more cellularly permeated showing both walls highly infiltrated at three months. No difference of wall infiltration can be stated between the MG/Med and the MG/SC groups.

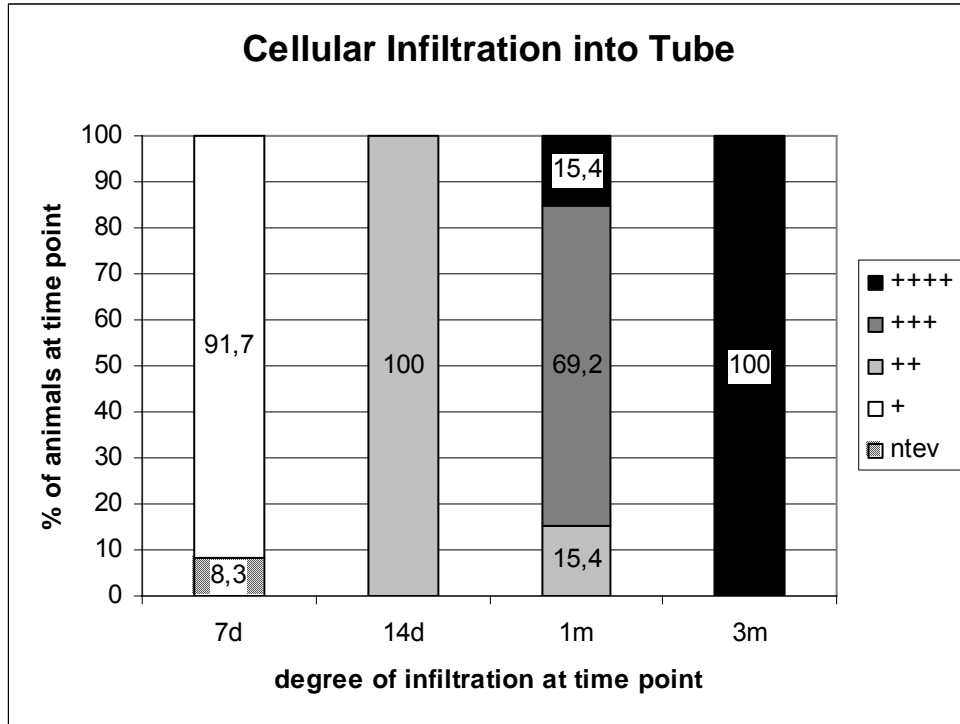


Fig. 3.12: Correlation of the amount and the temporal development of cellular infiltration of the guidance channel walls. Ntev: not to be evaluated for reasons of tissue or tube wall destruction.

### Quantity of cellular infiltration

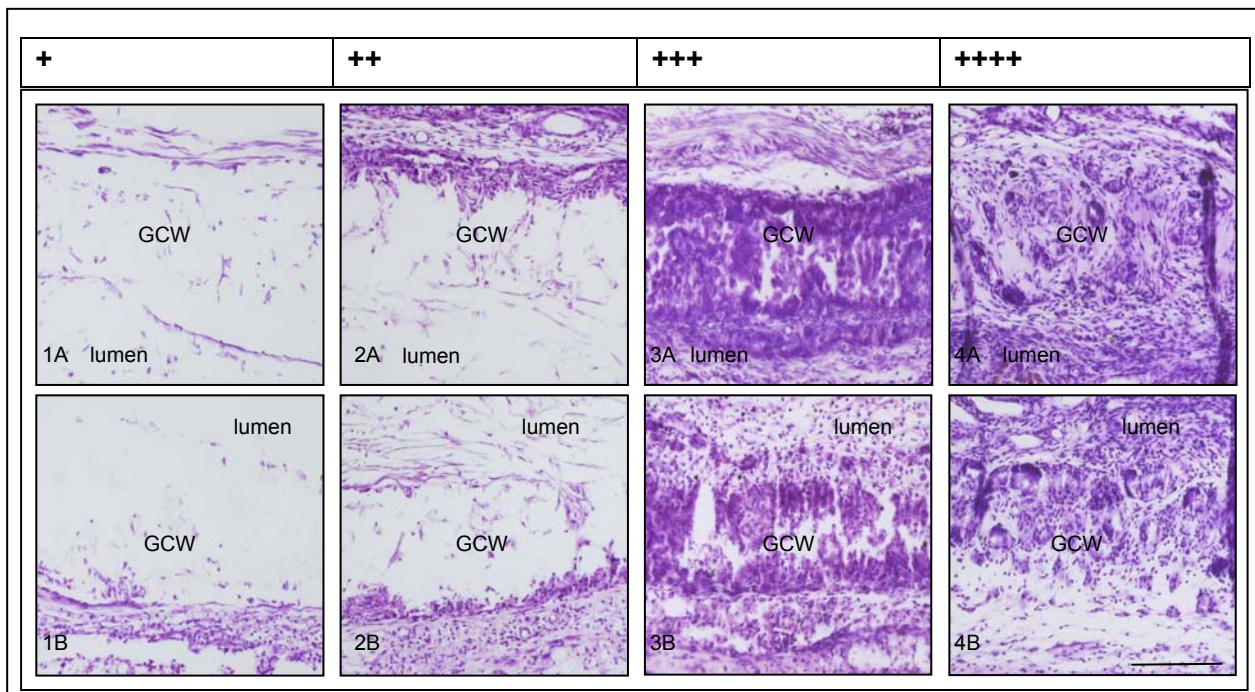


Fig. 3.13: Description of four categories to quantify cellular infiltration of the guidance channel walls (GCW): + very rare, ++ rare, +++ medium, ++++ many. (A) Dorsal guidance channel wall. (B) Ventral guidance channel wall. Scale bar: 200  $\mu$ m.

### 3.3 Characterisation of the Spinal Cord Lesion

#### 3.3.1 Lesion Size

Compared to the SWK lesion, the damage of spinal cord tissue in this injury model is more severe. The gap for guidance channel integration as well as lesions at both host tissue / tube interfaces create an enormous injury that has to be overcome by regenerating fibres. To best see the lesion's extent, staining with GFAP (glial fibrillary acidic protein) is examined (Fig. 3.14).

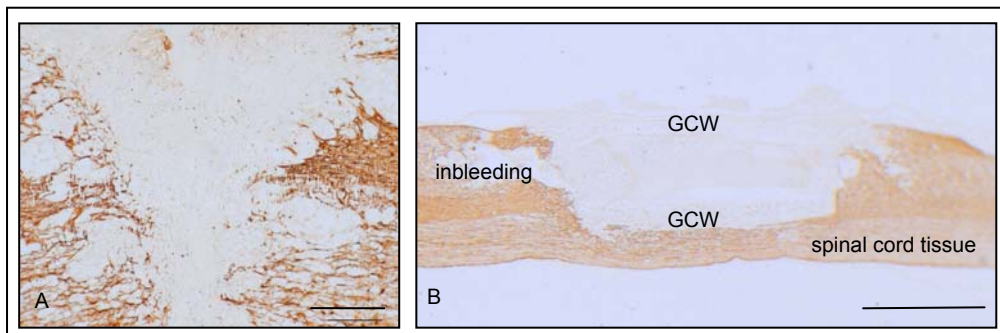


Fig. 3.14: Comparison of a SWK lesion (A) with an example of this injury model (B). Scale bars: (A) 500  $\mu$ m. (B) 2mm.

##### 3.3.1.1 Role of Inbleeding on the Lesion Size

Inbleeding can best be visualized by staining with ED-1 (Fig. 3.15 A) essentially presenting blood-borne macrophages and with applying a GFAP antibody (Fig. 3.15 B), as mentioned above, describing the lesions' extent relatively obvious.

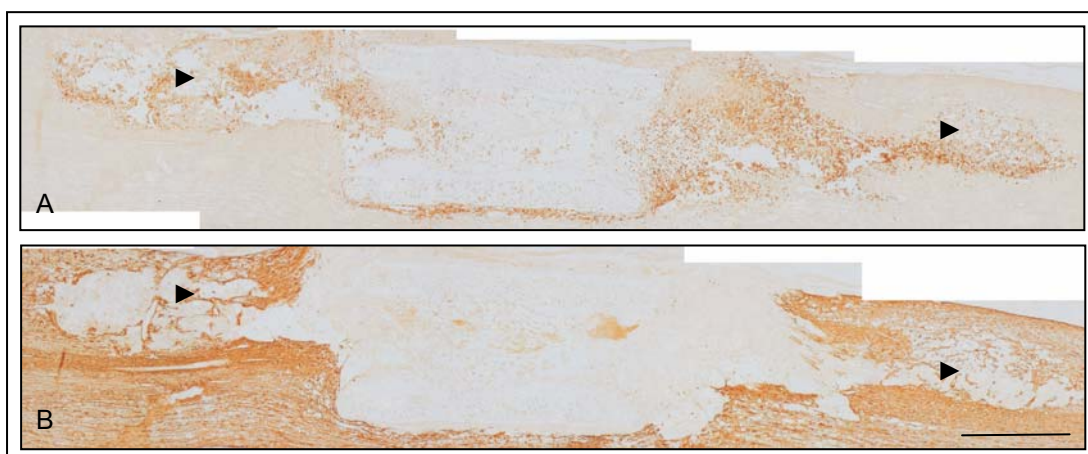


Fig. 3.15: Visualisation of sites of inbleeding indicated by arrowheads around the lesion. Comparison of different stainings on adjacent sections (A) ED-1 (B) GFAP in an example of enormous bleeding extents proximal and distal to the implant. Scale bar: 1mm.

Many different localisations of bleeding sites can be described (Fig. 3.16 for a schematic overview). Mainly animals at the 7d time point are concerned. Later on, bleeding size generally is less prevalent (data not shown, see Fig. 3.17 for measurements).

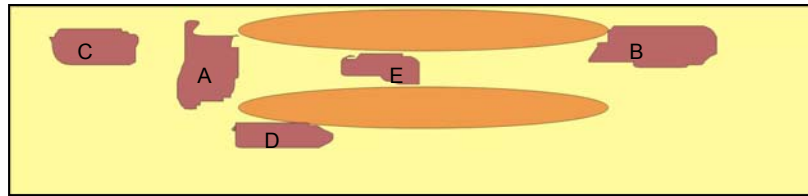


Fig. 3.16: Schematic overview over different bleeding locations. (A) immediately in front of the guidance channel, at the site of implantation, (B) at the other guidance channel end, often combinations of A and B, (C) rostral to the site of implantation, some spared tissue in between, (D) ventral to the guidance channel, (E) inside the guidance channel

As described in 2.9, lesion size was roughly measured. The aspired lesion (A) is enlarged by bleeding sites rostral and caudal to the implanted tube (B). With time, the difference between A and A+B+C decreases. Bleeding sites are more important at earlier time points. Non evaluable bleeding sites were found mainly at the 7d time point. Here, tissue was too destroyed in median sections to distinguish bleedings' limitations. Those sections were de-selected to create Fig. 3.17.

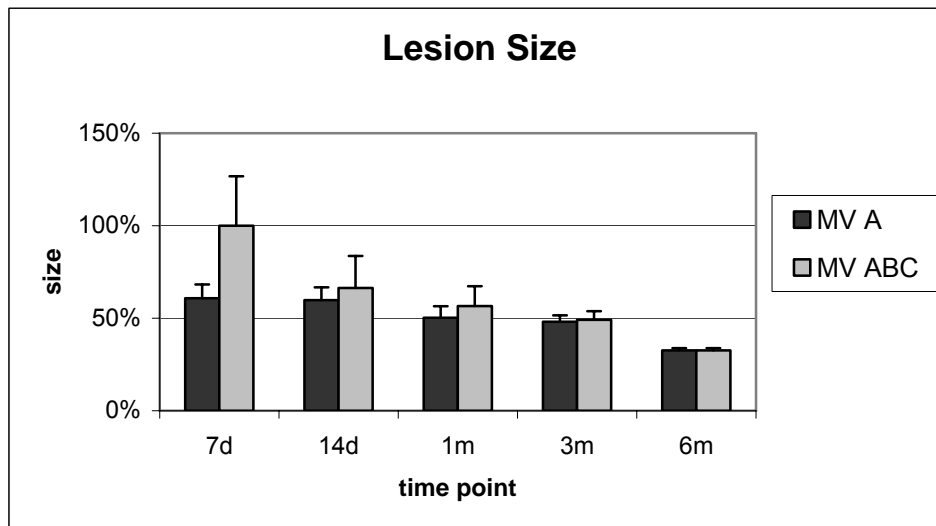


Fig. 3.17: Theoretic lesion size A compared to aspired lesion (A) plus inbleedings rostral and caudal to the tube (B+C) at different time points. Bleeding is most important at early time points, enlarging the functional lesion size. MV mean value. 100% is defined as the largest lesion ABC found, measuring about 9mm.



### 3.3.2 Cellular Reactions after Lesion

#### 3.3.2.1 Astrogliosis

An upregulation of the glial fibrillary acidic protein (GFAP) is taking place in the SWK lesioned animal (Fig. 3.18 B) as well as following guidance channel implantation (Fig. 3.18 C). It is visualised using a GFAP antibody (Chemicon). Unlesioned rat spinal cord tissue is less prominently stained by GFAP (Fig. 3.18 A).

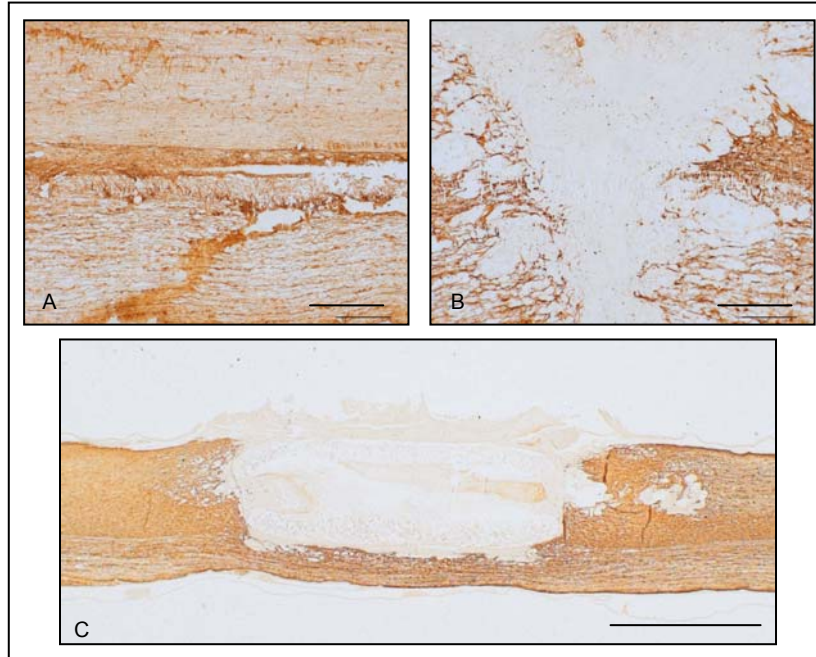


Fig. 3.18: Comparison of the GFAP staining in an unlesioned (A), a scouten wire knife lesioned (B) and a guidance channel implanted (C) animal. Scale bars: (A,B): 500 μm. (C) 2mm.

Astrogliosis in this lesion is complementary to the Collagen IV positive fibrous scar (Fig. 3.19).

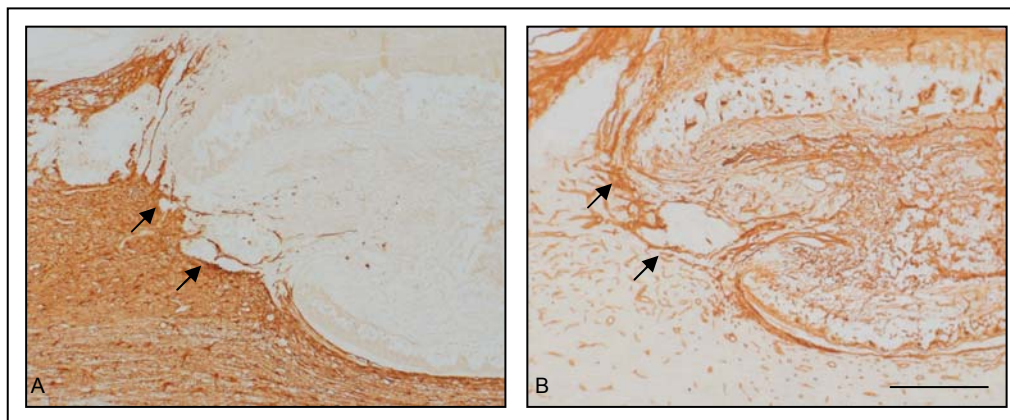


Fig. 3.19: Complementary distribution of astrogliosis and fibrous scar in injured spinal cord in this injury model. Adjacent sections show the complementary stainings of the GFAP-positive astrogliosis (A) and the Collagen IV - immunopositive fibrous scar (B). Scale bar: 500 μm.

No positive GFAP-staining can be found in the centre of the guidance channel lumen (Fig. 3.20 A) nor within the tube wall (Fig. 3.20 B) at any time point in the control MG/Med group (only 7d shown). Stainings of the MG/SC group do not show evident differences in the GFAP-upregulation compared to the control MG/Med group (data not shown). Channel lumen and tube wall remain negative for GFAP staining at all time points. Comparison of the tube opening areas and the developing glia limitans of the AST group with both, control MG/Med and MG/SC group, showed no differences of astrogliosis between these three groups (not shown).

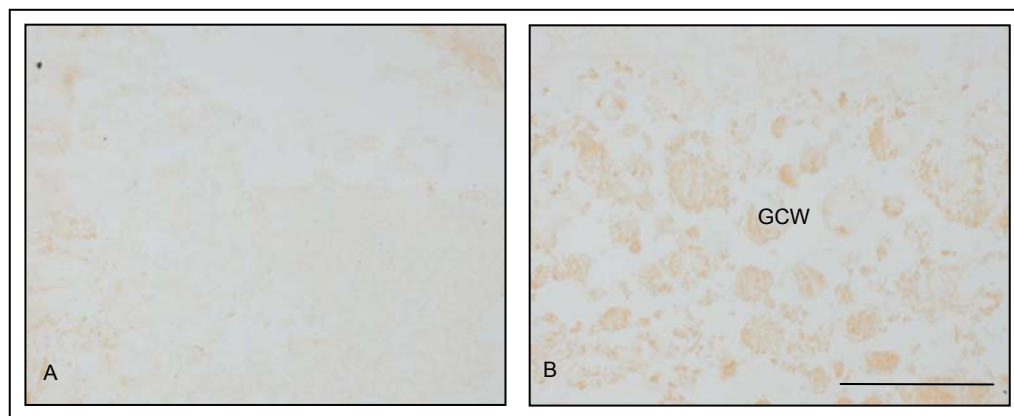


Fig. 3.20: Distribution of GFAP-positive staining at 7d in a MG/Med control (N482-54) (A) Guidance channel centre (B) Guidance channel wall (GCW). Scale bar: 200  $\mu$ m.

Having a closer look on the “tube opening area”, some cellular processes can be visualised within (Fig. 3.21). This phenomenon is not found at 7d. At later time points it can be observed in various extents in all three animal groups. One can have the impression that the MG/Med control group shows this potential astrocytic migration in a lesser degree but no real quantification is possible.

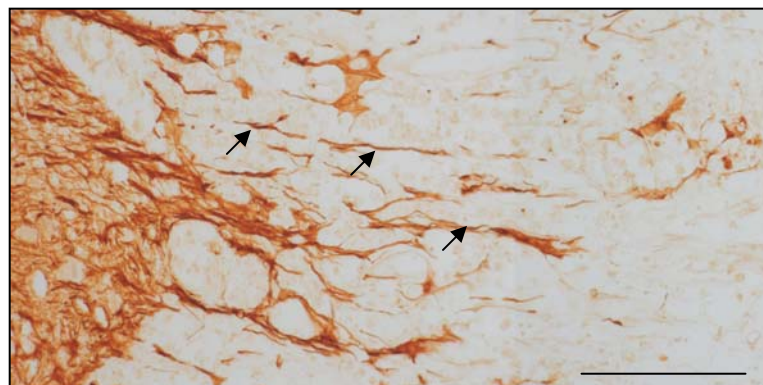


Fig. 3.21: Tube opening area illustrating GFAP-positive filiform staining as indicated by arrows at 1mo, MG/SC group. Scale bar: 200  $\mu$ m.

### 3.3.2.2 Inflammation

Distribution of ED-1 positive cells was investigated to have an idea of the number and location of potentially inflammatory cells (Fig. 3.22). Comparison with an unlesioned animal (A) and a SWK-lesioned animal shows (B) a higher repartition of ED-1 positively stained cells in this lesion model (C) than following a SWK lesion. In both injuries, cells are mainly found at the lesion site.

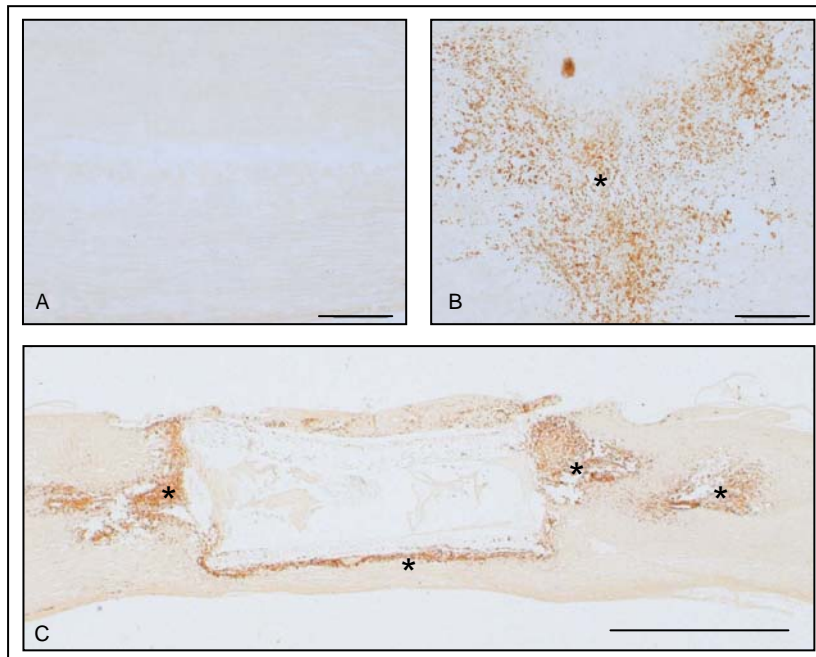


Fig. 3.22: Comparison of the immunohistochemical staining with ED-1 in sham tissue compared to different lesion models. (A) Sham animal (B) SWK lesion (C) Guidance channel implanted animal. Stars indicate areas of high ED-1 localisation and inbleeding. Scale bars: (A,B) 500  $\mu$ m. (C) 2mm.

In this injury model, ED-1 positive cells are mainly found around the implanted guidance channel (Fig. 3.23 A, F flashes) and at the sites of inbleeding (Fig. 3.23 A star) in close proximal and distal relation to the implant. No cells are observed in spinal cord tissue farther rostral (Fig. 3.23 C) nor caudal (Fig. 3.23 E) to the lesion site at 7d. The tube walls do not seem invaded by ED-1 positive cells (Fig. 3.23 B, F). Neither does the tube lumen (Fig. 3.23 D). Changes in the distribution of ED-1 positive cells over time cannot be quantified. At 7 and 14d, a very high number can be visualised rather located. Later, at one month, there seem to be less positive cells giving the impression to be more widely distributed over the spinal cord tissue. The ED-1 positive cells appear to follow the line of degenerated axons showing a high number of cells in the dorsal column (not shown). With time, the tube walls appear to be invaded by some rare ED-1 positive cells, the main number accumulating in the host tissue just around, though. Schwann cell implantation does not seem to have any effect on the distribution of ED-1 positively stained cells, neither does the application of the AST (not shown). No apparent differences are found in comparison with the MG/Med group

illustrated above. The three and six months time points do not allow any new observations concerning the evolution of cellular distribution in time.

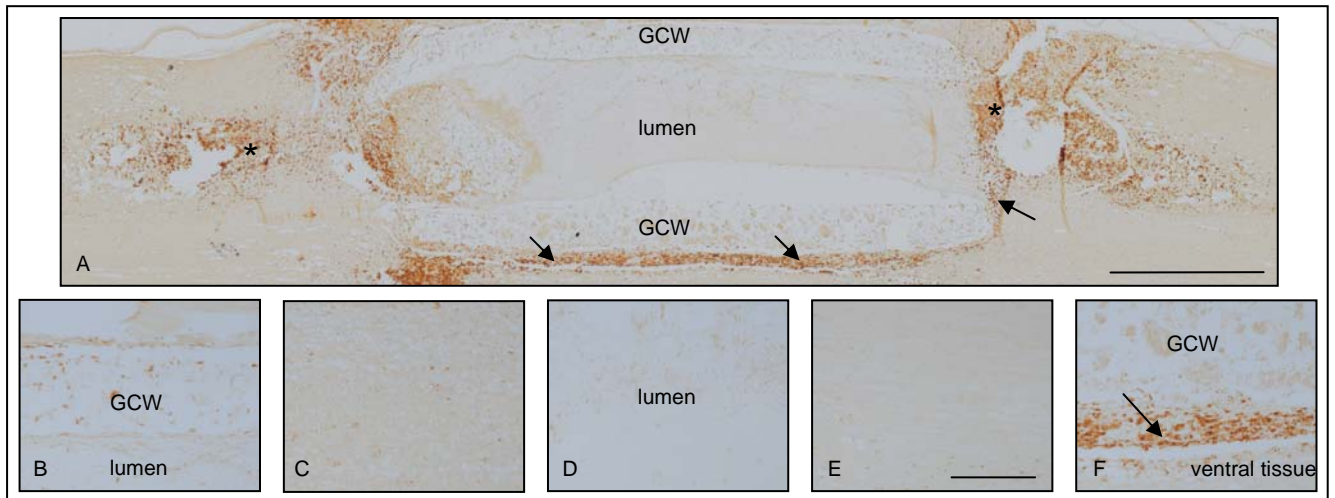


Fig. 3.23: Distribution of ED-1 positive cells in a 7d MG/Med animal (N482-78). (A) 4x magnification of the implantation site with ED-1 positive cells visible mainly around the implant (arrows) and at the site of inbleeding (star). (B) - (F) 16x close-ups of different locations (B) Dorsal guidance channel wall (GCW), (C) Spinal cord tissue rostral to the lesion site, (D) Tube lumen, (E) Spinal cord tissue caudal to the lesion site, (F) Ventral guidance channel wall and ED-1 positive cell-filled rim (arrow) around. Scale bars: (A) 1mm. (B-F) 200  $\mu$ m.

### 3.4 Visualisation, Localisation and Survival of Implanted Schwann Cells

#### 3.4.1 Visualisation of Implanted Schwann Cells

S100 revealed itself as not being specific enough for the visualisation of Schwann cells in this lesion model in rat spinal cord. Schwann cells and astrocytes are stained (Fig. 3.24).

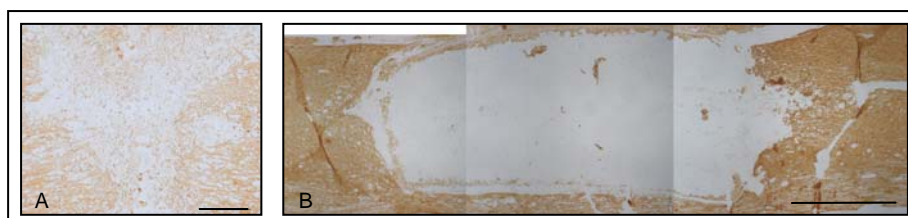


Fig. 3.24: Immunohistochemical staining with S100 in a SWK-lesion as well as in this lesion type shows prominent staining of the whole spinal cord tissue. No specificity for Schwann cells is given. Scale bars: (A) 500  $\mu$ m. (B) 1mm.

Schwann cells, 100% retrovirally infected with enhanced GFP, were created. All Schwann cells were green fluorescing at the time of implantation (Fig. 3.25 A, B), verified *in vitro* just before cell collection via trypsinisation. The Schwann cells' morphology *in vivo* might vary

from the *in vitro* shape (Fig. 3.25 C-E), appearing “fibre-like”. The increasing cell number with time in cell culture proves that descendant cells of proliferating Schwann cells *in vitro* express the fluorescent label as well (data not shown).

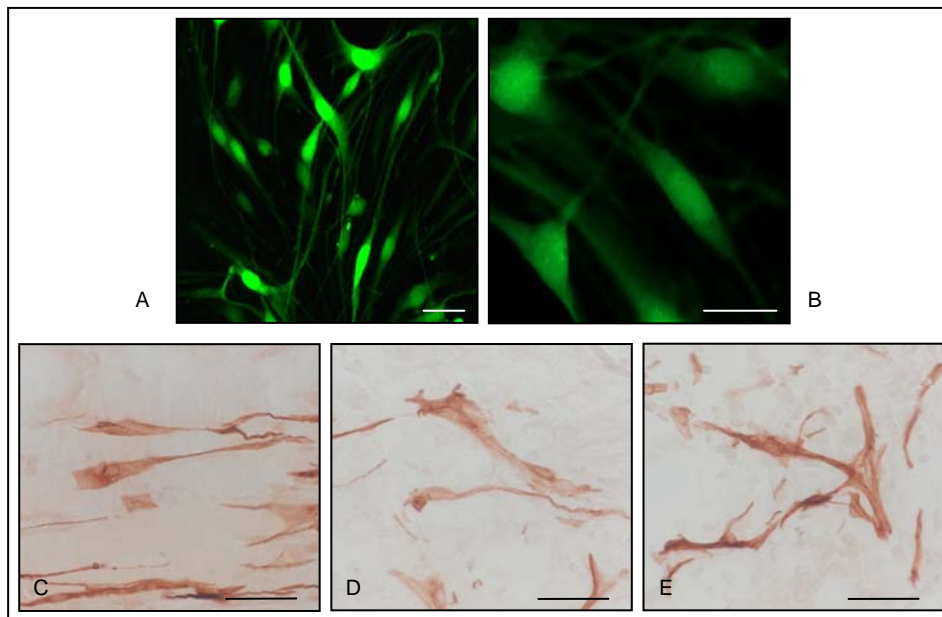


Fig. 3.25: Visualisation of eGFP-labelled Schwann cells. (A) and (B) *In vitro* fluorescence of the labelled Schwann cells. (C)-(E) *In vivo* immunohistochemical staining with an eGFP antibody against the labelling. Various morphologies are found. Scale bars: 50 µm.

### 3.4.2 GFP/DAPI Double-Staining

GFP/DAPI double staining (Fig. 3.26 A, B) proves the co-localisation of cell nuclei (DAPI) and eGFP-stained “fibre-like” structures (Fig. 3.26 A).

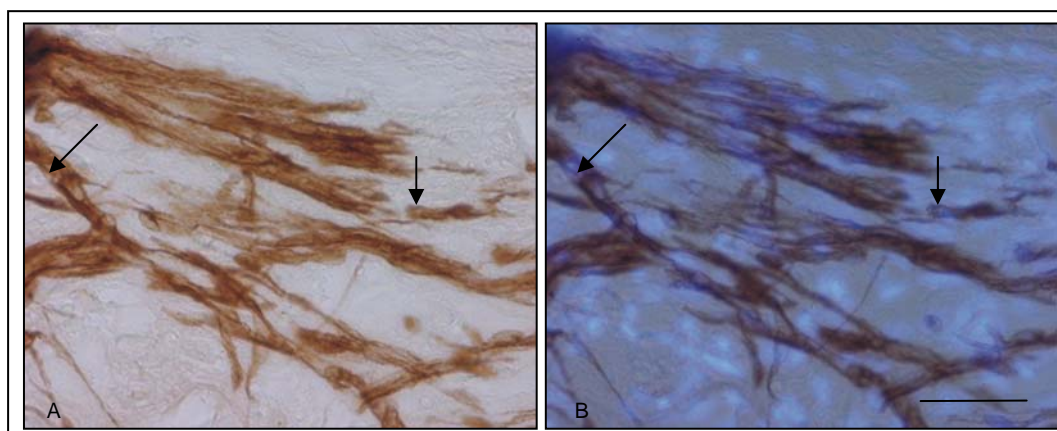


Fig. 3.26: Co-localisation of eGFP-positive structures and cell nuclei of a GFP/DAPI double-staining. (A) shows eGFP-positive “fibre-like” structures (B) presents the double-staining. Arrows indicate DAPI-positive nuclei in B and corresponding GFP-positive structures in A. Scale bar: 50 µm.

### 3.4.3 Survival and Quantity of Implanted Schwann Cells

The following observations were made:

- The iron chelator BPY-DCA tested on Schwann cells *in vitro* shows different effects depending on its concentration. Pure BPY-DCA application leads to cells death but if diluted, cells develop normally (data not shown).
- MG/Med channels do not show Schwann cells at any time point.
- No difference concerning Schwann cell behaviour can be stated between the MG/SC and the AST group.
- An increase of Schwann cell number inside the channel lumen with time was observed. At 7d, hardly any GFP positive cells are visible inside the tubes. The number increases up to the one month time-point. At three months, Schwann cells are found in only one out of four animals. The six months animal's sections do not present any Schwann cells neither.

### 3.4.4 Schwann Cell Localisation

To describe a potential Schwann cell migration, four categories of cellular location are created (Fig. 3.27 A-D) and all Schwann cell containing animals of the groups IIC2 MG/SC and IIC3 AST were classified. Multi- category-classification for an animal was possible.

- Categories A as well as category D can be found in most animals excluding the three and six months time points. Here, only one animal shows Schwann cells, the others not at all.
- Category B is present at the 14d time point and possibly found at one month for one animal of each group.
- Category C is found at the 7d time point only in both Schwann cell containing groups. For the AST group it can be found in all 7d animals.

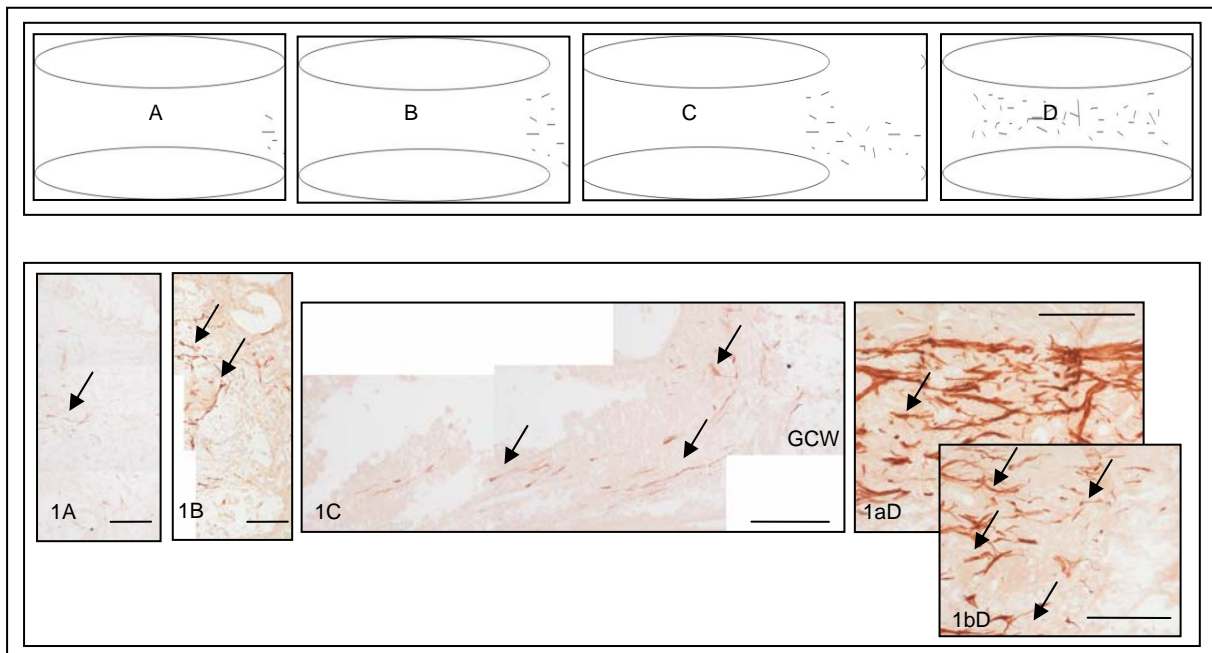


Fig. 3.27: Classification for Schwann cell localisation into four categories. (A) Schwann cells within the guidance channel, close to its openings (B) Possible Schwann cell-migration just across the tube end (C) Some Schwann cells migrating proximal or distal to a tube opening (D) Schwann cells in the middle of the tube lumen. *In vivo* examples for the demonstrated categories are given in (1A)-(1D). (1aD) shows the tube lumen centre, (1bD) a more distal part. The arrows indicate Schwann cells. Scale bars: 200 µm.

Tab. 3.2: Distribution of Schwann cells according to the in Fig. 3.27 mentioned classification in regard to animal group and time point. (ntev) not to evaluate

Group	Localisation	7d	14d	1Mo	3Mo	6Mo	Total
<b>MG/SC</b>	<b>A</b>	4/4	4/4	4/4	0/4	0/1	12/17
	<b>B</b>	0/4	1/4	0/4	0/4	0/1	1/17
	<b>C</b>	2/3 1ntev	0/4	0/4	0/4	0/1	2/16
	<b>D</b>	3/3 1ntev	3/3 1ntev	4/4	1/4	0/1	11/15
<b>AST</b>	<b>A</b>	5/5	3/3	3/5			11/13
	<b>B</b>	0/5	2/3	0/5			2/13
	<b>C</b>	5/5	0/3	0/5			5/13
	<b>D</b>	2/5	3/3	4/5			9/13

## 3.5 Cells Invading the Guidance Channel

### 3.5.1 Morphologically Schwann Cell-resembling Cells

In Schwann cell-filled guidance channels morphologically Schwann cell-resembling cells are found in Nissl staining (Fig. 3.28 A, B). Guidance channels of the MG/Med control group show similar cells as well as a very high number of more longitudinally oriented cells (not shown). At one month, the channels seem as filled with cells or even more packed as comparable tubes of the MG/SC group (Fig. 3.28 C).

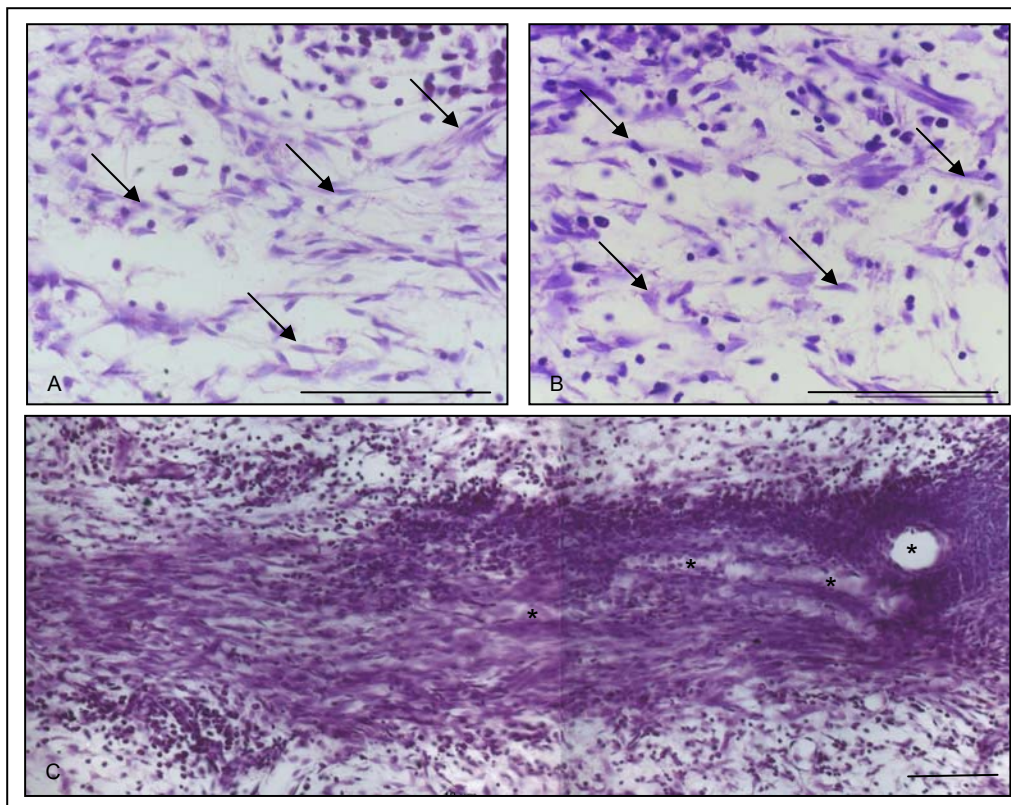


Fig. 3.28: Nissl staining demonstrating cells inside the guidance channel lumina. (A) and (B) Morphologically SC-like cells (arrows) within the lumen of a 1mo MG/SC animal. (C) Cell-loaded guidance channel lumen of a 1mo MG/Med animal. Stars indicate blood vessels. Scale bars: 100  $\mu$ m.



### 3.5.2 Small Round Cells

Clusters of small round cells are found inside the tube lumen (Fig. 3.29).

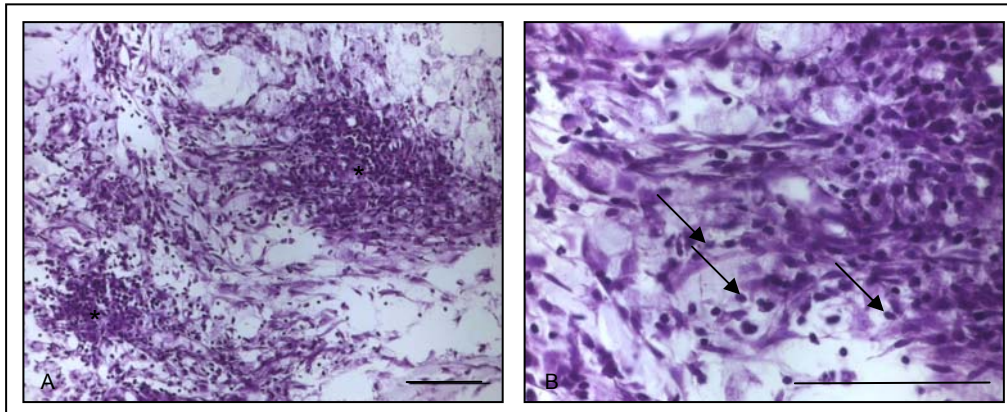


Fig. 3.29: (A) Cell clusters (star) within the tube lumen. Arrows in (B) indicate such small round cells. Scale bars: 100  $\mu$ m.

## 3.6 Scar Formation

### 3.6.1 The Glial Scar

The glial scar has been visualised by an anti-GFAP antibody and is found to be complementary to the Coll IV positive fibrous scar (Fig. 3.30) as already stated for other lesion types (see 3.3.2.1).

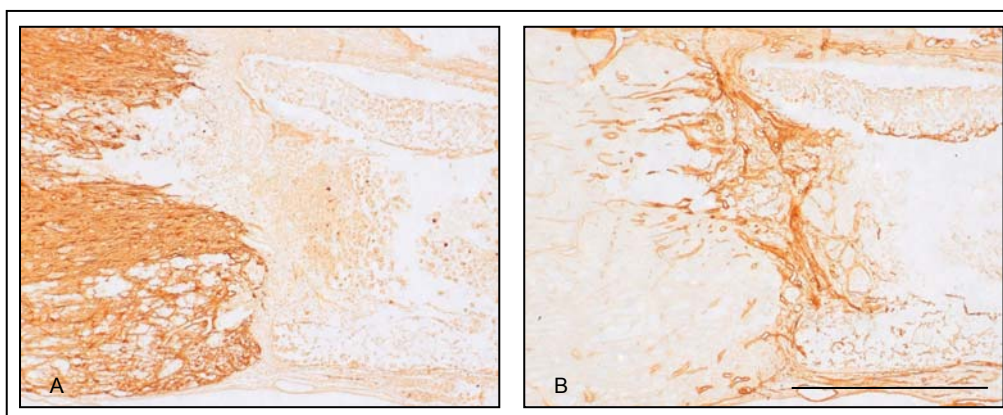


Fig. 3.30: Complementary distribution of glial and fibrous scars in this injury model. Adjacent sections show the complementary stainings of the GFAP-positive glial scar (A) and the Collagen IV - immunopositive fibrous scar (B). Scale bar: 1mm.

### 3.6.2 The Collagen IV containing Fibrous Scar

The development of the fibrous scar in the lesion epicentre was studied using an antibody against Collagen type IV.

#### 3.6.2.1 Description of the Fibrous Scar in this Injury Model

As in SWK lesion, a fibrous scar develops at the site of injury (Fig. 3.31). One important difference is the existence of two scars – one at each tube end – in the guidance channel implanted animals. The dimensions of the scars are difficult to compare with other models. MG/Med controls of different OP methods during establishment of this injury model (see 2.5.1) do not reveal any differences in scarring dimensions. At 7d, both tube ends seem capped by collagen layers of various extent and around the tube wall, a thinner scar layer can be found (Fig. 3.32). Tissue of a 4d time point could not be preserved during preparation procedures (data not shown). Scarring as depicted below can be observed in all 7d control animals (n=9).

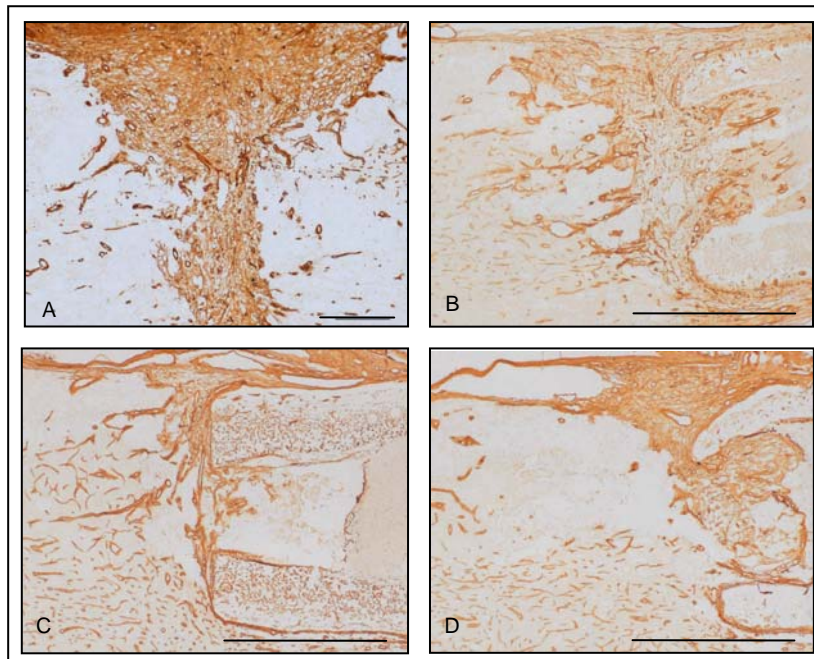


Fig. 3.31: Collagen IV positive fibrous scar in (A) a SWK lesion compared to (B) group I (empty implant) and (C, D) MG/Med controls (C) group III B1, (D) group III C1. Scale bar (A): 500  $\mu$ m. Scale bar (B,C,D): 1mm.

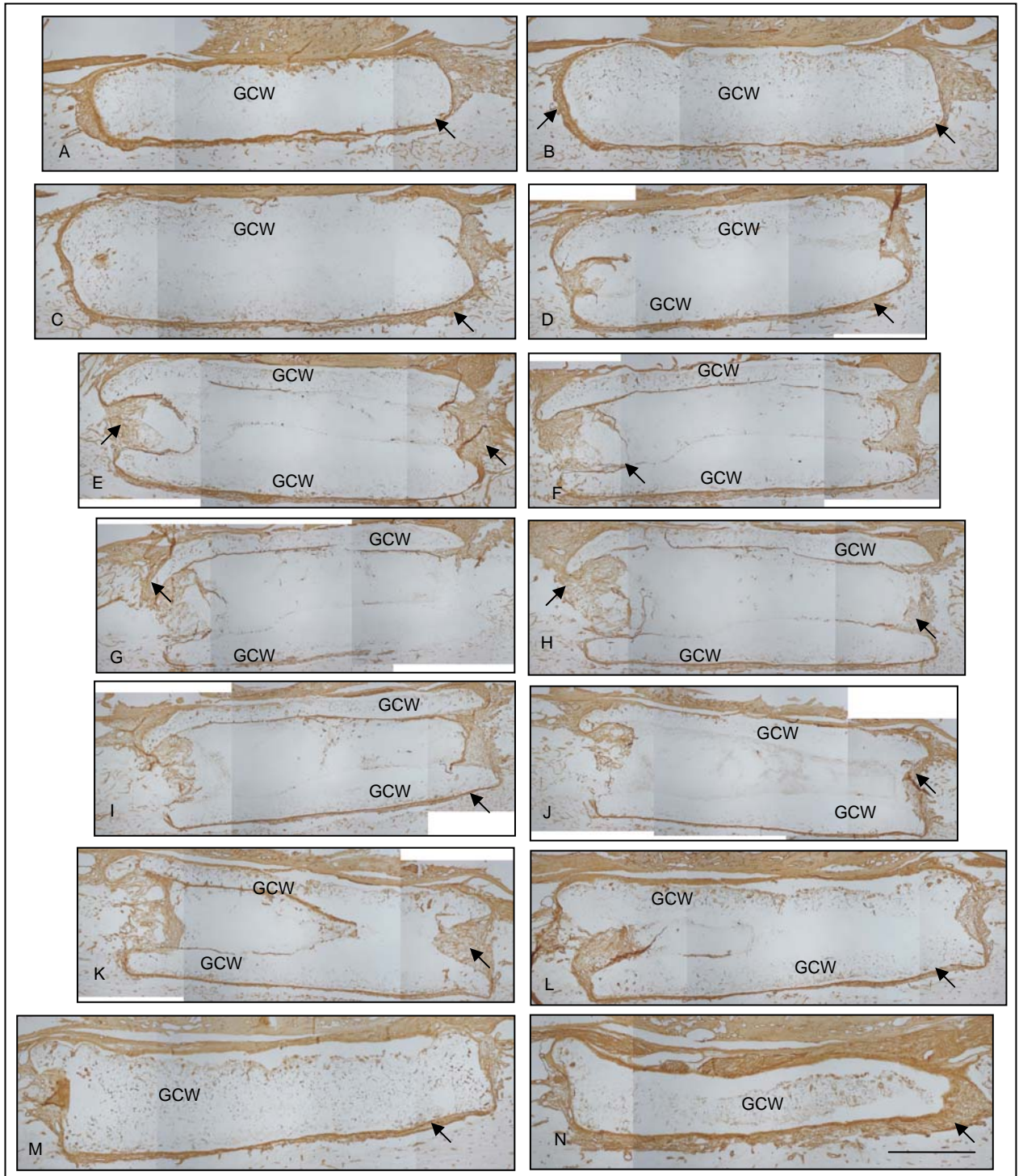


Fig. 3.32: Demonstration of the fibrous scar “capping” around the implanted guidance channel in a MG/Med control at 7d. (A)-(O) show adjacent sections stained with a Collagen IV antibody to well visualise the scarring over all sections. The arrows indicate the localisation of fibrous scarring around the guidance channel wall (GCW). Scale bar: 1mm.

### 3.6.2.2 Effect of Schwann Cells on Scarring

Both, the control group MG/Med (Fig. 3.33 A) (IIC1) as well as the MG/SC (Fig. 3.33 B) (IIC2) group show Collagen IV positive scarring around the implanted guidance channel. This fibrous scar resembles the “cap” shown in Fig. 3.32 at all examined time points. There is no difference obvious between both groups.

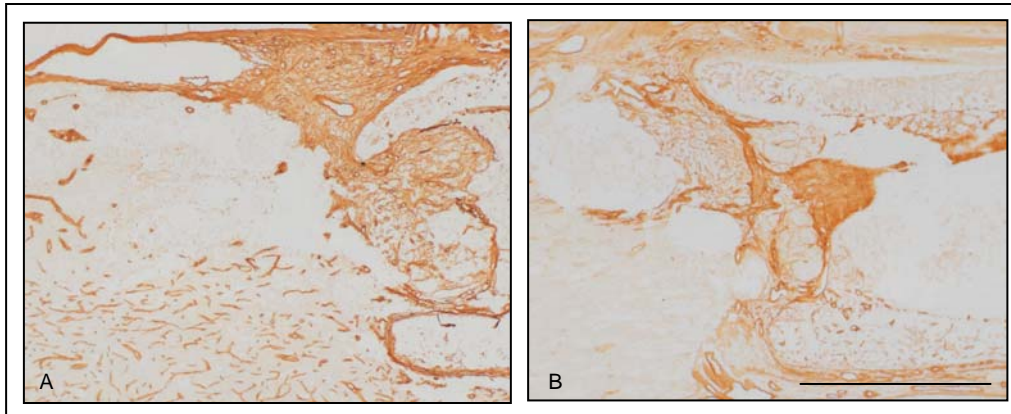


Fig. 3.33: Examples of Collagen IV immunopositive staining of the fibrous scar in (A) a MG/Med control versus (B) a MG/SC animal at 7d. Scale bar: 1mm.

### 3.6.2.3 Influence of the Anti-Scarring Treatment

All sections stained with an antibody against Collagen IV in the MG/SC and AST 7d animals were examined for any effect of the Anti-Scarring Treatment. Analysis was very difficult for several reasons (see 4.6.2). To classify different findings, sections were categorised as described below in complete reduction (-), partial reduction (+) and full scar (++). Two extra categories concerning the probable tissue loss due to inbleeding among other reasons were created: appearing partially reduced (\*+) and appearing fully scarred (\*++) (Fig. 3.34). No complete reduction of the fibrous scar could be found. Partial reduction was observed in some rare sections (10%) in one out of five AST animals (N405). The category “appearing partially reduced” (category \*+) was found in additional 20% in the same AST animal as well as in 17,6% in another AST animal. In contrast, none of the MG/SC animals presented this category (for details Tab. 3.3). The category “appearing fully scarred” (category \*++) was present in a rather high percentage in MG/SC and AST animals. Sites of inbleeding were found within the Coll IV positive tissue, seeming to loosen the scar. Comparing Collagen IV stained sections of the anti-scarring treated group IIC3 with different animal groups throughout this study at later time points up to one month, no significant change of scarring could be detected (data not shown).

### Classification of Scarring

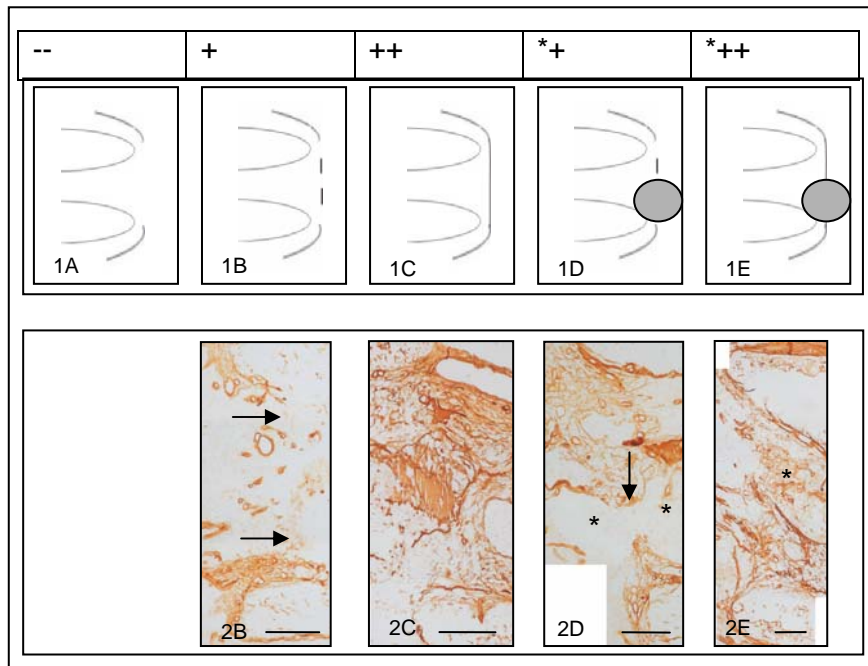


Fig. 3.34: Classification of Collagen IV immunopositive scarring. (1A)-(1E) present the chosen categories. (1A) Complete reduction (1B) Partial reduction (1C) Full scar (1D) Appearing partially reduced (1E) Appearing fully scarred. No *in vivo* example of a complete reduction was found. (2B)-(2E) show *in vivo* illustrations for the schematic categories. Arrows indicate the site of (appearing) partial reduction. Stars designate areas of inbleeding leading to tissue loss (2D, E). Scale bars: 200  $\mu$ m.

Tab. 3.3: Percentage of sections for each category showing a tube opening in the MG/SC versus the AST group. (ntev) not to evaluate. + designates partial reduction of fibrous scarring. \* indicates a probable tissue loss making classification difficult (see above).

Group							
MG/SC	<b>Category</b>	<b>N390</b>	<b>N392</b>	<b>N400</b>	<b>N401</b>		<b>Total</b>
	ntev	0	0	0	0		0
	-	0	0	0	0		0
	+	0	0	0	0		0
	*+	0	0	0	0		0
	++	62,5%	88,2%	94,4%	100%		85,7%
	***	37,5%	11,8%	5,6%	0		14,3%
AST	<b>Category</b>	<b>N405</b>	<b>N443</b>	<b>N444</b>	<b>N525</b>	<b>N526</b>	<b>Total</b>
	ntev	0	20%	0	0	0	4,4%
	-	0	0	0	0	0	0
	+	10%	0	0	0	0	2,2%
	*+	20%	0	17,6%	0	0	7,7%
	++	50%	40%	58,8%	100%	100%	68,1%
	***	20%	40%	23,6%	0	0	17,6%

### 3.6.2.4 Development of the Scar with Time

The Collagen IV positive fibrous scar seems fully developed at 7d (Fig. 3.35A). It remains present and unchanged at all time points. Distinction of scar-forming collagen sheets and stained Matrigel® at later time points is difficult (Fig. 3.35 B-E). The scar's extension within the tube lumen can only be speculated on. However, the scar-border to the host tissue clearly can be determined (thin arrows in Fig. 3.35).

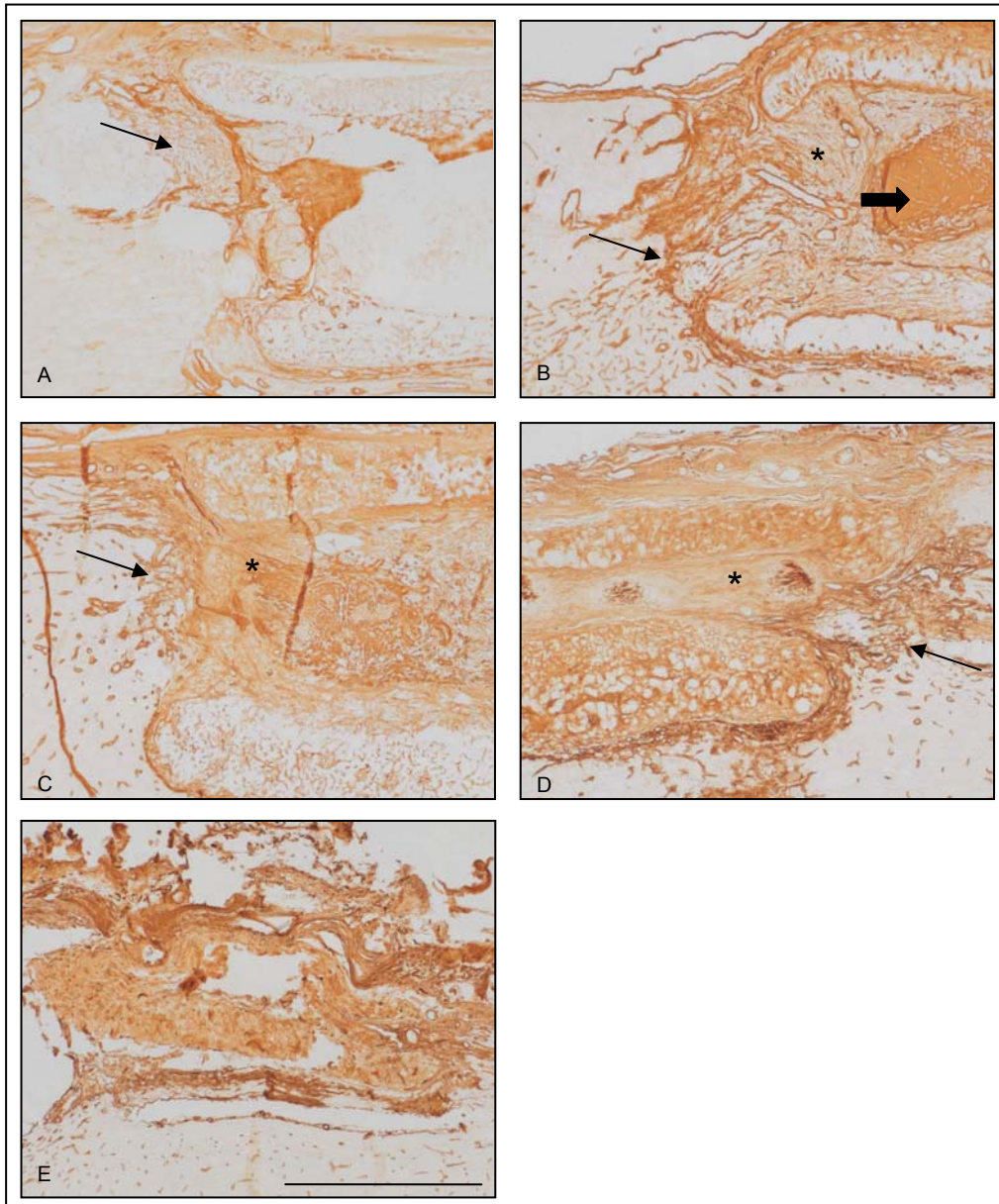


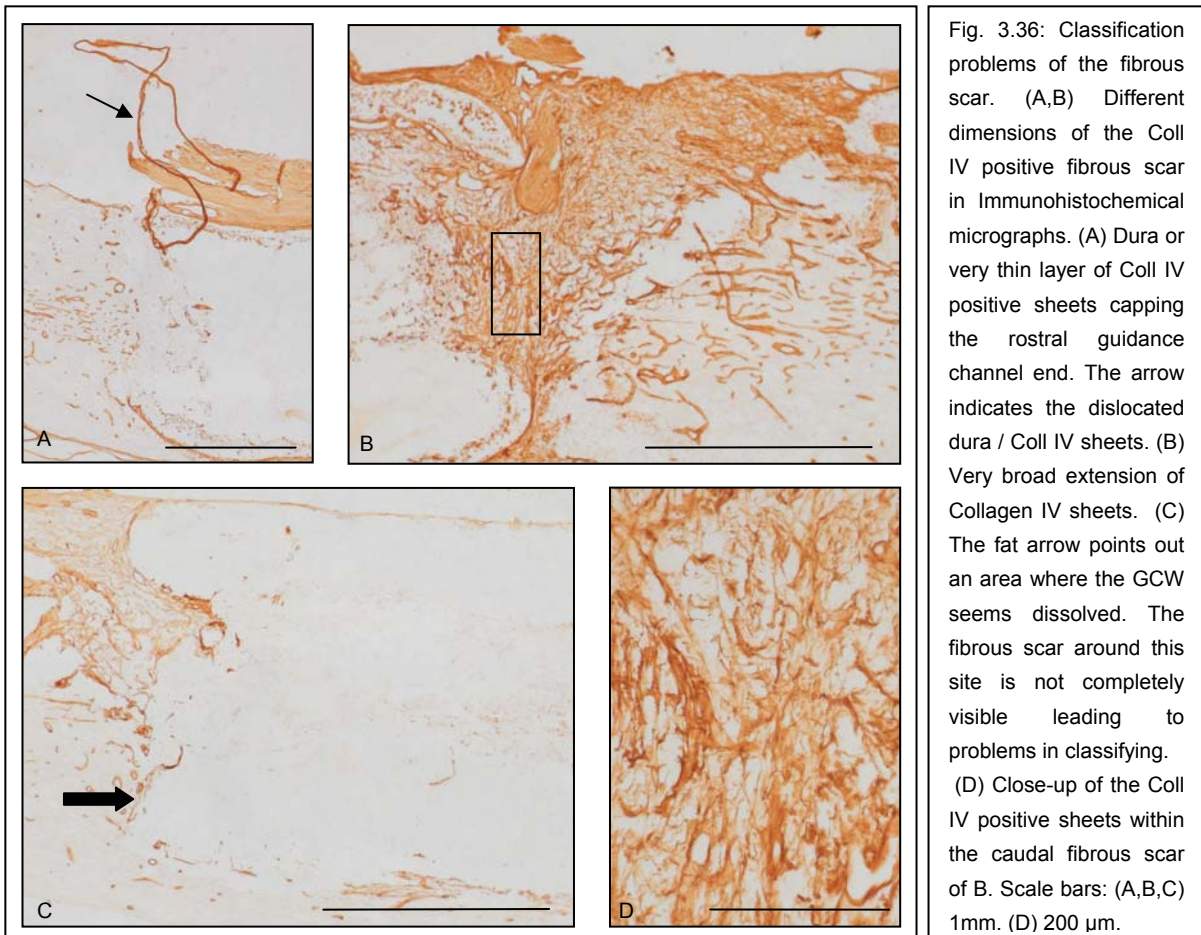
Fig. 3.35: Development of the fibrous scar in this lesion model with time. (A) 7d (B) 14d (C) 1mo (D) 3mo (E) 6mo The stars indicate Collagen IV immunopositive areas within the guidance channel lumen where a differentiation between Matrigel® and Collagen IV sheets of a fibrous scar is impossible. The fat arrow in B points out a site of MG collection. The thin arrows show the border of the fibrous scar to the host tissue. Scale bar: 1mm.

### 3.6.3 Phenomena observed in Collagen IV-immunostained Sections

Evaluation of the fibrous scar is not without problems for this complex type of injury. Fig. 3.36 - Fig. 3.39 demonstrate some of the difficulties arising.

#### 3.6.3.1 Classification of the Fibrous Scar

Scars of various dimensions from extremely thin layers to very broad accumulation of Collagen IV sheets are observed (Fig. 3.36 B, D). In Fig. 3.36 A, a thin, dislocated Collagen IV positively stained layer is visualised. It is difficult to distinguish between dura or thin scar. In case of scar, with some imagination, it is present and, therefore could be classified as being a full scar ++ (see 3.6.2.3). A problem for classification of the fibrous scar was due to a certain degree of guidance channel wall-dissolution in some sections (Fig. 3.36 C). The visualisation of the fibrous scar in those cases is incomplete. Fig. 3.37 A, at first glance, seems to demonstrate a partial reduction at the ventro-distal tube wall (arrowhead). A closer look shows the detachment of the innermost wall-layer from the ventral tube wall (Fig. 3.37 B, thin arrow). The fibrous scar in Fig. 3.37 A and B was classified as a full scar ++. Another example of “first-glance” partial reduction is demonstrated in Fig. 3.37 D (arrowhead). At the site of potential reduction, however, inbleeding can be visualised (Fig. 3.37 C, star). This scar was classified as “full scar appearing” \*++ for descriptive reasons.



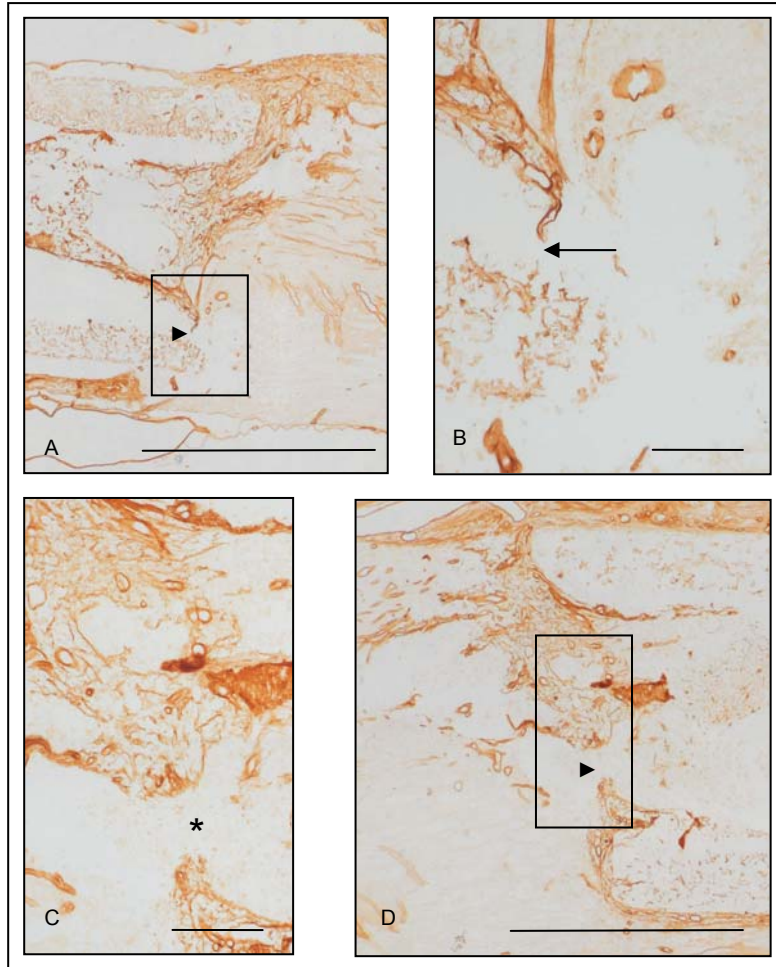


Fig. 3.37: First-glance partial reduction in stainings with a Coll IV antibody reveals itself as being not reduced at a second glance. (A) The arrowhead points at a site that might be reduced in Collagen IV positive sheets. (B) Close-up of A, the thin arrow indicating the same area and proving the detachment of the innermost GCW layer. No reduction in scarring is visible. (C) Close-up of the area indicated by the arrowhead in (D). The star points out the prevalence of a bleeding site at the area of potential scarring-reduction. Tissue is lost which qualifies this scar as \*++. Scale bars: (A,D) 1mm. (B,C) 200  $\mu$ m.



### 3.6.3.2 Cyst or Ripped Tissue?

Cysts and cyst-like structures have to be distinguished from torn tissue. Cysts, by definition, have a Collagen IV rim (Fig. 3.38 A, B, arrows). Inside of the structures, cell detritus is visible (stars). In case of tissue tearing, no structure is visible inside the designated area neither is a tissue loss (Fig. 3.38 C, D).

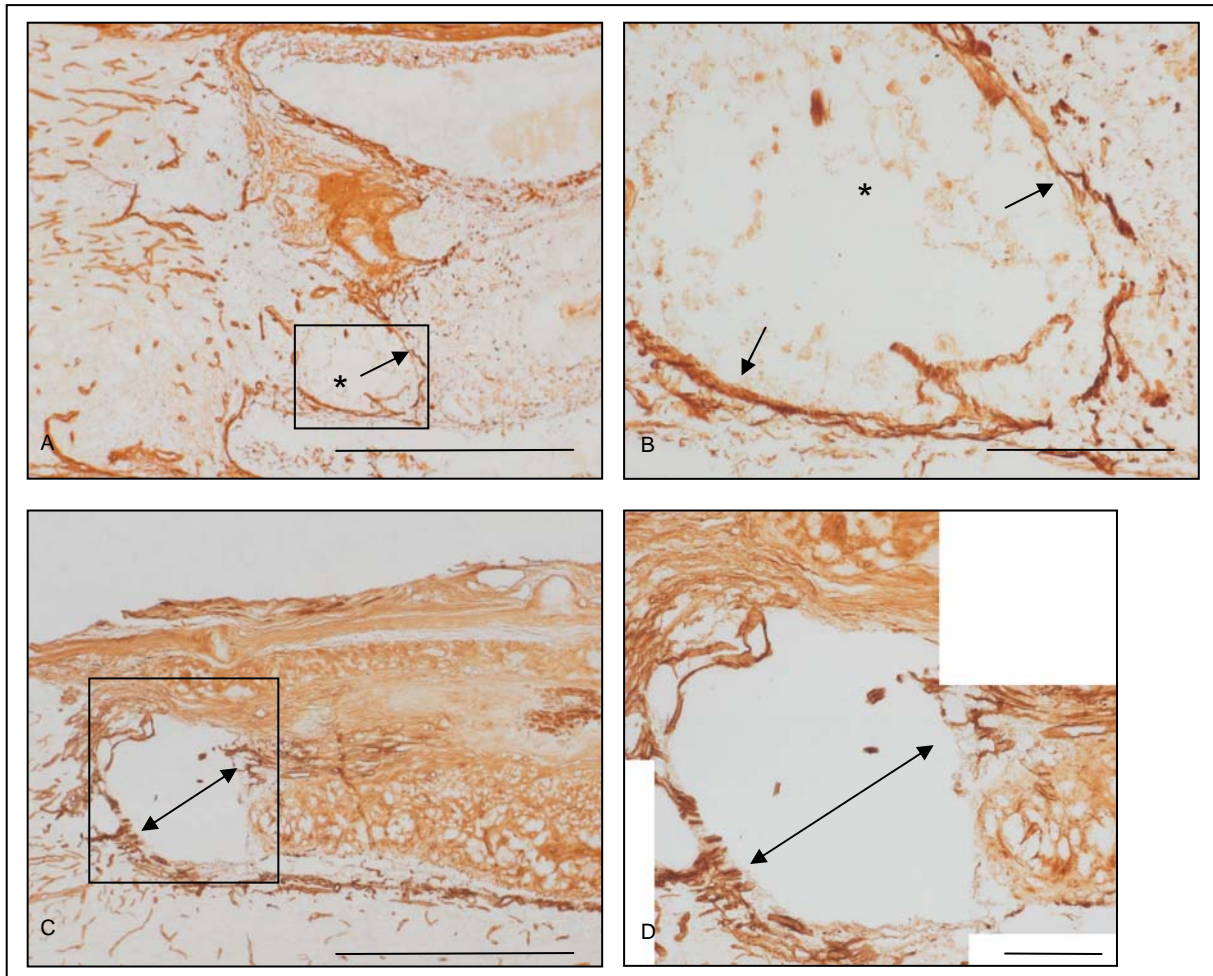


Fig. 3.38: Distinction between cyst-formation and tissue tearing in Coll IV immunopositive sections. (A) and (B) Inbleeding as indicated by the stars with a rim of Coll IV positive sheets around (arrows) lead to the classification as being a cyst. (C) and (D) show an example for torn tissue rostral to an implanted guidance channel. The double-sided arrows point at two borders that have been ripped apart. No structures are visible in the cyst-like area. No tissue is lost. Scale bars: (A,C) 1mm. (B,D) 200 μm .

### 3.6.3.3 Difficulties regarding the Application of Matrigel®

The Matrigel®-matrix in some animals, mainly at later time points, is heavily Collagen IV immunopositive (Fig. 3.39 B, D, E and F, also see 3.6.2.4 Fig. 3.35). In rare cases, the early 7d time point also shows Collagen IV positive Matrigel®-matrix staining (Fig. 3.39 A, C). No differentiation of structures can be made under conditions of such an important background staining to define or classify the fibrous scar. In the centre of Schwann cell-filled guidance channels vascularisation can be observed within the Matrigel®-matrix (Fig. 3.39D, E, F).

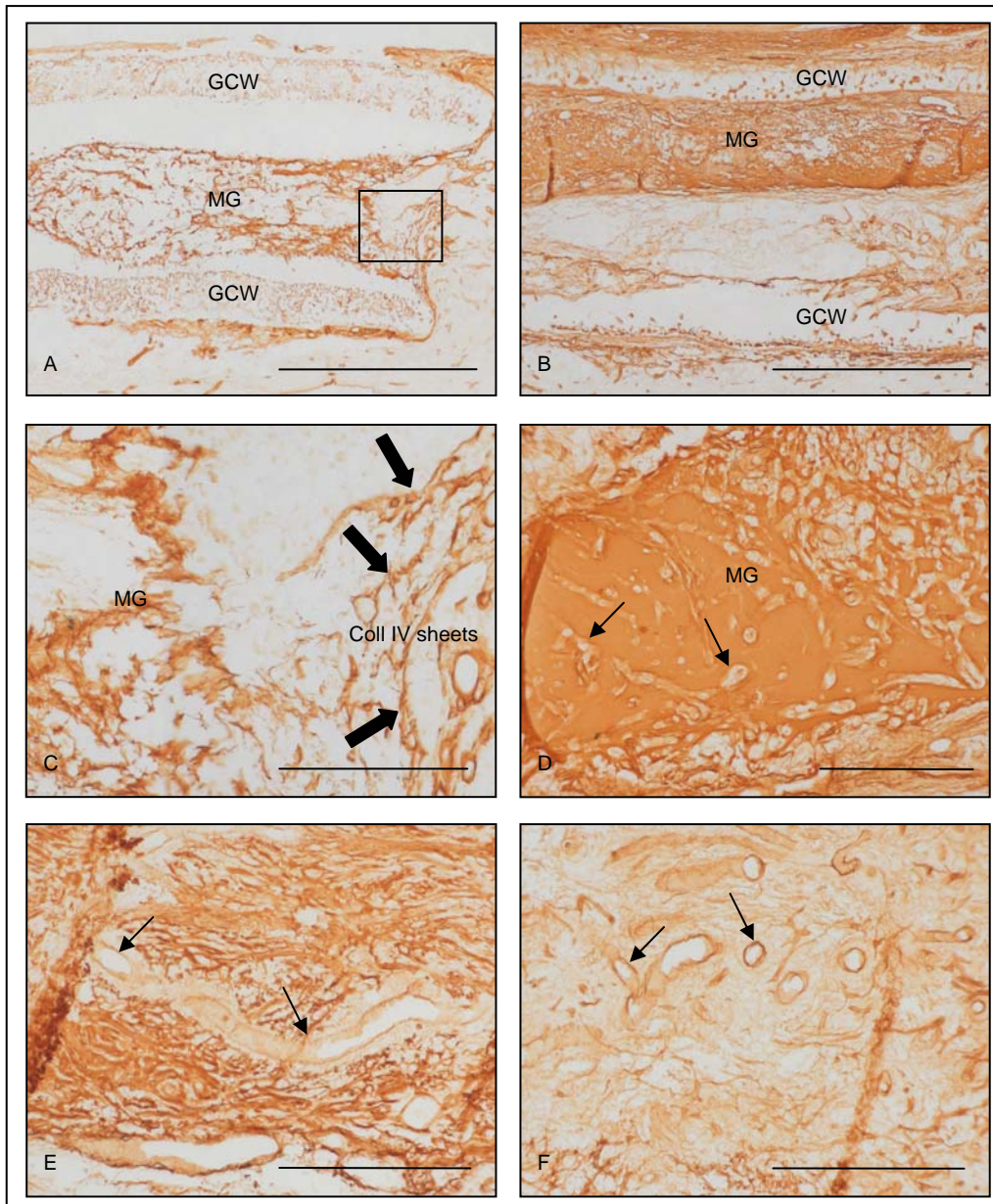


Fig. 3.39: Problems in the classification of scarring regarding the application of Matrigel® as a medium. (A) and (C) The MG is heavily stained by the applied antibody against Coll IV. A distinction between fibrous scarring and the MG is rather difficult. The scar being located as a capping around the tube end makes a differentiation to the host tissue possible. No exact definition of the interior end of scarring is valuable. (B) and (D) show the extremely orange background staining of MG clods. Again, no distinction of the interior border of scarring is possible. (D) - (F) Blood vessels within the Matrigel®-matrix clod are indicated by arrows (D) at a 14d time point (E) and (F) at 1mo. Scale bars: (A,B) 1mm. (C,D) 200 µm. (E,F) 100 µm.

## 3.7 Axonal Degeneration and Regrowth

Immunohistological staining with a Pan-Axonal Marker (PAM) was used to describe both, the degeneration processes going on in the rat spinal cord following the guidance channel implantation, as well as the observed over-all number of PAM-positive fibres visible in the tube lumen for evaluation of axonal re-growth.

### 3.7.1 Axonal Degeneration

#### 3.7.1.1 Description of Stainings with PAM in different Lesion Models

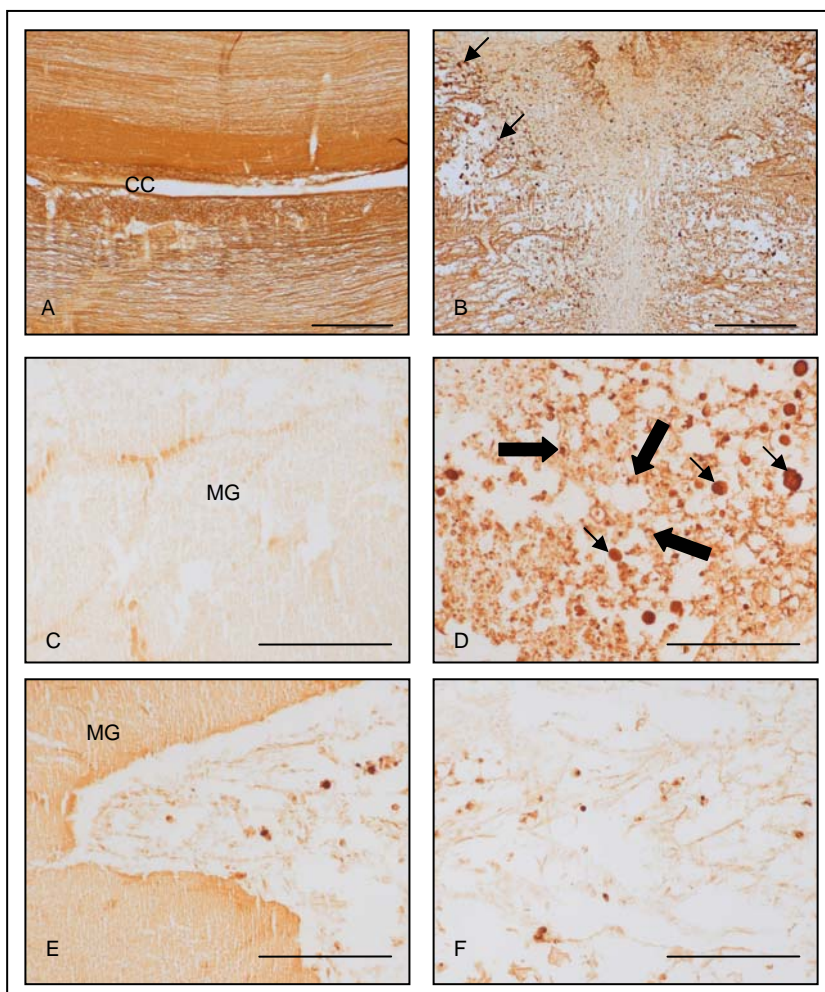


Fig. 3.40: Immunohistochemical micrographs showing staining with PAM in (A) unlesioned rat spinal cord, (B) a 7d SWK lesion and (C) - (F) luminal sections of 7d guidance channel-implanted animals. (A) PAM immunopositive fibres throughout the entire spinal cord. (B) Fibres stop around the lesion site. Retraction bulbs are formed (thin arrows). (C) MG matrix inside the tube lumen. (D) Phagocytosing cells (fat arrows), cellular debris and retraction bulbs (thin arrows) are found in Schwann cell-filled tubes at 7d. (E) and (F) present examples of difficult interpretation. (E) MG matrix. On the right side, the wall might be cut and its matrix including some cellular infiltration is shown. (F) Luminal section probably presenting wall structures (see 3.1.3.3). Scale bars: (A,B) 500 µm. (C-F) 200 µm.

Unlesioned rat spinal cord shows PAM immunopositive fibres over the whole spinal cord tissue. Dorsal column, CST and other fibre tracts are positively stained. The central canal serves for orientation (Fig. 3.40 A). In a 7d SWK lesion, the axons stop at the lesion site and form retraction bulbs (Fig. 3.40 B). No PAM stained structures are visible within the lesion site apart from some cellular debris (not shown). Guidance channel implanted animals in PAM staining present several aspects inside the tube lumen. Matrigel® matrix is visible in the MG/Med group's tube lumen (Fig. 3.40 C). Staining with PAM of Schwann cell-filled channels at a 7d time point often seems filled with phagocytising cells (fat arrows) cellular debris and little pieces of fibres with retraction bulbs (thin arrows) (Fig. 3.40 D). Fig. 3.40 E and F are examples of more complicated evaluation of the lumen contents. The first presenting partly MG matrix on the left hand side and partly probable tube wall material on the right side within the luminal sections (see 3.1.3.3 Fig. 3.4). For the second micrograph it can be questioned whether the visible structures are wall structures, some kind of cellular debris or maybe small fibre segments?

### 3.7.1.2 Axonal Retraction

Retraction bulbs can be found in a great variety in PAM-stained sections of animals in this injury model (Fig. 3.41). Distinction from blood-borne macrophages is important as the fibres often stop in bleeding areas (3.7.1.3). Retraction bulbs are homogeneously coloured. A continuity in fibres often is visible (thin arrows). Macrophages (fat arrows) are more irregular in its contents showing nucleoli. No fibre-like structures are visible in close proximity.

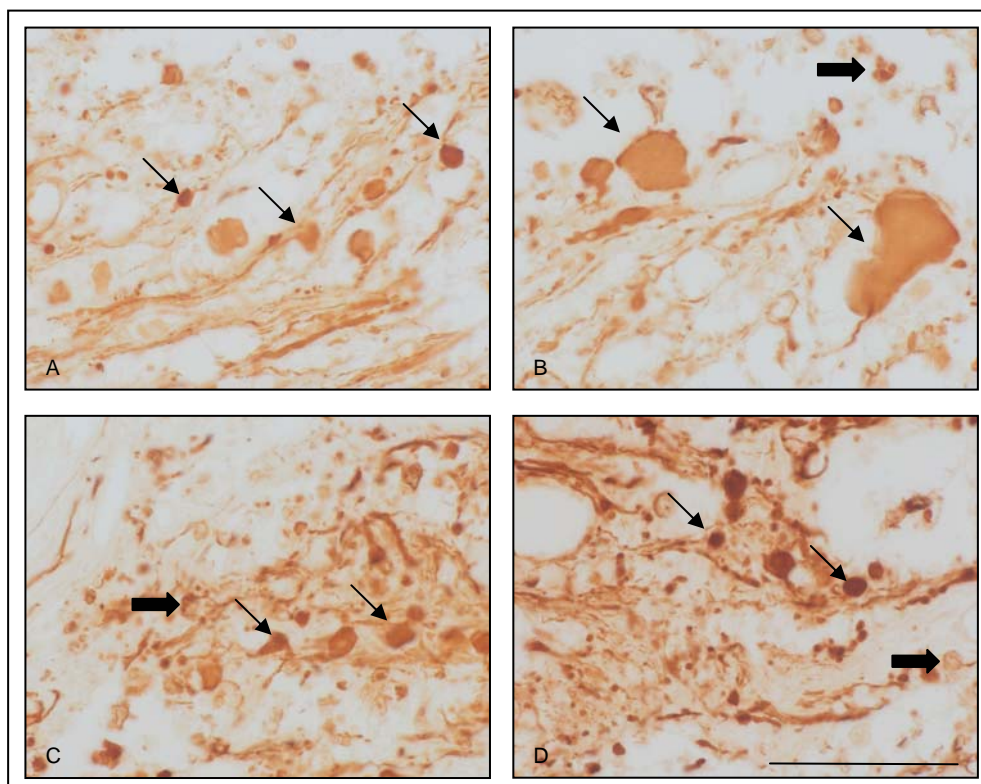


Fig. 3.41: Retraction bulbs as seen in 7d animals throughout this study. (A) - (D) Thin arrows indicate retraction bulbs. Fat arrows show macrophages. Scale bar: 100 µm.

Fibres are observed to stop and form retraction bulbs at the host tissue/lesion interface (Fig. 3.41). Examination of adjacent sections revealed that the Collagen IV containing fibrous scar (Fig. 3.42 1-3 B) is not passed by re-growing axons (Fig. 3.42 1-3 A). The glial scar (also see 3.3.2.1) is shown to be penetrated by some fibres as are sites of bleeding (Fig. 3.42 1-3 C).

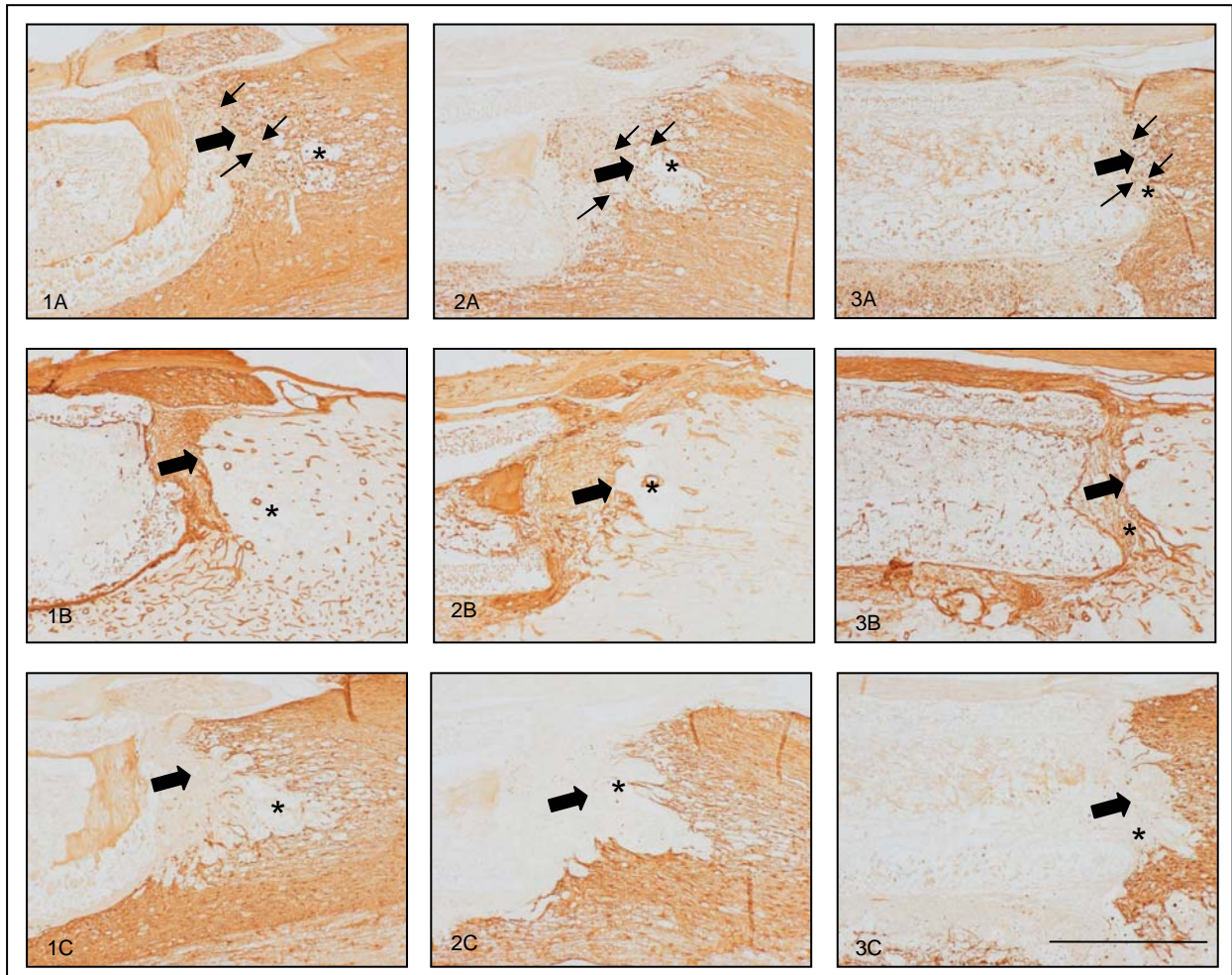


Fig. 3.42: Comparisons of immunostainings with PAM, Collagen IV and GFAP of adjacent sections at 7d in group IIIC3. (1) MG/Med (2) MG/SC (3) AST. (A) Immunohistochemical staining of fibres with PAM. (B) and (C) Complementary staining of the Coll IV immunopositive fibrous scar (B) and the surrounding GFAP-positive glial scar (C). Comparisons of (A)-(C) show fibres in the area of the glial scar whereas no axons are found within or even passed the fibrous scar. Some "loose" fibre-networks are found within areas of inbleeding (stars). Fat arrows indicate the border of the fibrous scar. Thin arrows point out some fibres in PAM stained sections. Scale bar: 1mm.

### 3.7.1.3 Role of Inbleeding on Axon Stop

If no bleeding enlarges the lesion, fibres stop at the collagen front (Fig. 3.43).

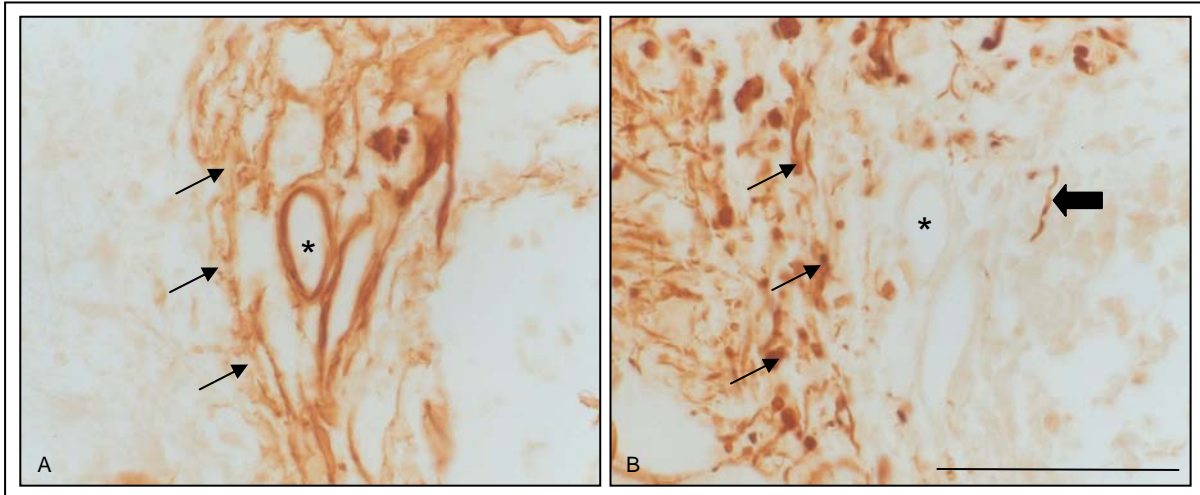


Fig. 3.43: Immunohistological stainings with Collagen IV and PAM of adjacent sections. (A) Coll IV immunopositive fibrous scar.. Thin arrows point at Coll IV depositions corresponding to fibre stop. (B) PAM immunopositive fibres stopping right in front of the collagen sheets. Retraction bulbs are shown, indicated by thin arrows. The stars point out a blood vessel for orientation. The fat arrow in B points at a fibre that seems to have achieved to regrow through a Coll IV "leak". Scale bar: 100  $\mu$ m.

Bleeding sites rostral (Fig. 3.44 A for ED-1 and B for GFAP immunohistological staining) or caudal (not shown here, see 3.3.9.2) to the implant widen the lesion and create new host tissue/lesion borders. Most fibres stop at this new front (Fig. 3.44 C). Some fibres can be observed twisting themselves through this damaged and loosened tissue area (arrows in Fig. 3.44 C), reaching the collagen layers of the original lesion site (Fig. 3.44 D) and stopping there.

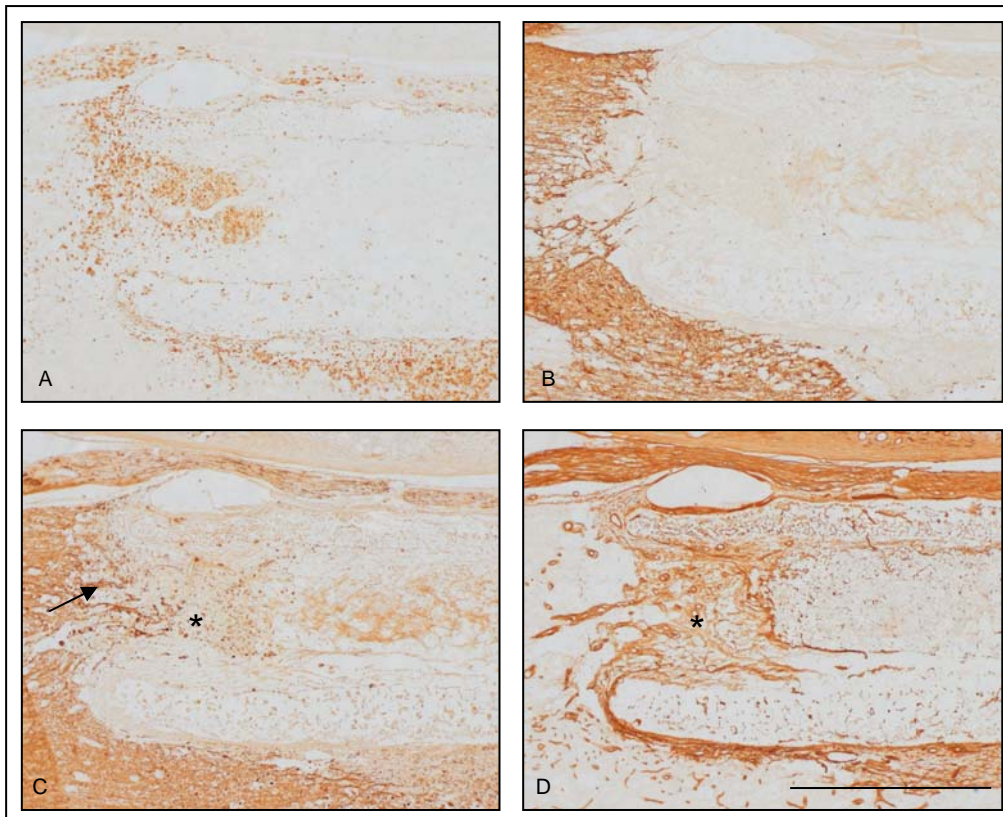


Fig. 3.44: Augmentation of the lesion area through inbleeding and its effect on axon stop. Immunohistochemical micrographs show the site of inbleeding rostral to the implanted guidance channel (A) by looking at ED-1 positive cells and (B) in a staining with GFAP for bleedings extent. The fibrous scar (D) is no more exactly complementary to the glial scar (B) for tissue damage due to the bleeding. The main number of PAM immunopositive fibres (C) stops at the bleeding border. Some axons twist themselves through the loosened tissue to reach the fibrous scar (arrow). Scale bar: 1mm.

### 3.7.2 Axonal Regrowth into the Implant

In most implanted animals fibre growth into the tube could be observed to a certain extent. The first surgical protocol though allowed only a very few axons to extend into the tube (data not shown). After establishment of the improved surgery the experimental group seen below was analysed. Compared to the first OP technique higher numbers of ingrowing fibres could be observed in the guidance channel lumina.

**Filling by capillary force, humid chamber, 1-5h at 37°C and optimized OP-technique, ME-021/PGA-tube**

	7d	14d	1mo	3mo	6mo
MG/Med	n=5	n=2	n=4	--	--
MG/SC GFP	n=4	n=4	n=4	n=4	n=1
AST	n=5	n=3	n=5	--	--

#### 3.7.2.1 Growth into Cell-free versus Schwann Cell-filled Tubes

##### *Fibre Quantity*

Comparing the quantity of fibres regenerated into the tube, animals of group IIIC1-3 are classified into four categories regarding the centre of the tube lumen and the openings: no (--), rare (+), medium (++) or many (+++) fibres visible. Examples for each category are given in Fig. 3.46. Both Schwann cell-filled groups present higher fibre numbers within the tubes than the MG/Med group (Fig. 3.45, no pictures shown).

##### *Time-dependent Growth*

A quantification of fibre number has not been elaborated. For each group, MG/Med controls and Schwann cell-filled (MG/SC and AST) animals, the impression of an increase in axon number with time - at least up to one month – can be gathered. In MG/Med animals at 7d, no axons are visible neither in the tube opening nor in the lumina. SC-groups only show fibres within the tube openings. At later time points, more and more fibres are visible within the openings and lumina (Fig. 3.45). At 14d post-implantation, more fibres are visible than at 7d, again showing more axons at one month than at 14d post-operation. Most Schwann cell-filled animals seem to present a higher axon number than the control group of the same time point. It is impossible to state whether the AST group shows better regenerative results than the MG/SC group, however. No further increase in fibre number is found for the three and six months Schwann cell animals compared to the one month time point of the same group.



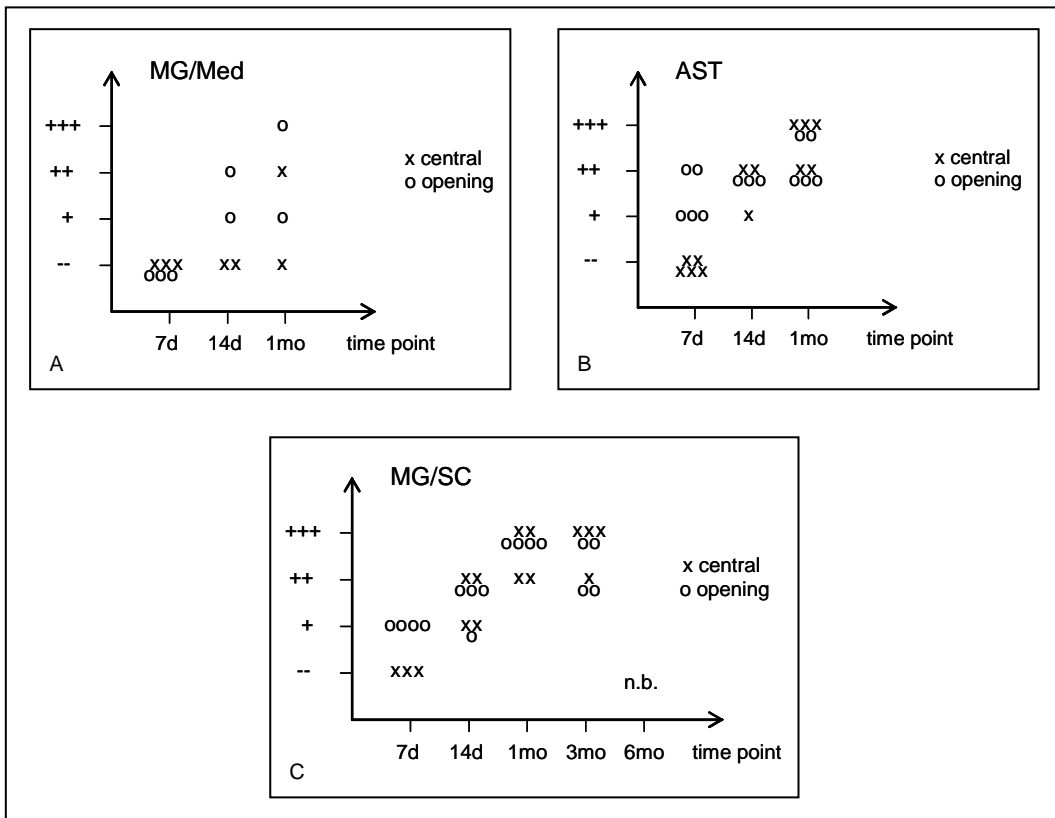


Fig. 3.45: Representation of the fibre quantity found within the guidance channel opening (o) and the guidance channel lumen (x) at different time points in the three different animal groups of IIC. (A) MG/Med group (B) AST group (C) MG/SC group. Both SC-groups are shown to present more regenerating fibres than the MG/Med group. In none of the 7d animals fibres are visible inside the tube lumen. Only the SC-filled groups present fibres in the tube opening at 7d. With time, more and more fibres are found within the tube lumen for both SC-filled groups. Differentiation between the MG/SC and the AST group is difficult.

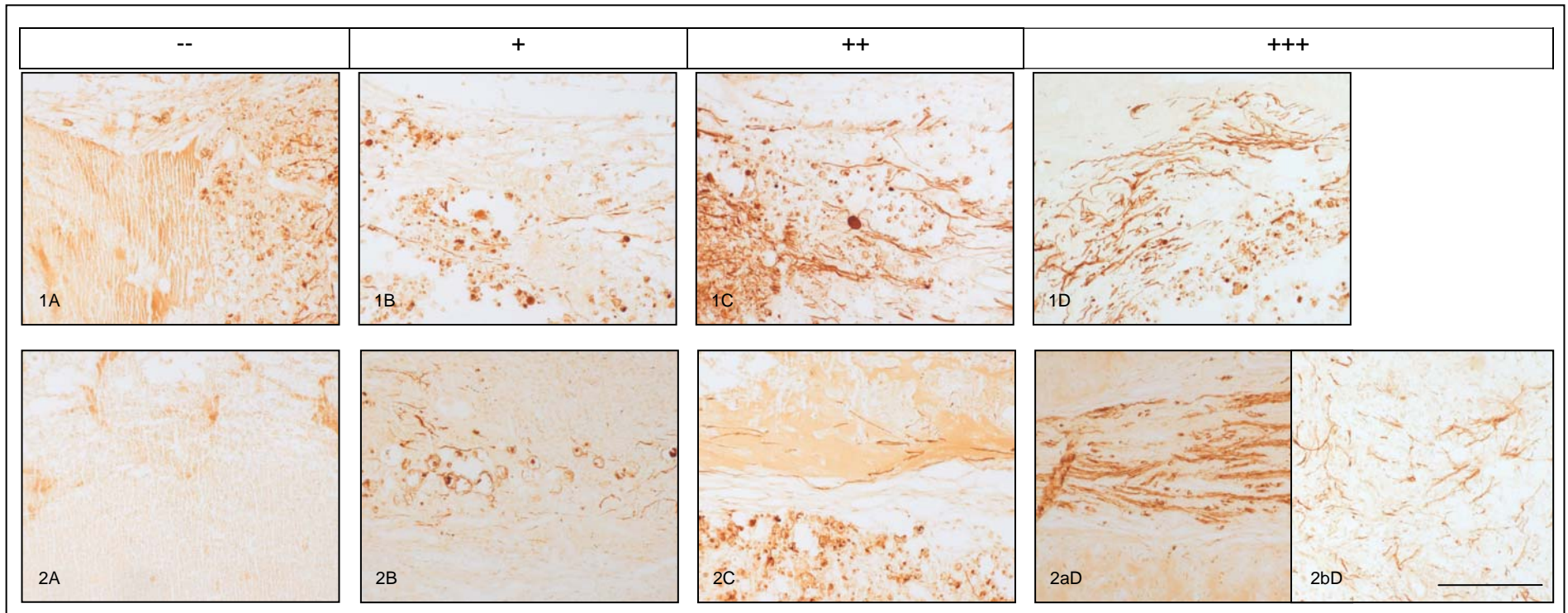


Fig. 3.46: Classification of fibre quantity. Two locations are distinguished : guidance channel openings (1) and guidance channel centre (2) (lumina). Examples of the four categories: (A) no (--), (B) rare (+), (C) medium (++) or (D) many (+++) fibres visible are given for both locations. Scale bar: 200  $\mu$ m.

### 3.7.2.2 Untreated Animals versus Anti-Scarring Treated Animals

At 7d some thin axons are found inside the tube lumen in MG/SC and AST groups. No obvious difference can be stated between treated and untreated animals. The tube opening area comparing the partially reduced animal N405 (Fig. 3.47 A,B) with a MG/SC animal (Fig. 3.47 C,D) shows PAM positive fibres (A) in the reduced area of the Coll IV immunopositive fibrous scar (B) of the treated animal. In contrast, fibres (C) in the MG/SC animal stop right in front of the Coll IV sheets of the fibrous scar (D). At one month, many fibres can be visualised inside the guidance channels (Fig. 3.48). An assessment of fibre number is hardly possible as is a judgement in between both Schwann cell containing groups.

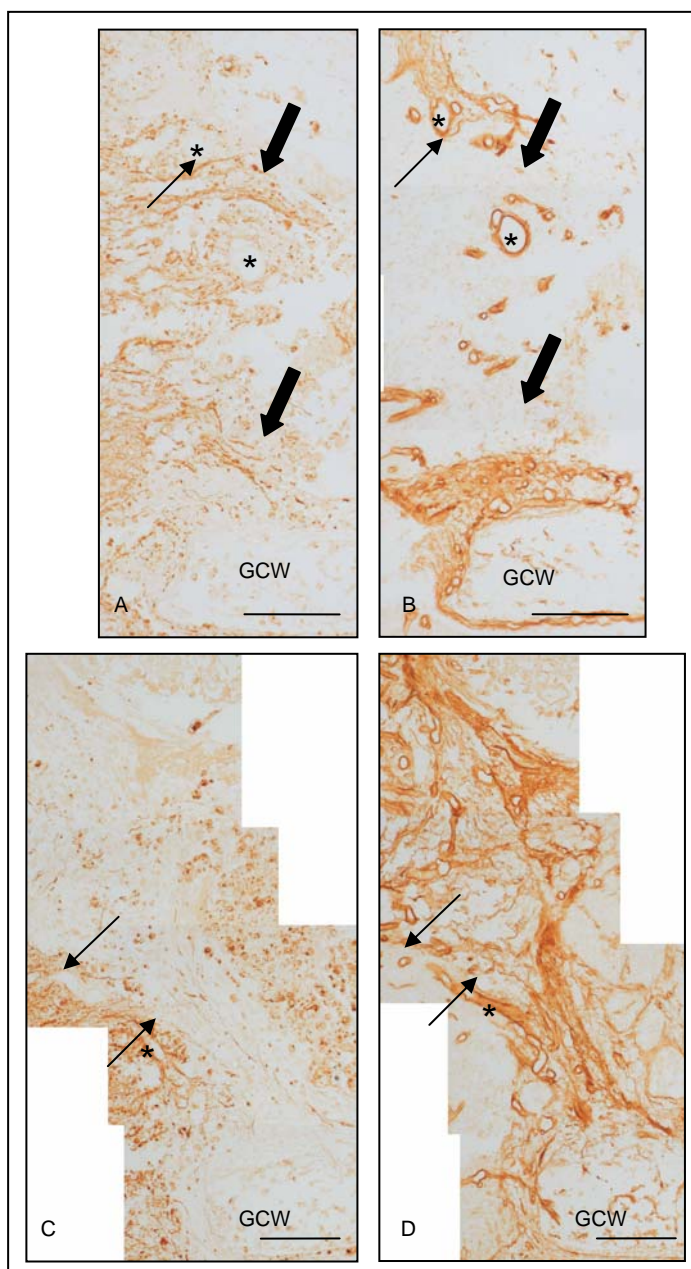


Fig. 3.47: Axonal regeneration at sites of partial reduction of the fibrous scar.

Immunohistochemical micrographs showing (A,C) PAM-immunopositive fibres and (B,D) the Coll IV-immunopositive fibrous scar. (A,B) Fibres are visible in (A) at sites of partial reduction of the fibrous scar in an AST animal (B) as indicated by fat arrows. (C,D) Example of a full fibrous scar in a MG/SC animal (D). Fibres stop where Coll IV positive sheets are found (C). Thin arrows point out the corresponding site of fibre stop. Stars point at blood vessels for orientation. Scale bars: 200  $\mu$ m.

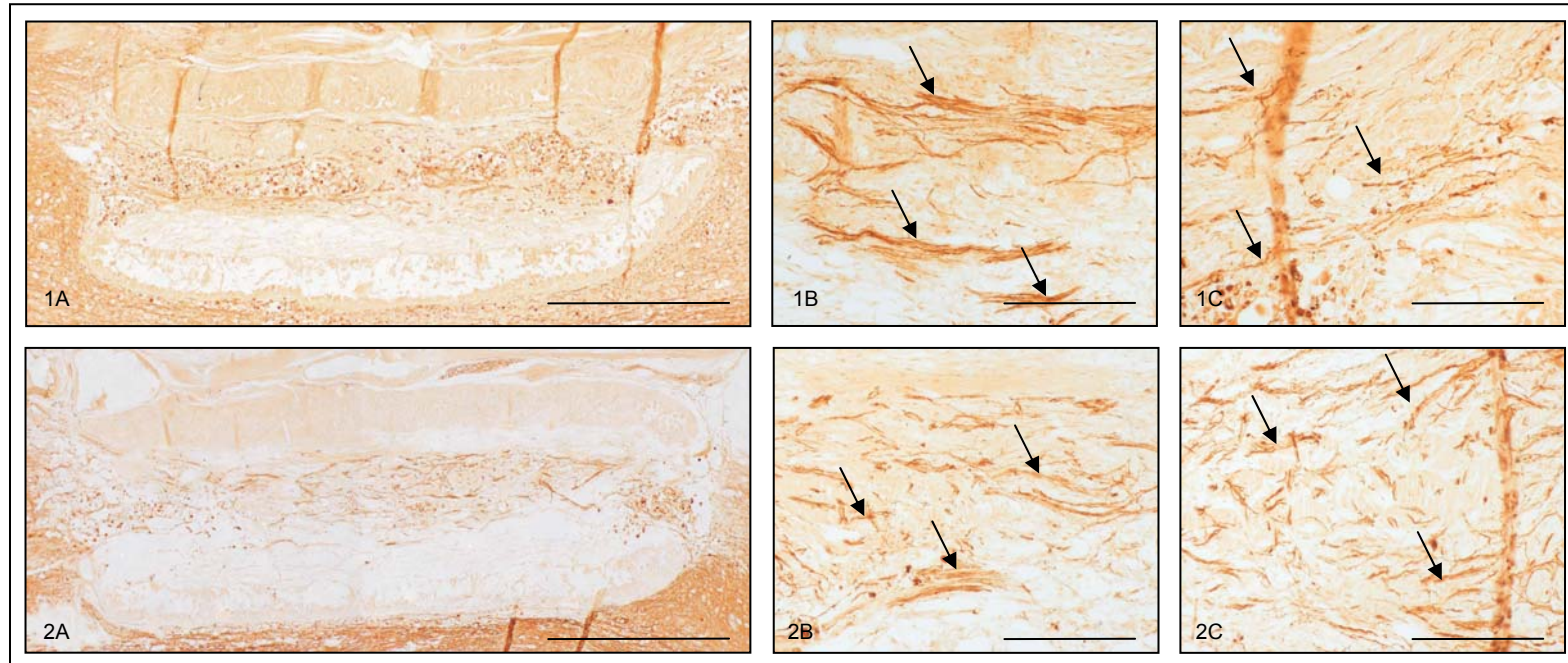


Fig. 3.48: Axonal regeneration in the Schwann cell-containing groups at 1month. Immunohistochemical micrographs comparing PAM-positive sections of MG/SC (1) with AST (2). (A) Overviews of the entire guidance channel length to get an impression on the number of fibres inside the tube lumen. (B) and (C) show magnifications of stainings with PAM at different locations – (B) more centrally located, (C) closer to a tube end. Many regenerated fibres are visible inside the lumina of both groups (arrows). No differentiation is possible. Neither is a valid assessment of fibre number. Scale bars: (A) 1mm. (B,C) 200  $\mu$ m.

### 3.7.2.3 Association of Schwann Cells with regenerating Fibres

The staining of adjacent sections of 10-40  $\mu\text{m}$  with PAM showing fibres and eGFP visualising SCs demonstrates a close proximity of these structures. Fibres and SCs are associated with each other in many cases (Fig. 3.49).

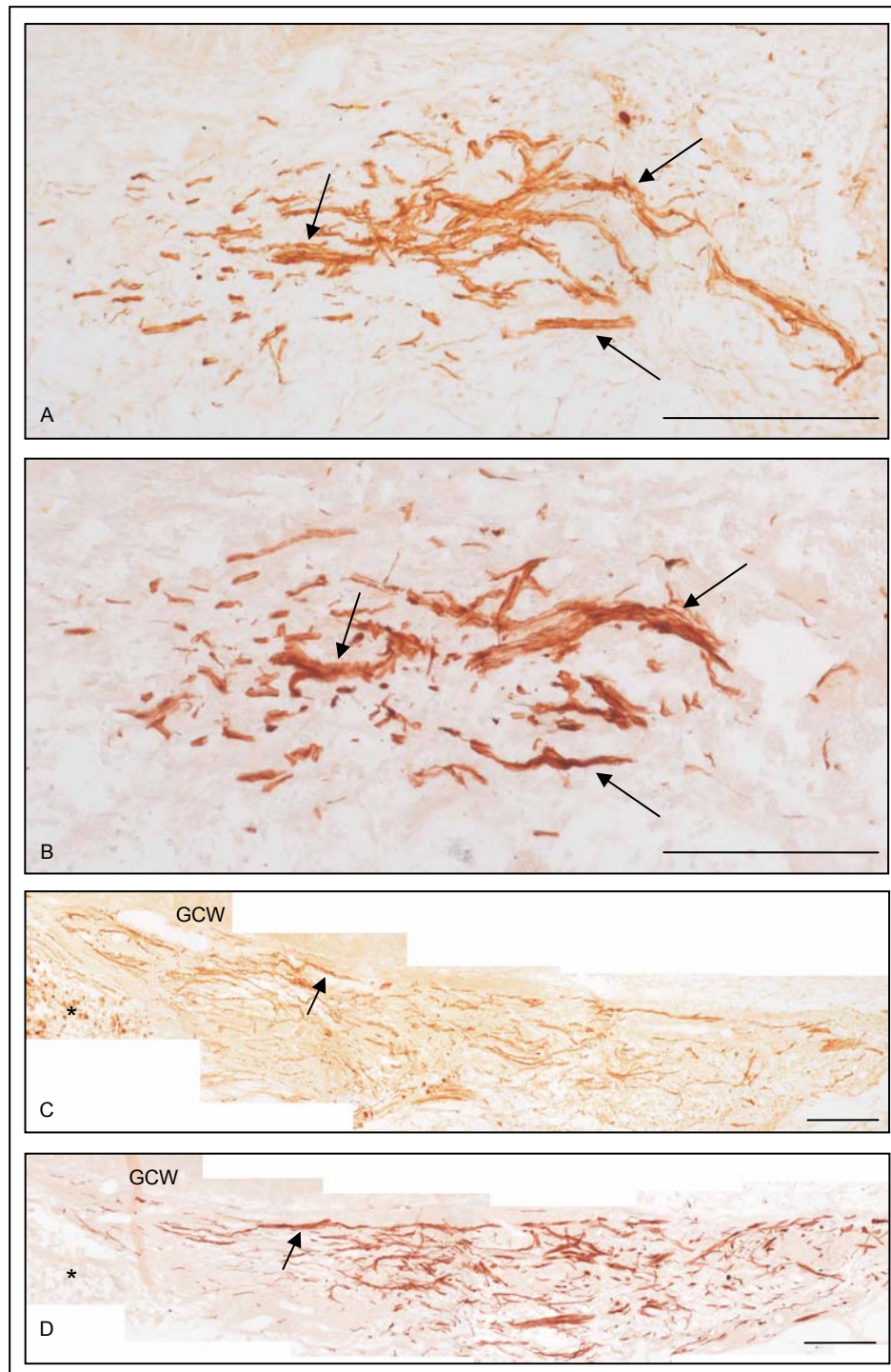


Fig. 3.49: Close association of PAM positive fibres and eGFP positive implanted Schwann cells. (A) and (C) Immunohistochemical micrographs showing PAM-immunopositive fibres at 1month. (B) and (D) DAB-visualisation of eGFP-labelled Schwann cells in sections adjacent to (A) and (C) respectively. Arrows indicate the close proximity of fibres and SCs. The star in (C) and (D) points out a site of bleeding for orientation. Scale bars (A,B) 100  $\mu\text{m}$ . (C,D) 200  $\mu\text{m}$ .

### 3.7.2.4 Observations in Immunohistological Stainings with PAM

To demonstrate some of the difficulties or surprises observed in PAM positive immunostaining, some examples are given in Fig. 3.50.

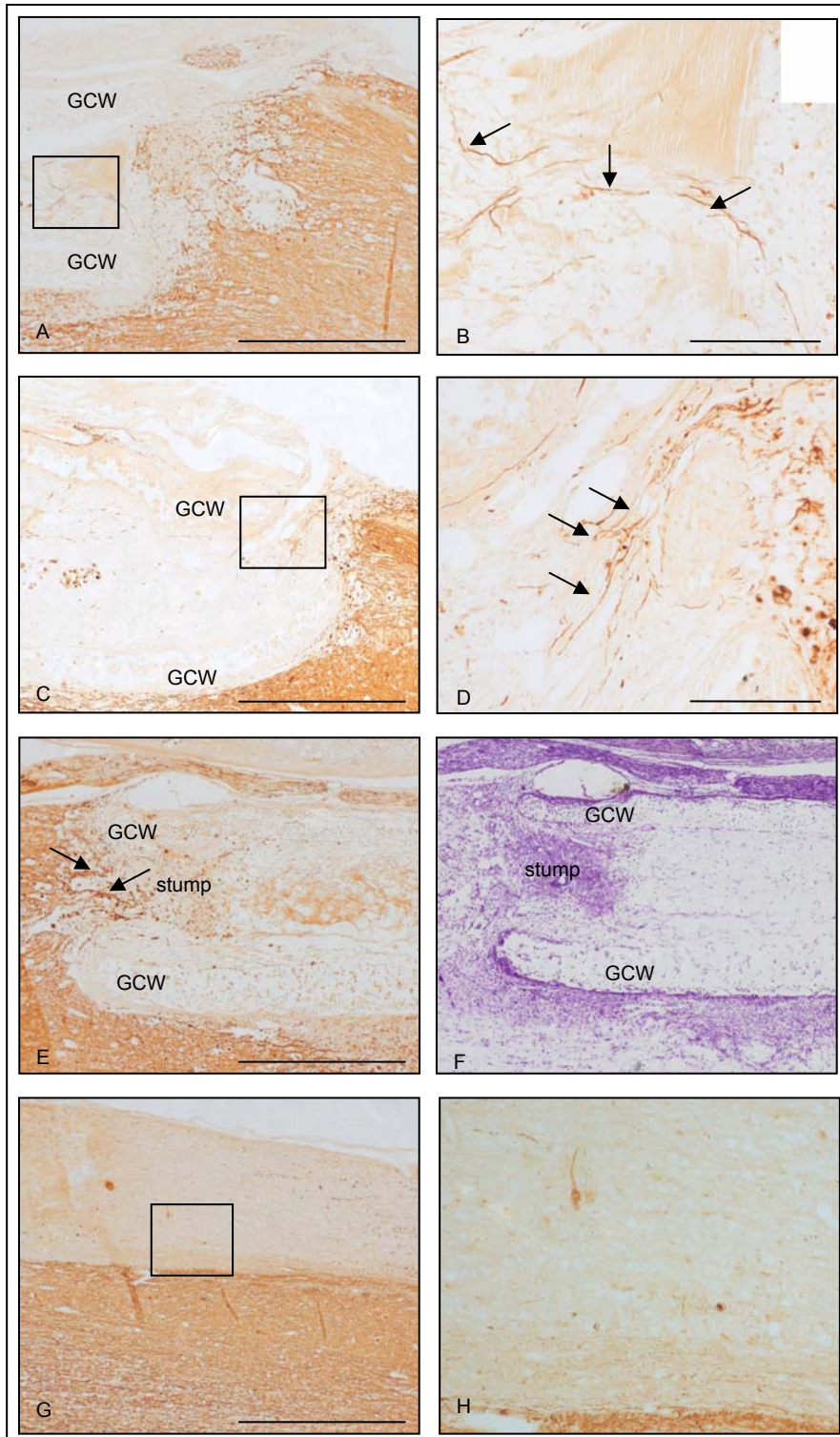


Fig. 3.50: Observations made in staining with PAM. (A,B) Quite a number of fibres are visible within the guidance channel opening at 7d (arrows). (C,D) The guidance channel is bend at its distal part. The number of entering fibres is limited. (E,F) Rather a number of fibres are visible in the proximal tube opening of the section stained with and antibody against PAM. The introduction of the proximal tissue stump can be visualised in Nissl staining of an adjacent section. (G,H) Little PAM immunopositive staining in the dorsal column is found at three months. Scale bars: (A,C,E,F,G) 1mm. (B,D,H) 200  $\mu$ m.

### 3.7.3 Traced Fibre Tracts

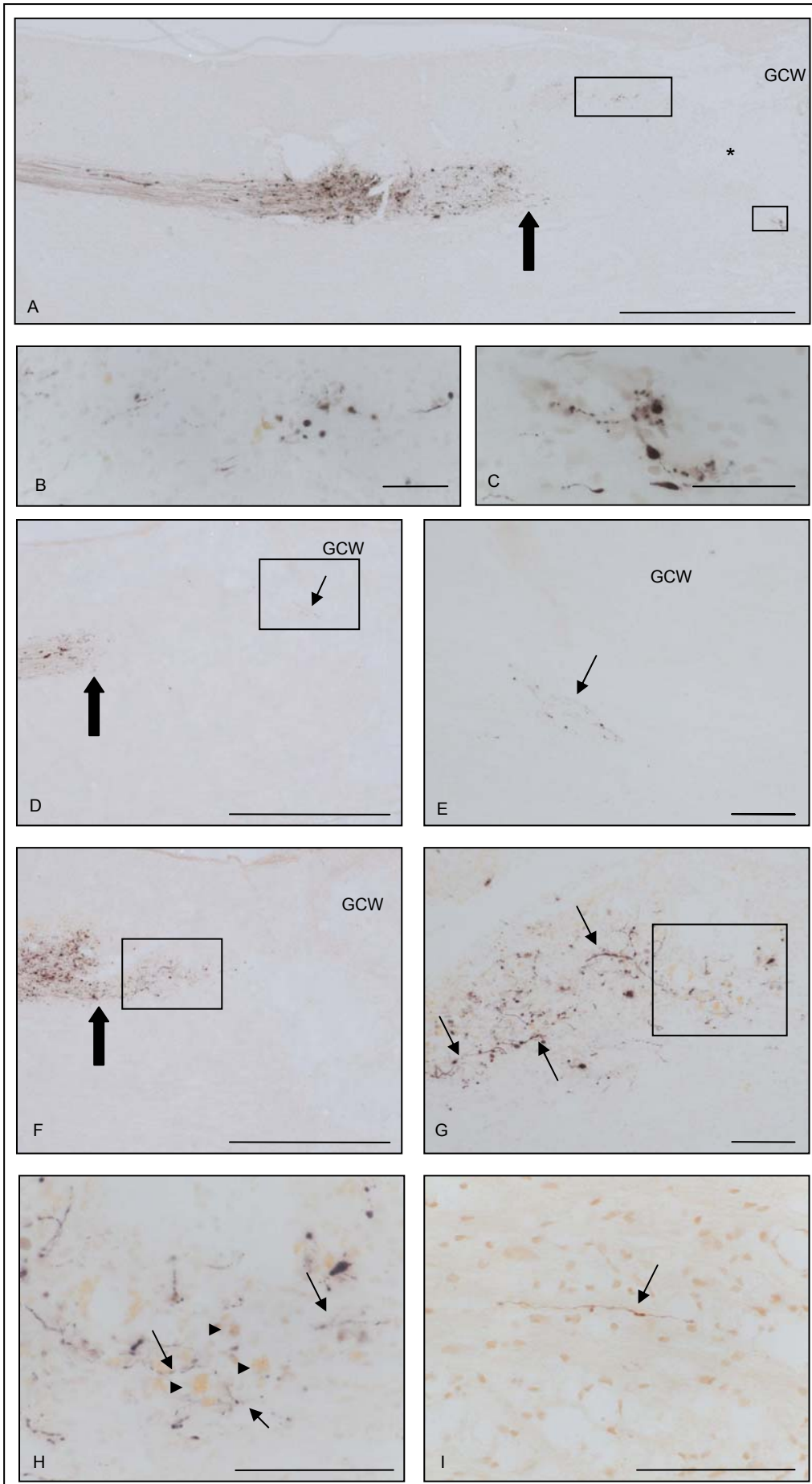
#### 3.7.3.1 Fibre Origin

Immunohistochemical staining against PAM reveals the presence of fibres. Fibre origin and differentiation of re-growing fibre tracts is not possible by such a staining. Regeneration into and through the implanted guidance channel as well as fibre re-entry into the host-tissue at the other tube end cannot be evaluated. Tracing studies are necessary for further information on fibre origin.

#### 3.7.3.2 CST Tracing with BDA

The course of the CST was taken as a marker for guidance channel placement (see 3.1.3.1). Its facing luminal sections is essential for potential positive CST fibre regeneration through the implant (Fig. 3.52 A, C). It was observed that in some animals the guidance channel's lumen was not open in the sections where the CST was best traced but in sections before or after (Fig. 3.52 B, D). CST tracing did not show regenerating fibres neither inside the tube lumen nor distal to the lesion in any of the animal groups (data not shown). The CST stopped rather far in front of the implanted guidance channel, at the most proximal point of the lesion's inbleeding (Fig. 3.51). The spinal cord parts distal to the tube, cut on the frozen microtome as 50µm sections, did not reveal any regenerated fibres in fluorescent Avi-Alexa 488 staining neither (data not shown).

Fig. 3.51 (next page): Staining of BDA-traced CST fibres with ABC. The stopping of the main fibre tract rather far in front of the GCW is indicated by the fat large arrows in A, D and F. Thin arrows point out regenerating fibres. The star shows tissue destruction rostral to the tube opening in A. Fat arrowheads in H point at cell debris of blood-born cells in a bleeding site. (A) Overview of a traced fibre tract with the main part stopping far before reaching the GCW. (B,C) are magnifications of regenerating fibres much closer to the GCW. The locations are squared in A. (D) demonstrates another overview of a fibre tract stop far in front of the implant. (E) Magnification of some regenerated fibres close to the dorso-rostral GCW as seen in D. (F-H) Some fibres twist themselves through a site of bleeding. (I) A solitary thin regenerated fibre in spinal cord tissue rather close to the rostral GCW. Scale bars: (A,D,F) 1mm. (E,G,H,I) 100 µm. (B,C) 50 µm.





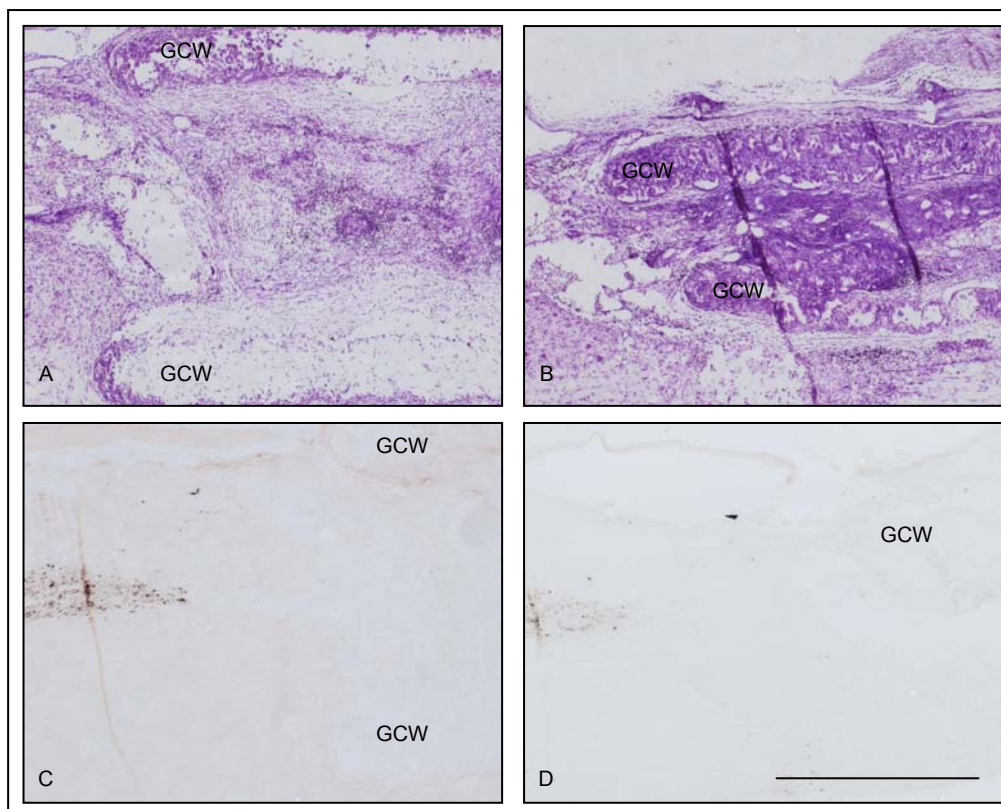


Fig. 3.52: Guidance channel placement in regard to the course of the traced CST. (A,C) Examples for good guidance channel positioning, the traced CST stump facing the tube lumen. (B,D) Bad tube positioning. The CST stump faces an already closed implant. (A,B) Nissl staining. (C,D) ABC immunostained sections. Scale bar: 1mm.

### 3.7.3.3 Dorsal Column Tracing with BDA

The dorsal column tracing with a BDA-soaked piece of gelfoam introduced at the Th 11 level did not reveal any fibres inside the tube lumen nor proximal to the implanted channel. The labelled axons stop before entering the tube lumen at the inbleeding's border to host tissue. This tracing model first was tested on three animals, a control animal without any lesion, a SWK-lesioned and a guidance channel-implanted animal. In the control tracing, dorsal column fibres from Th11 on over the whole spinal cord specimen were labelled, the number decreasing with distance. The SWK - lesioned animal showed less positive staining. Fibres did not reach or cross the lesion site, no fibres were found proximal to it.

In the guidance channel animal receiving the tracing and channel implantation during the same operation, only in the distal parts of the dorsal column traced fibres are observable. Fibres stop far from the lesion site, none were found within the tube or proximal to it. It is to be recognized that the stained fibres give a degenerating aspect (data not shown).

## **4.0 Discussion**

### **4.1 Improvement of the Experimental Setting**

#### **4.1.1 Improvement of the Guidance Channel Filling Procedure**

Guidance channel filling under reproducible, sterile, controllable conditions as objective, the filling procedure applied for this study imposed a certain development. It had to be assured that by the time of implantation, the tube piece of several millimetres is still filled. The idea to implant an empty guidance channel and, once placed, fill it by injection of MG/MedSC mixture rapidly has been abandoned. The tube material did not resist the pressure applied when trying to pierce the wall but was deformed and compressed in the middle. No control of complete tube filling would be possible neither.

One theory for the diminution of the MG/Med mixture inside the tube lumen in setting A (see 2.3.2) was the MG consistency. Matrigel® was very liquid and thought to be able to invade the wall structure micropores. Incubation at 37°C was said to change MG's consistency into a more gelified state (Schlosshauer et al., 2003). The filling could still not be guarded 100%, however. Histological observations (see 3.1.3.3 Fig. 3.4 D) might underline the suspected decrease in filling. Other groups (Xu et al., 1997) describe similar effects regarding histology: the tissue cable diameter is smaller than the guidance channel diameter in several animals. Possible explanations might be an insufficient filling or its retraction for unknown reasons. More probable, however, is a shrinking / detachment of the tissue cable from the tube walls during tissue preparation (see 3.1.3.3). The fixative perfusion with PFA or high temperatures necessary for Paraffin-embedding could be accounted for. Unfortunately, visualisation of the tissue cable in control tissue or in un-implanted SC-filled guidance channels was not possible. Prepared for Frozen Microtome sectioning, the tube broke out or the tissue cable was lost in PBS just before mounting of the section.

The incubation technique applied in method C is based on the humid chambers existing in histological staining procedures where antibodies have to be incubated over a longer period of time. Less antibody is necessary since the applied amount does not evaporate. Same is valid for the guidance channel incubation. Histologically, the impression of better filling than in previous techniques can be drawn. The filled channels' incubation time at 37°C varied between one to five hours before implantation. This was due to facilitation of the experimental setting. Channels were filled first, incubation was started and then the operations began. Incubation time before implantation should not make crucial differences, though, since 37°C is body temperature as well.

### **4.1.2 Optimisation of the Surgery**

Lesion models are created to mirror certain aspects of human SCI in structural lesion gravity as well as for measurement of functional improvement. Sharp transection lesions are applied to visualise the axonal regeneration of specific tracts whereas blunt lesions like the contusion or compression model are more realistic compared to human SCI. The neuropathological evolution over time is very important in human SCI and can be simulated by blunt injury models (Kakulas, 1999b;Kwon et al., 2002b). One negative aspect, however, of blunt injury models for regeneration studies is the occurrence of spared fibres. It is always questionable if regeneration or functional improvement is due to those spared fibres or to real regeneration.

None of the three current lesion models described in 1.10 seemed appropriate for this study. Leading ideas for the development of a new injury model were animals' health and a better transfer to human SCI's pathology. Even in completely paraplegic patients, the cord rarely is entirely transected but there is some residual parenchyma in the lesion's periphery (Kromer and Cornbrooks, 1987). An incomplete lesion combining partial cut and aspiration was developed in regard to the potential interest in neurosurgery following chronic SCI where resection of tumor, metastase, scar or syringomyelia would be necessary. The development of such a model made improvements and modifications necessary.

Facilitation of the implant handling and tube positioning to reach a certain degree of reproducibility were important factors (see 2.5.1, 2.5.2). It was decided not to modify the modus of the AST application bringing good results in SWK lesions (Hermanns et al., 2001b;Klapka et al., 2005) to restrain the number of modified variables where possible. Since in this injury model two lesion sites are created, the AST is applied at both tissue/tube interfaces. The injection of BPY-DCA, however, posed some problems. Piercing the dura with the glass capillary was not possible. Other essays failed as well. This led to the conclusion that injections had to be placed directly into the spinal cord tissue at both host tissue/guidance channel interfaces. To achieve this, the dura-opening needed to be longer than the aspiration-lesion to leave visible and accessible the rostral and caudal host-tissue/implant interfaces for the AST-injections. cAMP application did not pose any problem. The "powder" was placed on top and cautiously into the fissure at both interface areas. Elvax copolymer handling in the final experimental injury model is a little delicate for its dislocation when bleeding occurred during dura closure but without further difficulties.

### **4.1.3 Histological Phenomena observed in Nissl Stainings**

Improvements of the guidance channel filling method and the surgery led to the elimination of some of the in 3.1.3 stated phenomenons. Others are still found in histology of groups IIIC 1-3, the last animal groups operated.

### *Guidance Channel Positioning*

In this injury model, tube positioning is one of the most important factors of the experimental setting influencing the regeneration results. Good guidance channel integration into the spinal cord depends very much on the aspiration lesion. The reproducibility of this injury has its limits, though. The exact median location is difficult to achieve, same is valid for a reproducible aspiration depth which should be a must in a standardised operation. For this model, however, standardisation of lesion depth is not applicable. The outer guidance channel diameter varies extremely with the inconsistent wall thickness of the channels (see 2.3.1, 4.2.1). This problem is due to manufacturing. If the lesion depth is not modified according to the guidance channel to be implanted, a complete channel's integration into the host tissue would not be possible. The preliminary operating techniques (see 2.5) first placing one tube end, then the second one are suspected to be another reason for channel mal-positioning. Optimisation providing tube placement in a lesion site of exact size as well as re-suture of the dura for stabilisation of tube placement led to better results - no more inclination or incomplete channel integration as demonstrated in 3.1.3.1 Fig. 3.1 and 3.2 can be observed in the latest animal groups IIC 1-3.

### *Tube Stability*

Handling too mellow material might result in guidance channel compression with the effect of filling loss but also diminution of inner diameter and therefore less space for regenerated fibres. Hints for that are given by the shown examples of down-bent tube ends and median walls in 3.1.3.2 Fig. 3.3. A functional closure of the channel end can be the consequence of such down-bending leaving less possibility for potentially regenerating axons to enter the lumen (see 3.7.2.4 Fig. 3.50 C, D). Median compression has to be differentiated from tube deformation discussed in 3.2.1. The time point and the degree of cellular infiltration of the tube walls might count as leading factors for differentiation. Tube material's stiffness could cause additional micro-lesions at the host tissue / implant sites with, in consequence, more important scarring inhibiting regeneration.

### *Tissue Bridge*

Description and clear distinction of a forming tissue bridge proves to be rather delicate. The tissue bridge in the tube lumen has been shown to "shrink" (3.1.3.3 . Fig. 3.4 D). Similar observations can be made regarding histological stainings published by other groups (Guest et al., 1997b; Ramon-Cueto et al., 1998; Xu et al., 1995b; Xu et al., 1999). Surprising was, that not all of the implanted tubes presented such a tissue-bridge-shrinkage. Sections showing a complete guidance channel filling were observed. This, among other facts, led to the idea that shrinkage might be due to desiccation of the tube material with, in consequence, modification of the filling technique (see 2.3.2). Another possible explanation is tissue processing necessary for histological evaluation of the study. PFA, the alcohols or the heated paraffin might result in such "shrinkage". Distinction of a potential tissue bridge in

the centre of the lumen and wall structures invaded by some cells often poses a problem. Little tube stability might have led to some squeezing of the guidance channel while handling, the tube usually touched in the middle with a pincette (see above). The consequent diminution of the tube's inner diameter could explain that the filling can only be visualised in a small number of luminal sections. Adjacent sections present themselves as being "empty" which refers to the space in between the tissue bridge and the tube wall described above due to the shrinking processes. Next sections show the cellularly-invaded wall. Surprising to see was the high cell number present in the dorsal tube parts demonstrated in Fig. 3.4 B and C in 3.1.3.3. Since no filling at all had been administered into the channel, invasion of some kind of cells has to be suspected. Dura was left open after tube implantation in the animal discussed on. Dorsal location as well as cell morphology lead to think of fibroblasts in the first place (also see 3.5.2). Another possibility is that Schwann cells originating from the dorsal root ganglia might have invaded the guidance channel. Cell morphology is similar to fibroblasts (see 3.5.2) and the dorsal location could be explained by the vicinity to the ganglia.

#### *Tube Wall Dissolution*

A further probable consequence of tissue processing might be the observed "dissolution" of tube wall segments or even the entire tube material (3.1.3.4 Fig. 3.5). This hypothesis could be emphasised by the fact that the phenomenon was found throughout all animal groups and for both materials applied (ME-008 and ME-021). An effect on regeneration could only be speculated on and seems rather not probable. Depending on the amount of tube wall material disappeared, histological evaluation of the fibrous scar, however, is not representative and therefore worthless (see 4.6.3).

#### *Bleeding Sites*

Bleeding sites can be understood as functional regeneration inhibiting barriers (see 3.3.1). Bleeding proximal or distal to the tube opening also disturbs the continuity of a tissue bridge formation for fragility of the spared host tissue. Same is valid for bleeding sites within the tube lumen. It seems very likely that there is a link between the occurrence of inbleedings, cyst formation and tearing of the tissue. The bleeding thrusts aside tissue. Cavernous structures are found and, with time, cysts might form if the blood is not fully re-absorbed. This could explain the higher prevalence of cyst-like structures at later time points. Cysts, as sites of inbleeding, can block the tube openings leading to a functional barrier if located close to the tube ends. At other locations, they might exert pressure on the tube end to bend and, again, lead to a functional regeneration barrier. Inbleeding itself leads to a loosening of the tissue interactions. Tissue is damaged and ripping is facilitated. Some imagination might be necessary to visualise the complementary split ends (data not shown). Whether seen as one or several phenomena, the importance lies on the potential functional consequences.

## **4.2 Material Properties of the Implant ME-021/PEG**

### **4.2.1 Material Properties**

The implanted tubes showed differences in stability and flexibility which might pose problems of facilitated breaking when longer pieces are integrated (Sinis et al., 2005). Some other possible consequences have been demonstrated in 3.1.3.2 Fig. 3.3 and discussed earlier (4.1.3). Differences in wall thickness lead to a discrepancy in the outer tube diameter. It is unknown if nutrient diffusion and prevention of cell invasion are comparable in between the channels. For further information on the material used refer to (BMBF, 2000;BMBF, 2002;Lietz et al., 2005;Schlosshauer, 2003). A similar material has been studied and considered a potential effective in nerve repair (den Dunnen et al., 1996;Fabre et al., 2001).

### **4.2.2 Tube Degradation**

The coincidence of the three in 3.2.1 depicted observations leads to the conclusion that cellular wall invasion, wall deformation and diminution of the number of luminal sections can be seen as important factors in tube degeneration processes. If any of those on-goings plays a leading role is not known. Combined, though, the three factors might be evaluated as a marker for guidance channel degradation. Nevertheless, this rests a hypothesis and needs to be proven with higher animal numbers. The continuous deformation of the implanted tubes is no surprise since the material was said to be degradable. If its deformation is a descriptive factor for degradation cannot be proven. Nonetheless, the time points of deformation correspond to the time points of higher cellular infiltration of the tube walls and, at later time points, also with the decreasing number of luminal sections. Exceptions for visible deformation at early time points (3.1.3.2 Fig. 3.3 E) could be explained by material manufacture time differences, the used material being “elder” at the time of implantation, having begun degradation already. It rests unclear whether the described cellular infiltration of the GCW is a cause for tube material degradation or a consequence. In this study, a time point for complete disappearance of the tube material could not be defined. At six months, there is still material to be seen at the lesion site. Complete biodegradability rests to be demonstrated in a follow-up study. Whether the degradation of the guidance channel material affects the axonal regeneration can only be speculated on. With the diminution of the number of luminal sections at later time points, the inner tube diameter is probable to decrease as well. A spatial restriction for regenerating fibres could be the consequence. Deformation of the GCW could also lead to a similar narrowing of the inner diameter. Cellular infiltration of the GCW might be a reason for tube deformation. An effect on regeneration due to the invading cells themselves is not very probable.

## 4.3 Characterisation of the Spinal Cord Lesion

### 4.3.1 Lesion Size

Characterisation of the lesion and its extent is extremely difficult in this injury model. There are discrepancies in lesion size between different animals and even between various sections within one animal, mainly due to the length of the aspiration lesion (also see 3.1.3.1 and 4.1.3) and the occurrence of bleeding at various locations (3.3.1.2 Fig. 3.16). The size of the cut-aspiration lesion, for best case the implant length, describes the actual lesion dimensions. The easiest way to describe the lesion extent would therefore be the measurement of the implanted guidance channel including a small margin of lesion around due to tube integration. In practice, this is not applicable. Inbleeding at various locations and of different dimensions modifies the lesioned host tissue quantity. Functionally, such sites of bleeding act as additional regeneration inhibitory barriers (see 3.7.1.2 and 3.7.1.3). The theoretic lesion size, therefore, is not equal to the functionally relevant lesion. There are several explanations for occurring bleeding. Every *operation* leads to a certain degree of bleeding at the lesion site. The spinal cord pre-cuts, the aspiration and tube integration are just some examples of steps during surgery that might provoke blood to enter the lesion site. Animals' *anaesthesia* has to be considered when discussing bleeding. Depending on the depth of anaesthesia, bleeding was provoked by more or less important manoeuvres during operation. The time point of the rats' *first movements*, possibly influencing post-operative bleeding at the lesion site, also depends on the depth of anaesthesia during operation.

In regard to the above stated, visualisation of the sites of inbleeding is necessary for determination of the lesion dimensions. Measurements have to include the sites of inbleeding rostral and caudal to the implant. Staining with ED-1 (3.3.1.2 Fig. 3.15 A) illustrates lysosomal cells (Leskovar et al., 2000), in this case essentially blood-born macrophages. The distribution of ED-1 immunopositive cells seems to be co-localised with the "vacuole-like" structures visible in stainings with GFAP on adjacent sections (Fig. 3.15 B). The measurement of lesion size has been carried out on GFAP-stained sections since a delimitation of bleeding from spared host tissue is more obvious. Median luminal sections were compared. Only two to four sections per animal have been stained with the GFAP antibody, however, and the median section might not be among these. Variations in lesion size could be due to this fact. It would be interesting to check whether the bleeding in AST treated animals and in group IIB2 (TRIS-injections) in dorsal spinal cord is broader than in control or Schwann cell-only animals. If this was the case, a correlation with injections damaging the until then spared, healthy host tissue, could be suspected. Another interesting correlation would be the comparison of fibre number and bleeding size. Less fibres would be suspected in animals presenting large lesions, that is large inbleedings. In this study, such a statement would not be integer for too little animal numbers.

## 4.3.2 Cellular Reactions after Lesion

### 4.3.2.1 Astrogliosis

As expected, immunohistochemical micrographs in unlesioned rat spinal cord tissue show a positive but not very prominent staining with GFAP (Eng et al., 2000). Any lesion of the spinal cord leads to an upregulation of glial fibrillary acidic protein in astrocytes that can be visualised by applying the described GFAP antibody (Reier and Guth, 1983; Fawcett and Asher, 1999; Eng et al., 2000; Silver and Miller, 2004). Quantification is not possible, though. Neither the prominence of the brown staining nor cell morphology nor cell number can be understood as hints for the quantity of upregulation. Morphology is more related to cellular location within the spinal cord. Star-like cells are found more often within the white matter whereas longitudinal, fibre-like cells, most often are located in the gray matter. Cell number is impossible to assess and the darkness of the staining mainly depends on minor variations following the immunohistochemical staining protocol. Fig. 3.18 in 3.3.2.1 gives two examples, the SWK lesion and the injury applied in this study. The observed distribution of the positive staining with GFAP leads to the following conclusions:

1. The complementary distribution of immunohistochemical stainings with GFAP- and Collagen IV antibodies in this study, already described for other lesion models (Hermanns et al., 2001a; Hermanns, 2001; Klapka, 2003), underlines the repartition of scarring in two components, the fibrous and the glial part (Klapka et al., 2002) (1.7 Fig. 1.4).
2. Astrocytes are said to have a repulsive effect on SCs and vice versa (Franklin, 2003). The lack of astrocytic invasion of the tube lumen and wall is, therefore, not surprising for the SC-filled groups. SCs potentially have a “loosening” effect on the glial scar. The presence of some astrocytic processes observed in tube opening areas as shown in 3.3.2.1 Fig. 3.21 only at later time points underlines the necessity of time for the processes to newly grow into the tube opening.
3. Regarding the enormous lesion in this study, it does not surprise seeing the GFAP-upregulation still prevalent at six months. The longest time point at which a still high GFAP-upregulation has been observed in our laboratory was at 6 months in spinal cord and at two years following a fornix lesion (unpublished data). Examination of spinal cord segments more proximal or distal to the actual lesion site would be interesting. GFAP-upregulation extending for at least one centimetre around the lesion site in rats is described (Fawcett and Asher, 1999).
4. No differences in GFAP upregulation of the treated and the untreated SC-containing groups are suspected. The AST focuses on the delayed development of Collagen IV sheets (iron chelator) and inhibition of fibroblast proliferation (cAMP) (1.7.6). Astrocytes are not supposed to be influenced in any way.



#### 4.3.2.2 Inflammation

In an injury model like this one it is very important to find out whether any of the implanted material leads to an inflammatory response of the host tissue. The guidance channel material itself, its degradation products or the implanted Schwann cells could trigger and promote inflammatory reactions within the rat spinal cord (Nicholas and Arnason, 1992). To illustrate such an inflammatory response, T-cell stainings for CD4 (helper cells), CD8 (cytotoxic cells) and CD3 (pan-T-cells) are imperative (Wekerle and Meyermann, 1986;1994). Since the establishment of those antibodies has not been positive yet, an ED-1 marker visualising activated phagocytic cells has been applied. The origin of the ED-1 positively stained cells, however, remains unknown. It cannot be distinguished between cells reactive to inflammation like microglia cells or blood-born cells as macrophages “flooded in” by inbleeding (Leskovar et al., 2000;Fitch and Silver, 1997;Dusart and Schwab, 1994).

The scarce invasion of the guidance channel walls by stained cells could be a sign for little inflammatory properties of the tube material. The rare ED-1 immunopositively stained cells found inside the walls might be blood-born. An argument for the blood-born origin of most of the visible ED-1 positive cells is their *distribution* at early time points. Cells are mainly located *at sites of inbleeding* and in a rim just around the implant, another site predisposed for bleeding due to guidance channel implantation. Erythrocytes flooding into the lesion site are not probable to have invaded the channels’ micropores. Erythrocyte with a diameter of about 6µm are unable to invade far smaller pores (about 20kDa pore size for molecules of the size of Dextraneblue)(Lietz et al., 2005;Schlosshauer, 2003;Sinis et al., 2005). Furthermore, erythrocytes are anucleate. Cell morphology is relatively typical and should be more obvious in Nissl stainings. Accompanying the blood, numerous macrophages are transported into this area explaining the high number of ED-1 positive cells. *Wider spreading at later time points* with a predominance in the dorsal column can be understood as another factor underlining the macrophage-origin of the stained cells. Several dorsal column axons degenerate following injury. It is not astonishing that macrophages follow the line of their degeneration. The lack of any observed differences in stainings between the control MG/Med and the Schwann cell implanted MG/SC group could be explained by the fact that Schwann cells of syngeneic origin are not very inflammatory. For handling of the cells and surgery, the same protocols were employed in both groups. Discrepancies in bleeding extensions as well as the possible existence of any cellular contamination due to semi-sterile surgical conditions should therefore be statistically equalised. Anyhow, the ED-1 staining cannot supply more than a questionable information on presence and origin of potentially reactive cells around the lesion site. Establishment of T-cell stainings is imminent.

## 4.4 Visualisation, Localisation and Survival of Implanted Schwann Cells

To ascertain the success of Schwann Cell implantation and survival, it was necessary to state whether Schwann cells were actually found inside the tube lumen and to prove their survival giving information on the efficacy of the channel micropores and material. Distinction of the transplanted cells to picture potential migration into the host tissue around the lesion site is another interesting point. The Schwann cell marker S100, usually applied to specifically show Schwann cells in the PNS, is of no use in this CNS lesion model (3.4 Fig. 3.24). In spite of its use by other groups (Brook et al., 1998), it was revealed to be not specific enough for the histological evaluation of Schwann cells survival and number in rat spinal cord in this injury model. Applied on spinal cord SWK-lesioned sections, spinal cord parts proximal and distal to the lesion site were stained. The lesion itself seemed to be of less positive staining (Fig. 3.24 A). In a guidance channel implanted animal (group IIIB2), positive staining is found all over the spinal cord as well, the implantation site being the only unstained spot Fig. 3.24 B). These two test stainings led to the conclusion that the S100 antibody is not useful for these purposes. Even if Schwann cells within the tube lumen had been illustrated, no differentiation could have been possible of whether those cells were of implanted or of dorsal root origin. Neither could a potential cellular migration have been visualised. Another standard way of illustrating Schwann cells is labelling by bisbenzimidazole (Baron-Van Evercooren et al., 1991). The Hoechst labelling is only applicable when working with frozen tissue. Fluorescent labelling is quenched by organic solvents as used in paraffin tissue embedding processes needed in this study. Therefore, bisbenzimidazole labelling is of no use in this work. A different marker to trace the transplanted SCs had to be found.

To accurately determine whether there *are* Schwann cells inside the tube lumen, to give an idea of the *cell number*, to illustrate *potential cellular migration* out of the guidance channel and to further *differentiate* whether the found cells are really the transplanted Schwann cells, 100% of the transplanted cells were 100% retrovirally infected with enhanced GFP (2.1). *In vitro* and in frozen sections, the cells could be identified by their green fluorescence (3.4.1 Fig. 3.25 A, B). All Schwann cells were green fluorescing at the time of implantation. In the paraffin embedding procedure necessary for this experimental setting, the fluorescence is lost. Nonetheless, the protein can be traced by an antibody against eGFP (3.4.1 Fig. 3.25 C-E) (Walter et al., 2000; Howe and McCarthy, 1998). Due to the method of infection, the eGFP protein being transferred into the SC genome, it is likely to assume that descendant cells of proliferating Schwann cells will show the fluorescent label as well. The increasing cell number with time in cell culture can be seen as a proof for this assumption. The discordance in Schwann cell morphology between unimplanted cells *in vitro* and implanted Schwann cells *in vivo* (3.4.1 Fig. 3.25) has already been described earlier (Raisman, 1997; Scherer and Salzer, 2001). Visualisation *in vivo* is made possible by a secondary

antibody and DAB-reaction, the fluorescence lost due to tissue processing. To prove if the applied staining is specific and does not, for any reason whatsoever, picture other structures, a GFP/DAPI double staining was carried out. The observed co-localisation of cell nuclei (DAPI) and the GFP-stained structures sustains evidence for the cellular origin of those “fibre-like” structures (Fig. 3.26). The negative staining for eGFP in MG/Med animals at any time point underlines the above made conclusion.

It remains unclear, however, why the number of visible Schwann cells in SC-containing groups is so disappointingly low. One explanation could be a *low SC transplantation rate*. Schwann cells might have been *too diluted* by the medium added at time of trypsinisation. The applied dilution in medium was chosen to provide an environment nutritive enough for the cells within the guidance channel, though. Schwann cells, medium and MG might *not* have been *mixed well* enough before tube filling although the components were well intermingled with a pipette before filling of each channel. An indication for this hypothesis could be the observed MG clods within guidance channel lumina of SC-filled tubes. The aspect of these clods is similar to the relatively homogenous MG filling found in MG/Med tubes. To achieve a MG fluid enough for capillary channel filling (2.3.2), it needed to be cooled down. The MG was placed in a box with ice cubes. In consequence, same had to be done in order to mix the MG with SCs. This “cooling down” might have had a negative effect on the SCs. Freezing is supposed to harm SCs (Plant et al., 2000). The guidance channel *filling* itself might be *insufficient*. With the optimised method, however, no obvious diminution of filling was found at the time of tube implantation. Minor discrepancies in guidance channel filling or handling during operation, even the operation itself with little or much bleeding could have led to differences in the number of implanted cells. Another possibility for a low cell number is the occurrence of *cell death of the transplanted SCs* within the first 7d. No eGFP stained cell debris was observed within the tube lumen, though. Hill et al. recently described an important cell loss at two weeks following acute SC transplantation (Hill et al., 2006). The number of transplanted SCs was descending with time. In spite of increasing p75+ staining at the same time, the co-localisation with eGFP labelled transplanted SCs diminished. The group concluded on cell death of transplanted SCs and, simultaneously, replacement by endogenous SCs. Delayed transplantation combined with immunosuppression improved results. This observation underlines the hypothesis, that the acute injury environment as described in 1.3 and acute rejection play a role in cell death of transplanted SCs (Oudega et al., 2005; Hill et al., 2006). Third, the implanted SCs *might have migrated* out of the tube lumen. Little eGFP positive structures are visible in the host tissue around the tube, however, although comparison of the different time points illustrates a top position of the 7d time point, mainly in the AST group (3.4.4 Fig. 3.27, Tab. 3.2). But the applied classification is questionable. Only two to four sections per animal have been stained with the eGFP antibody. This leaves a large number of sections unevaluated which might present more migrated cells, thus possibly allowing a classification yet not made. The given example of a 7d AST animal (N525) presenting a relatively high number of SCs might

as well be an exception. A section of high cell number could have been stained. Furthermore, there is said to be a “mutual exclusivity” between SCs and astrocytes. If in proximity, SCs induce astrocytic hypertrophy and prevent contact (Franklin and Blakemore, 1993; Franklin, 2003; Lakatos et al., 2000; Lakatos et al., 2003). Since astrocytes are present in the host tissue around the implanted guidance channel, a migration into such a disfavoured environment is improbable. In combination with the minor number of migrating cells, the hypothesis of cellular migration as an important factor in the prevalence of the low SC number within the implanted tubes is practically invalidated. In contrast, it could rather be a hint for sufficient nutrition within the guidance channel. Cells probably would try to search a more nutritive environment in case of malnutrition. The observation of some migrating cells at the early time point in the AST group underlines the assumption that the injected BPY-DCA does not have any negative effect on the Schwann cells *in vivo*. In such a case, a migration closer to the points of injection would not be suspected. In *in vitro* experiments, SCs have been shown to die or proliferate very slowly when a pure or high concentration of the iron chelator BPY-DCA was administered. The exact reason for cell death when confronted with high concentrations of the chelator has not been examined. Changes in the pH could be a possible explanation. With higher dilution, this negative effect had disappeared and the cells developed as in the control. *In vivo*, the BPY-DCA probably is highly diluted at the site of application around the implant/host tissue interface. It most likely is confronted with an enormous “bloody” dilution for the amount of chelator applied. Additionally, each injection into the unlesioned spinal cord tissue provokes minor bleeding, the blood diluting the BPY-DCA. It is unlikely that the *in vitro* findings (not shown) concern the SC survival in the AST group. Application of cAMP or cAMP analogues is supposed to have a mitogenic effect on Schwann cells *in vitro* (Monje et al., 2006; Raff et al., 1978). If this was also the case *in vivo*, it could be one explanation for the increasing Schwann cell number up to the one month time point found within the channel lumen and occurring in both SC-containing groups in this study. Another explanation could be a proliferation effect of the implanted SCs, once the acute injury survived. The eGFP-labelling is transferred to descendent cells (Walter et al., 2000; Howe and McCarthy, 1998). Why this trend seems to stop at the three and six months time points is not fully understood. Long-time rejection processes could take place. No explicit references were found in literature. Not easier to explain is the observation that three of the 3mo animals as well as the only 6mo animal do not reveal any singular eGFP-immunopositive cell in the stained sections whereas the fourth 3mo animal shows a rather high cell number, similar to the one month time point. These discrepancies might be a mere impression due to low animal numbers at later time points. On the other hand, tube degradation processes could play a role in the decreasing SC number. Time points co-incide (3.2 and 4.2.1). With cellular infiltration of the tube walls during tube degeneration, the micropores might be plugged by such invading cells rendering nutrition of Schwann cells within the tube lumen more delicate. Diminution of the lumen diameter accompanying the decrease of luminal sections as well as the channel deformation

could lead to a reduction in space for the SCs. Nonetheless, no dead Schwann cells are observable within the tubes at late time points. The eGFP-labelling might be lost with cell death due to catalytic processes. Cultivated 4% PFA-fixed Schwann cells have been shown to continue fluorescence, however, although formally the cells undergo cell death due to fixation (unpublished data). Migration to the tube ends for better nutritive conditions cannot be found. Whether the lack of SCs within the guidance channel lumen at the three months time point has any consequence on axonal regeneration is not known. Time points coincide, however, for the diminution of SC number and no further notable increase in estimated fibre quantity.

## 4.5 Cells invading the Guidance Channel

Implanted Schwann cells have to be distinguished from other cells invading the guidance channel. This is possible by eGFP-labelling as demonstrated in 3.4. Comparison of sections showing eGFP-immunopositive Schwann cells with Nissl-stained sections, however, leads to the assumption that far more cells are infiltrating the tube lumina and walls. The origin of these invading cells, until now, is unknown.

Before establishment of the staining protocol for application of an eGFP-antibody (Molecular Probes 11122), the tube filling was tried to be verified in Nissl stainings. Morphologically, many cells inside the channel-lumen matched the description of Schwann cells and their *in vitro*- morphology (compare 3.4 Fig. 3.25 A, B and 3.5.1 Fig. 3.28), other were longitudinally oriented. Several details were surprising, however. First, clusters of small round cells are found mainly in areas rich in morphologically SC-resembling cells within the tube lumen (3.5.2 Fig. 3.29). The first idea was them being dead SCs. Second, MG/Med channels, i.e. channels without Schwann cell-implantation, seemed as cell-laden in Nissl stainings as the implants actually filled with Schwann cells. Most cells were oriented in a longitudinal manner and the nuclei were more visible but overall, they were similar to the cells found in SC-filled tubes. The introduction of a working staining protocol for the implanted eGFP-labelled SCs demonstrated a discordance between the high cell number stained in Nissl and the visible eGFP-immunopositive cells found on adjacent sections. This detail questions the assumed Schwann cell-derivation of the cells found within the tube lumen and leaves space for discussion. The origin of the high number of cellular guidance channel invasion remains unclear. It is uncertain as well whether the SC-resembling cells and the small round cells found within the tube lumen are of the same origin. The mentioned clusters of small round cells probably are not composed of dead SCs. The small cells were not immunopositive in staining with the antibody against eGFP-labelling. As stated in 4.4, eGFP labelled SCs might lose the eGFP due to catalytic processes but cultured PFA-fixed SC have been seen to

continue fluorescing (unpublished data). Compared to the number of eGFP positive Schwann cells that can be observed in the guidance channels (see 3.4), the quantity of those small round cells seems very high. This, again, makes the possibility of them being dead SCs rather less probable. The hypothesis of those cells being *erythrocytes* as proposed by Montgomery (Montgomery and Robson, 1993) is rather unlikely. Erythrocytes are anucleate and Nissl negative. *Macrophages* or *Granulocytes* have not been specifically searched by immunostaining. The ED-1 staining performed reveals activated phagocytising cells (Leskovar et al., 2000). In the spinal cord, local microglia as well as invading macrophages should be visible. ED-1 positive cells, as shown in 3.3.2.2, are mainly found in close relation to the site of implantation and the implant's outer face, at sites prone to show inbleeding. It is possible, though, that granulocytes participate in the cell number inside the tube lumen. *T-cells* are not very probable to play an important role in filling the tube lumen. Their number seems very limited (data not shown). The most likely hypothesis of cellular origin for the cells found within the guidance channel lumen as well as for the cells that have been shown to occupy the GCW in 3.2.1.3 seems to be fibroblasts. The guidance channel openings might have become invaded by fibroblasts. A close proximity to the meninges is given at least around the dorsal GCW. Some of those fibroblasts could die and form clusters of small round Nissl positive cells. The important dorsally located tube filling visible in 3.1.3.3 (Fig. 3.4 B,C) underlines the assumption of fibroblastic tube invasion. The animal in question had been implanted with an empty tube. Dura was left open after implantation (former operation protocol). Fibroblasts easily could have entered the cell-free dorsal tube lumen due to the proximity of meningeal tissue. In the SC-filled channels, SCs inside the tube could secrete factors preventing cellular invasion as they are known to secrete various molecules (Bandtlow et al., 1987; Bixby et al., 1988; Bunge, 1993). This would explain the impression of more cell-laden tubes at late time points in the control group (3.5.1 Fig. 3.28C). Schwann cells originating from the dorsal root ganglia are another cell type potent to have invaded the guidance channel. Cell morphology is similar to fibroblasts (see 3.5.2) and the dorsal location could be explained by the vicinity to the ganglia. Neither hypothesis could be verified yet. No specific fibroblast marker exists to my knowledge. Staining with RALDH<sub>2</sub>, a marker said to be rather specific, does not give any reliable result. Schwann cells are proven to be both, eGFP and RALDH<sub>2</sub> positive in *in vitro* studies (data not shown). In 2004, RALDH<sub>2</sub> has been shown to stain various cell types (Mey et al., 2005). Effects of fibroblast presence within the guidance channel on regeneration have not been examined in this study. Since fibroblasts secrete ECM molecules including Coll IV, they participate in BM construction at the lesion site, thus, in the formation of the fibrous scar. In theory, the conclusion could be drawn that the more fibroblasts are present, the more ECM molecules and consequently more Coll IV sheets are present at the lesion site. The fibrous scar acts as a barrier for regenerating fibres (see 1.7.2).

## 4.6 Scar Formation

### 4.6.1 Glial Scar

In literature, the definition of “scar” or “glial scar” is not uniform (Fawcett and Asher, 1999;Hermanns et al., 2001a;Klapka et al., 2002;Liesi and Kauppila, 2002;Silver and Miller, 2004). It is said to be inhibitory for regeneration. Astrocytes, among other cells, secrete ECM molecules and inhibitory molecules like CSPGs following SCI (1.7.1.2) (Fitch and Silver, 1997;Heck et al., 2003). The accumulation of these secreted molecules within the glial network, though, rests pure speculation. It is highly probable that the inhibitory proteins attach to the BM within the fibrous core of the scar (Klapka and Muller, 2006;Klapka et al., 2002;Stichel et al., 1999b;Reier and Guth, 1983). This hypothesis is underlined by follow-up Piromen® studies showing that Piromen® has no effect on glia but is able to modify the connective tissue (Reier and Guth, 1983). Another observation emphasising this theory is the depletion of astrocytes via Ethyidium bromide (Moon et al., 2000) not showing any regrowth nor sprouting after four days. A coincidence with the increase of the inhibitory proteoglycan NG2 attached to the BM at the lesion site (Klapka and Muller, 2006;Masannek et al., 2003;Moon et al., 2000;Grimpe and Silver, 2002) is found. A further hypothesis for astrocytic implication in regeneration inhibition is their failure to produce supportive factors. Liesi et al. (Liesi et al., 1984) showed that astrocytes *do* produce supportive molecules but it is unknown until today whether those molecules are secreted in a sufficient quantity, in a correct spatial or temporal sequence and whether there is a receptor re-expression on regrowing axons. Astrocytes not being a good substrate for axonal elongation has been refuted by *in vitro* experiments. It has been shown that neurons grow on astrocyte monolayers, myelin itself and MAG are not inhibitory (Stichel et al., 1999b). The GFAP-positive glial scar being complementary to the Collagen IV positive fibrous scar in this lesion model (3.6.1 Fig. 3.30) confirms former results of our group in different SCI models (Hermanns, 2001;Klapka et al., 2002). For further information see 1.7.2.

### 4.6.2 The Collagen IV-containing Fibrous Scar

The development of the fibrous scar in the lesion epicentre was studied using an antibody against Collagen type IV (first Progen, later Biodesign). Staining protocol problems with the first led to the establishment of other connective tissue stainings as van Gieson-Trichrome or Picrofuchsin (data not shown). Collagen IV staining was more specific in illustrating the fibrous scar, however, and the latter Collagen IV antibody was applied. Scarring studies were mainly focussed on the 7d time point. Earlier time points than 7d were not further

investigated. In two 4d test animals, the implant “broke out” during tissue preparation leading to the hypothesis that the tissue cable present is not strong enough at 4d (data not shown).

#### *Description of the Fibrous Scar*

A Collagen IV positive “cap” around the guidance channel implant comparable to Fig. 3.31 and Fig. 3.32 shown in 3.6.2.1 is present in all animals. The sheet-like structures forming the fibrous scar-cap around the tubes in this injury are equivalent to the scar formation following other SCI lesion models (Hermanns, 2001;Stichel et al., 1999b). The lesion and therefore scar dimensions, though, vary in each of these models. The reason for this discrepancy in BM-expression might be due to the difference in location of the lesion site in relation to the meninges. In SWK lesion, the meninges are in close proximity to the site of injury whereas the fornix lesion is performed in deeper brain regions, the meninges being located further away. If the meninges are lesioned within the scope of a SCI, fibroblasts and meningeal cells invade the lesion site, secreting BM-proteins, probably to re-establish the function of the BBBs BM (Carbonell and Boya, 1988;Hermanns, 2001). Migrating fibroblasts are known to secrete many ECM-molecules (Halfter et al., 1990) as well as Coll IV among other collagens (Eckes et al., 2000).

The “cap-like” scar around the implanted guidance channel present in this lesion model (see 3.6.2.1 Fig. 3.31) is in accordance with earlier results (Feringa et al., 1980;Hermanns, 2001) showing electron-microscopic proof that after total transection of the spinal cord both stumps are enclosed with BM. Scar dimensions - examining each host tissue/implant interface separately - are more important than in the fornix model [data not shown, (Stichel et al., 1999b)] but appear to be smaller compared to the SWK lesion (Hermanns et al., 2001b;Klapka, 2003;Klapka et al., 2005). By re-adaptation of the dura post-implantation, a lesion’s proximity to the meninges would be suspected with all the above stated hypotheses on scar development. One reason for the intermediate scar size in this injury model could be the fact of implanting a guidance channel. The tube taking up room, cell invasion might be prevented where it is placed. Instead, the fibroblasts and other invading cells disperse where they can – around the tube – and produce Collagen IV leading to fibrous scar formation. Another, though less probable hypothesis, could be the inhibition of the Collagen IV producing cells by the implant through an unknown mechanism. This, however, as well as the suspicion of an intermediate scar size, rests pure speculation. Quantified comparison of scar dimensions with other injury models is not valuable, not even within groups of this study. Scar size varies from one animal to another (see 3.6.3.1). Scar density, that is the number of Coll IV sheet layers, cannot be evaluated. The differences in extensions of the fibrous scar are likely to be relevant for scar’s permissiveness and, in consequence, on axonal regeneration. In this study, importance was laid on the functional relevance. A complete scar capping represents a barrier for regenerating axons, regardless its width and density. Even a thin Collagen IV layer presents an obstacle for axonal regeneration



(Hermanns et al., 2001b;Stichel et al., 1999b). According to these observations, the category “full scar” ++ was accounted for when a fibrous cap covered the tube opening from dorsal to ventral (see 3.6.2.3 Fig. 3.33). Possible explanations for differences in scar extension mainly are based on the occurring inbleedings (see 4.3.1) and the variations in the operating technique not being a hundred per cent reproducible.

The described Collagen IV positive “cap” around the guidance channel implant present at 7d does not change with time but remains visible at later time points. As illustrated in 3.6.2.4 Fig. 3.34, the fibrous scar easily can be distinguished from the host-tissue. In contrast, a distinction of scar-forming collagen IV sheets and stained Matrigel® within the tube lumen is difficult. MG seems to develop an important background staining within the tube lumen in immunostaining with an antibody against Collagen IV at later time points. Why the Matrigel® matrix is hardly stained at the early and more heavily stained at the late time point rests unclear. By later time points, vascularisation has occurred within the guidance channel lumen leading to a more abundant positive staining in Collagen IV. This does not explain background-staining of the matrix, though. The application of Matrigel® in this or future studies has to be discussed for different reasons. It had been selected for its easy acquisition and its utilisation in comparable studies in literature. In practice, however, several difficulties for its application were observable in this study. The above stated mystery in the description of the fibrous scar at later time points is only one important factor. MG consistency had to be controlled at various stages of the setting. Intermingling the Schwann cells and guidance channel filling were possible only in a liquefied state. For tube implantation, however, the MG needed to be in a more gelified state. Furthermore, MG is a solubilised basement membrane preparation extracted from EHS mouse sarcoma. Its major component is laminin, followed by collagen IV, heparan sulphate proteoglycans and entactin. Therefore, Coll IV-immunopositivity is not surprising. Matrigel components are not well described. The influence of the present collagens on axonal regeneration is unclear. They might function as scaffolds for inhibitory molecules as well.

#### *Effect of Schwann Cells on Scarring*

Schwann cells are shown to have several regeneration promoting effects (see 1.9, 4.4). The mere presence of Schwann cells at the guidance channel ends could have the effect of loosening the tissue interconnections of the developing fibrous scar. In this study, however, the presence of implanted Schwann cells as well as their continuous secretion of NTF's appears to be without obvious consequence on the formation of a fibrous scar (see 3.5.2.4). Whether SC implantation influences the development of the fibrous scar cannot be excluded, however. As mentioned by Guénard (Guenard et al., 1993), the number of implanted SCs is important for axon regeneration (see 4.7). It might be the same effect for their influence on scar formation. Visualisation of Schwann cells revealed the small number actually present within the guidance channels (3.4.3, 4.4) and in 3.4.4, tube opening areas were examined according to SC migration. Only a rare cell number has been found showing

such “migratory” behaviour at the host tissue/implant interface, the actual site of scarring. Lakatos et al. has depicted the SCs ability to induce astrocytic hypertrophy with upregulation of CSPGs (Lakatos and Franklin, 2002;Lakatos et al., 2003). Plant (2001) has demonstrated a high increase of CSPG accumulation at the caudal and less expression at the rostral host tissue / tube interface area following implantation of SC-filled channels in comparison with MG filled channels where CSPG is upregulated at both interface areas (Plant et al., 2001). CSPGs are inhibitory to axonal regeneration and accumulate within the fibrous core of the scar (Klapka, 2003). These findings could explain fibre ingrowth into the tube as well as the inability of fibres to re-enter the host tissue. Nevertheless, this rests a speculation. It remains unclear whether Schwann cells, the implanted channel material, continuous microtraumata at the interface areas or the mechanical factors during implantation technique are responsible for Plant’ s finding. In this study, no obvious differences in scarring were observed between the rostral and caudal guidance channel ends.

#### *Application and Effect of the Anti-Scarring Treatment*

Determination of an effect of AST on the fibrous scarring in this study imposed a classification of histological findings (Fig. 3.34 A-C in 3.6.2.3). Two extra categories were added to the rough classification of complete reduction (-), partial reduction (+) and full scar (++). The category “appearing partially reduced (\*+)” (Fig. 3.34 D) was created to demonstrate the observed occurrence of those findings in the partially reduced animals only. No definite partial reduction could be designated in these sections but a hint might be given. The extra-category “appearing fully scarred (\*\*+)” (Fig. 3.34 E) was appended to separate clear from suspected results. No definite full scar is visible for tissue loss due to various reasons, inbleeding being the main aspect. A partial reduction of the fibrous scar in those sections being very unlikely, a full scar must be assumed.

The failure of complete scar inhibition and the rare partial reduction observed in this study in contrast to the postcommissural fornix model (Hermanns et al., 2001b;Stichel et al., 1999b) as well as the SWK lesion (Hermanns and Muller, 2001;Hermanns et al., 2001b;Klapka, 2003;Klapka et al., 2005) is probably due to the mode of AST application. Lesion’s extent in this model is enormous compared to any of the previous studies (3.3.1). Exact transmission of the AST application in the SWK lesion to this model was given a try in order to keep as many experimental variables as possible unchanged. The injected chelator might mix with the inbleedings around the lesion site leading to a dilution of the active ingredient and loss of chelating effectiveness. Six injections of BPY-DCA at each host-tissue/implant interface probably do not offer enough chelator volume to compensate for such a loss. The liquid application form seems to have an effect too transitory. Application in a gel-form or through micropores containing BPY-DCA could be more appropriate. The Evax copolymer seems not to be potent enough in this type of injury. It is to discuss whether application difficulties arising due to the re-adaptation of the dura led to any less functioning. Difficulties in guarding the Elvax in place arose when bleeding occurred during dura re-closure. The blood

flooded the Elvax pieces away. In spite of this delicacy during operation, in most cases the positioning right on top of the lesion site could be assured. Another possible explanation for the probable insufficiency of the Elvax application could lie in the “sealing effect” of the copolymer piece placed. The introduced piece of Elvax might have been too small to prevent fibroblast invasion for such a rather big lesion. The implant’s length and the described inbleedings at both tube ends form a lesion of immense dimensions (see 3.3.1). If the cAMP showed any effectiveness as fibroblast proliferation inhibitor cannot be evaluated. The same is valid for the Schwann cell proliferation enhancing effect described (Monje et al., 2006; Raff et al., 1978).

It is not surprising that no scarring differences were found at later time points when comparing the AST group to other animal groups at 14d and 1mo. In the fornix and SWK lesion models, a scar is reforming at day 14 after AST admission (Hermanns et al., 2001b; Klapka, 2003). At one month, this “time window” has largely been closed and a scar should therefore be present. At later time points, Collagen IV sheets are suspected to be “loosened” by regenerating fibres. In practice, however, visualisation of such gaps in the fibrous scar is impossible when examining the sections with the used light-microscope. Double-stainings for Collagen IV and PAM are necessary to prove such a complementary localisation.

#### *Classification Difficulties*

In 3.6.3, a number of phenomena have been depicted leading to difficulties in classification of the fibrous scar into the above stated categories. Dislocation of collagen caps probably is due to tissue processing influencing the integrity of the tissue to be stained. Fig. 3.36 A probably pictures Coll IV positively stained dura. The layer is very fine and seems connected to the meninges. Distinction from a thin scar might be difficult. The already in 3.1.3 mentioned phenomenon of guidance channel wall disappearance is relevant in Collagen IV stained sections since the scar cap’s integrity might be destroyed (3.6.3 Fig. 3.36 C). Tissue-bridge shrinkage, most likely being responsible for detachment phenomena as in Fig. 3.37 A and B (also see 3.1.3, 4.1.3), also renders evaluation of the fibrous scar more difficult or even impossible for some guidance channel ends. Evaluating the efficacy of the AST, a very close look at all seemingly reduced sites is essential to differentiate reduced scars and scars merely appearing so. At sites of inbleeding, blood might expand and displace the formed Collagen IV sheets. An indicator for this hypothesis is the fact that sections classified as “partially reduced appearing” mainly are found within the median luminal sections where most inbleeding is observable (3.1.3.5, 3.3.1.2). Bleeding sites are demarcated. Coll IV sheets are deposited at the inbleeding’s borders to host tissue. If unresorbed, cysts might form at the site of former inbleeding, the newly formed Coll IV positive rim possibly presenting one more barrier to be overcome by regenerating axons (3.6.3.2 Fig. 3.38 A, B). As discussed in 4.1.3, a distinction between bleeding, cyst-like structures and areas of probable tissue tearing is delicate but should be attempted (3.6.3.2

Fig. 3.38). Imagination has to be used in search for corresponding tissue segments to decide whether tissue loss has occurred or not. The word “imagination” implies the subjectivity of this differentiation. Nevertheless, the subject is important when considering SCI. The development of syringomyelia, a process of slow and progressive cyst cavitation, is a complication following human SCI which can rapidly deteriorate even after years of stability (Radojicic et al., 2005). Observation of cyst formation implied the absence of host tissue, fibres or scar at the site of interest. It is unproven, however, whether a real cyst formation is taking place. Hermanns et al. describes the dependence of collagenous scar preservation on tissue processing. Cryostat sectioning and direct free-floating staining destroys the tissue (Hermanns and Muller, 2001). Many other groups work on frozen tissue and cryostat sections, however. This could be one explanation for them describing large cyst-like cavities (Meijs et al., 2004). Interesting is the description of some fibres within the septations of cavities found in chronically injured rat spinal cord (Radojicic et al., 2005). This observation is important for future application of therapies in human SCI if the same is valid in humans. In case of resection of scar tissue or cyst-like cavitations, a risk-benefit consideration is crucial.

## **4.7 Axonal Degeneration and Regrowth**

### **4.7.1 Axonal Degeneration**

Following axotomy due to an injury, spinal cord axons distal to the lesion undergo Wallerian degeneration (see 1.2 Fig. 1.1). Fibres in the proximal spinal cord segment have been shown to retract for several millimetres before sprouting (Ramon y Cajal, 1928). While doing so, retraction bulbs are forming. Such retraction bulbs can present themselves in a variety of size and form. In areas where many phagocytising cells are present, distinction might be difficult. Retraction bulbs are homogeneously stained whereas macrophages usually contain several vacuoles (Fig. 3.41). This is visible when focussing through the section. Differentiation from growth cones, the “clublike structures” that have already been described in 1928 by Ramon y Cajal as “conductors that turn back on encountering the scar near which they accumulate, forming complicated plexuses...”, is not possible using a light microscope. Fibres are observed to stop and form retraction bulbs at the host tissue/lesion interface (Stichel and Müller, 1994). The Collagen IV sheets present an insurmountable barrier. As demonstrated by Stichel et al. (Stichel et al., 1999a) and Hermanns et al. (Hermanns et al., 2001a), axonal degeneration in a fornix lesion is taking place within one week. Retraction bulbs are built and sprouting occurs until at day 14 the fibres stop right at the site of Collagen IV deposition (Stichel et al., 1999b). Same has been shown in a SWK transection lesion of rat spinal cord (Hermanns et al., 2001a; Klapka et al., 2002; Klapka,

2003). Regarding this entubulation model, special interest has to be directed on the already described site of bleeding proximal and distal to the tube opening at the site of guidance channel implantation. The general principal of fibres stopping in front of the Collagen IV sheets is still valid. In case of no inbleeding, fibres stop close to the guidance channel wall (Fig. 3.43). In most cases, however, inbleeding sites of various extents can be found (see 3.3.1.2) and the majority of fibres stop at the newly created host tissue/bleeding front. Its effect on axonal regrowth probably is very important. The farther cranial or distal to the implanted tube this front is located, the longer the distance for regenerating fibres to overcome. Some evidence for a penetration of the glial scar by several fibres contradicting its barrier effect (Fawcett and Asher, 1999; Moon et al., 2000) can be drawn from Fig. 3.42 A,C and Fig. 3.44 B,C. At the same time, these observations underline the invincibility of the fibrous scar (3.7.1.2 Fig. 3.42 A,B and Fig. 3.44 C,D) as described previously (Hermanns et al., 2001a; Stichel and Müller, 1998b; Stichel and Müller, 1998). The impression of a “loosened” area of inbleeding mainly visible in stainings with GFAP and PAM is due to the above described fibres and astrocytic processes accomplishing a passage through the bleeding area. A distinction between degeneration and regeneration regarding the often thin and short fibre segments is difficult. A continuity of such a fibrous structure with a retraction bulb has to be searched by focussing through the section. Likewise interesting for distinction of axonal structures is the content of the guidance channel lumen. As mentioned in 4.1.3, guidance channel wall structures infiltrated by some rare cells have to be distinguished from a tissue bridge containing Schwann cells and fibrous components.

#### 4.7.2 Axonal Regrowth into the Implant

Fibres have been visualised with a pan axonal marker (PAM), i.e. phosphorylated axons are stained by the antibody. The assessment of regenerating fibres is very difficult, quantification of *fibre number* therefore extremely laborious. One reason is that the cutting edge of the sections is not exactly parasagittal in most animals which might disturb observation. Parasagittally cut sections showing many longitudinal fibres might give the impression of better regeneration than looking at sections presenting a number of shorter fibre segments diffusely located within the tube lumen. Those dispersed segments could represent a high number of regenerating fibres. On the other hand, they could be different parts of one and the same axon since especially regenerating fibres show a more twisted aspect (Brosamle et al., 2000). In this study, an estimation of fibre number has been applied. *Fibre origin* cannot be differentiated in stainings with PAM. Regarding the operation protocol, it seems rather possible that many axons found in the tube are of sensory origin since the dorsal column has been damaged completely. In the Bunge group, regenerated axons found in SC seeded tubes were mainly CGRP positive, a marker for sensory motor neurons. Neither serotonergic nor noradrenergic axons were found in those studies (Bunge

and Pearse, 2003; Xu et al., 1995b; Xu et al., 1999). Bunge's results give a hint on axons' origin. To be certain, immunostainings for neurotransmitters could be performed in the future. The establishment of tracing studies as discussed in 4.7.3 would be the next step to determine fibre derivation.

#### *Evaluation of axonal regeneration*

For evaluation of axonal regeneration, only the animals of the last group IIC3 have been examined. A higher over-all number of PAM-immunopositive fibres was estimated within the guidance channels of these animals than in the groups before. This might be due to several factors. Both, the guidance channel filling mechanism as well as the operating protocol have been optimised. Relative reproducibility is given for both protocols (see 4.1.1 and 4.1.2). Guidance channels are well integrated into the lesion site, no more dislocation occurs. Experience in operating probably plays a role as well. Axonal regeneration can be studied regarding fibre quantity on the one hand and time-dependant regrowth on the other hand. It has been observed that both categories actually correlate (3.7.2.1 Fig. 3.45). The temporal progression of axonal regeneration seems logic. Time allows more axons to elongate. Schwann cells' regeneration promoting capacities (see 1.9) are underlined by the observation that a higher number of axons is present in Schwann cell-filled guidance channels than in the MG/Med control at any time point. The occurrence of actual axonal regeneration is emphasized by the evolution of fibre in-growth. Early time points reveal fibres mainly located around the tube opening areas whereas with time the number of fibres in the centre of the tube lumen increases up to one month (3.7.2.1 Fig. 3.45). Both tube ends are supposed to be invaded by fibres of different origin. CST fibres, for example, should enter the proximal opening whereas dorsal column fibres would enter the tube from the distal end to regenerate. With time, the fibres will elongate and eventually reach the tube centre, maybe regenerate even further to the other tube end. Peripheral nerve axons are known to regenerate for about 1-2mm per day. For CNS axonal regeneration, a similar time frame is agreed on. As stated earlier, regenerating CNS fibres do not regrow straight forward but in a twisting and turning manner (Brosamle et al., 2000). Whether any fibre in this study crosses the second lesion site to re-enter the host tissue is unclear. To demonstrate this, specific neurotransmitter stainings or tracing studies are necessary (see above and 4.7.3) and need to be established in the future. Any re-entrance of fibres into the spinal cord tissue at the other side of the guidance channel is very unlikely to have occurred, however, in this study.

#### *Effect of Schwann Cells on Axonal Regeneration*

Comparing the MG/Med control with SC-filled animals, it is evident that Schwann cell-filling stimulates axonal regeneration. Exceptions like some of the one month MG/Med animals showing good results partly can be explained by rather exact parasagittal sectioning of those animals giving a good impression of longitudinal regeneration (see above). Two of the

specimen have been cut in 20µm sections. In consequence, the visible axon number cannot be compared to the other animals. The impression of the fibre number not further augmenting at time points later than one month remains unexplained. This observation has been made in a very little animal number, therefore not being representative. Tube degradation processes could possibly play a role in explaining these findings. As demonstrated in 3.2, the tube material appears to degrade in a temporal progression. Around the three months time point, the number of luminal sections decreases. The inner diameter diminished, less room for axons is left inside the guidance channels. Same is valid for the observed tube deformation around a similar time point. Coinciding with the same time point, Schwann cells were found in only one of four three months animals and not within the tube lumen at the six months time point (see 4.4 for further discussion). These results in addition to the observation that regenerated fibres stained with PAM are often found in close vicinity of eGFP-stained implanted Schwann cells (see 3.4.2, 3.7.2.3) emphasise the good regeneration stimulating capacity of Schwann cells (Bunge, 1994;Guenard et al., 1993;Montgomery et al., 1996;Oudega et al., 2005;Stichel, 1997) and findings of axonal regeneration in other studies (Bamber et al., 2001;Plant et al., 2000;Tuszynski et al., 1998;Xu et al., 1999). The number of fibres regenerating into the guidance channel could probably be increased if more SCs were implanted with the guidance channels or kept alive for a longer time. Guénard (Guenard et al., 1992;Guenard et al., 1993) has shown that the higher the number of transplanted SCs is, the more axons are visible (see 4.4 for further discussion). A double-staining of PAM/eGFP is crucial to prove a co-localisation of SCs and regenerating fibres. Unfortunately, it has not been possible to establish yet. Nevertheless, a staining of two adjacent sections of 10-40 µm offers evidence for a close Schwann cell - fibre association (Fig. 3.49). These findings are supported by similar observations of regrowing axons associated with transplanted SCs (Plant et al., 1995;Plant et al., 1998). In none of the described literature, regenerated fibres were found to re-enter the host tissue after having crossed the lesion site in Schwann cell-only groups. Only combined treatments have shown some axons to do so until now (Reier, 2004;Plant et al., 2000;Zhang et al., 2005;Fouad et al., 2005).

Important to discuss at this point is the question whether OECs do not show more regeneration promoting capacities than SCs used in this study. They seldomly have been directly compared to SCs but seem to be faster in enhancement of functional restoration (Keyvan-Fouladi et al., 2003;Keyvan-Fouladi et al., 2005). Garcia-Alias et al. have shown better results for OECs in behavioural tests and MEP amplitudes. Astrocytic activity and proteoglycan expression were reduced compared to the SC group (Garcia-Alias et al., 2004). Myelin-forming OECs and SCs are impossible to distinguish. They have a close resemblance in morphology, ultrastructure and biochemistry, even have been shown to use the same transcription factors (Franklin, 2003). One important difference seems to be OECs capacity to mingle and interact with astrocytes to create a new transitional zone at the lesion site (Lakatos et al., 2000;Ramer et al., 2004) whereas SCs show a “mutual exclusion”

(Franklin and Blakemore, 1993), even inducing astrocyte hypertrophy (Lakatos et al., 2000;Lakatos et al., 2003). On the other hand, OECs are more difficult to acquire (Oudega et al., 2005). They do not myelinate in situ in CNS as SCs are shown to do (Takami et al., 2002). OECs might possess better regeneration promoting capacities than SCs, acquisition and implantation seem more complicated, however. SCs have a constant regenerative, myelinative and neuroprotective potential (Keyvan-Fouladi et al., 2005). These properties might be enhanced by combination therapies to reach OEC level, guarding the easy acquirement.

#### *Application and Effect of the Anti-Scarring Treatment*

As stated above, Coll IV sheets present an insurmountable barrier for regeneration. Fibres are only able to cross a lesion site where the Coll IV network has not yet been built. As described in 1.7, long distance axonal regeneration has been promoted by the application of the AST in the fornix model (Hermanns et al., 2001b;Stichel et al., 1999b). Functional improvement resulted following application in a SWK lesion (Hermanns, 2001;Klapka, 2003;Klapka et al., 2005). In regard to the above mentioned search for combinatory approaches, the application of the AST in an entubulation study in combination with other treatments, in this case Schwann cell implantation, is promising. In this study, probable regeneration facilitation in one partially reduced animal can be suspected (3.7.2.2). Exact description of these observations on adjacent sections not being possible, a double-staining for PAM and Collagen IV is indispensable in the future. To determine fibre growth in general, a 7d time point is far too early since the axons find themselves in their initial growth period. A reason for the rather high number of axons in a 7d MG/SC animal (3.7.2.4 Fig. 3.50 A,B) might be the fairly rapid regeneration especially of sensory fibres. If outgrowth did begin at the day of injury, they could have grown a distance of about 7mm. A judgement concerning possible differences comparing the number of regenerated axons present in guidance channels of the untreated Schwann cell-containing and the treated group at later time points would not be integer. Quantification of fibres, as stated above, is extremely difficult, the impression gathered therefore subjective. Variations within each animal group exist but no obvious differences were found. Guidance channel stability as well as its integration into the lesion site has to be accounted for (3.7.2.4 Fig. 3.50). Fig. 3.50 E and F illustrate the effect an introduction of the host tissue stump into the tube can have on the evaluation of regrowing fibres. The axons pointed out within the rostral tube end have not regenerated but have been introduced with the tissue stump. Animal groups are too small and variations too important to draw a statistically exact conclusion. The data shown can only give an impression on axon regeneration and inspire to further work on this subject. It is necessary to first establish another application form for the AST in this injury model to ensure the efficiency of the treatment (see 4.6.2). If this has been verified on Collagen IV immunostained sections, an evaluation of axonal regeneration should be carried out in larger studies.



### 4.7.3 Traced Fibre Tracts

Immunohistochemical stainings with PAM neither differentiate different fibre tracts nor the direction of axonal growth. As visible in 3.7, staining with an antibody against PAM often visualises short PAM-immunopositive fibre segments within the guidance channels instead of fibres in continuity with axons in the host tissue. It is impossible to distinguish which tract the observed axon segments within the tube lumen can be accounted for. Located in the caudal part of the implanted tube, for example, they could be regenerating fibres of the dorsal column just having entered the tube at the caudal end. On the other hand, the same segments could belong to the CST or other descending fibre tracts having passed the entire tube length. Same is valid for visible fibre segments proximal or distal to the implant. Fibre origin cannot be inferred from the distribution of the PAM-immunopositive segments. Tracing studies are important to observe axonal re-growth and gather information on the origin of regenerating fibres. Especially in entubulation studies, it is principal to distinguish re-growing fibre tracts and to illustrate regeneration into and through the implanted guidance channel. Re-entry into the host-tissue at the other tube end could be illustrated by such a tracing. In this study, three tracing protocols have been applied. Although no sufficient results have been provided yet, tracing studies are essential to be continued. Distinction of regenerated fibres and their location is crucial for conclusions on the sufficiency of entubulation, Schwann cell implantation and the application of the AST. In case of no positive axonal tracing within the guidance channel lumen nor distal to the implant, the PAM-immunopositive fibres might be of interneuronal or DRG origin, for example. Xu et al. demonstrate a mainly interneuronal origin up to nine segments rostral to the implanted SC filled guidance channel (Xu et al., 1995b). As described by Hill et al., the number of transplanted SCs seems to decrease with time whereas endogenous SCs apparently invade the spinal cord tissue simultaneously (Hill et al., 2006). Ingrowth of endogenous SCs without previous transplantation of exogenous SCs, however, does not lead to a positive effect on regeneration (Keyvan-Fouladi et al., 2005).

#### *CST Tracing with BDA*

In this injury model, CST-tracing with BDA is not very efficient. The lesion size, enlarged by bleedings often located at the tube ends, definitely is an important factor for the fibre stop rather far from the tube opening (see 3.7.1.3 ). In literature, the CST is described as one of the fibre tracts difficult in regeneration (Schnell and Schwab, 1990). Such poor regenerative capacities render it the best tract for research. The choice of CST tracing to verify regeneration success was also made for practical reasons - it was well established in our laboratory for other lesion models. For establishment of a new injury model in this study, however, the efficiency of CST tracing is questionable. An incongruence of tube opening and CST location was observed in some animals. The CST is quite small in diameter,

located a little dorsal to the central canal. Aspiration lesion and tube positioning in this study is rather delicate, reproducibility of exact three-dimensional location within the spinal cord not given. If the guidance channel is not placed exactly in the middle of the spinal cord so that the CST can be directed inside its lumen, it is rather probable that no axons are growing through it but facing its wall (see 4.1.2 and 4.1.3 for further discussion). Furthermore, tissue processing and cutting in 10µm sections was necessary to obtain a sufficient number of sections showing the tube lumen. This compromise was indispensable since other stainings had to be carried out on adjacent sections although regenerating fibres would be very hard to visualise in ABC staining on 10µm sections. The 50µm sections of the distal spinal cord parts did not provide evidence of any regenerated fibres, neither. The notion of a lack of CST regeneration is confirmed. Xu et al 1999 (Xu et al., 1999) stated that CST fibres do not regenerate into a PN/Schwann cell environment (Bunge et al., 1989), Cheng et al., however, was pro-regeneration (Cheng et al., 1996). This deficiency of CST regeneration should not surprise or demotivate, though, even considering the AST group. The application of the AST did lead to CST axonal regeneration in other models (Hermanns, 2001;Klapka et al., 2005), the SWK transection lesion as such being less important, though.

#### *Dorsal Column Tracing with BDA*

This novel tracing method was thought of when searching to stain a higher amount of fibres than the CST. The dorsal column represents large fibre tracts relatively easy to attain. Lesioning was possible in a rather reproducible fashion. Animal sacrifice in test animals was at 7d to leave a timeframe for BDA transport up to more cranial spinal cord levels. The observed fibres' aspect resembling rather degenerating than sprouting could be explained by the extreme damage of the tract. Fibres in the control animal were cut at Th11 only. For both other test animals, the additional injury, SWK and cut-aspiration lesion, represented a second more cranial fibre destruction. Axons were harmed at two levels at the same time. Since the three month animals were very valuable, this not well established tracing technique with uncertain results was applied on only two of them. Tracing was carried out ten days before sacrifice instead of seven days in the test animals to allow a longer and thus maybe farther BDA transportation closer to the lesion site. This was not the case, however. Again, no traced axons were found in proximity of the caudal guidance channel opening. The 10d timeframe might still not be long enough to ensure the transportation of BDA from spinal cord level Th11 up to Th8 or further. It is not well known how BDA is transported in unlesioned axons in the first place. What happens in damaged fibres has not been described yet. This uncertainty in addition to the poor results (little fibres traced at all) and the suspicion of fibre degeneration led to abandoning of this tracing model.

## 5.0 References

1. (1994) Immune Responses to Tissue Transplants. In: Cellular and Molecular Immunology (Abbasth, Lichtman AH, Poher, eds), pp 339-355. Philadelphia: Saunders.
2. (2001a) Peripheral Nerve Regeneration. In: Brain Damage, Brain Repair (Fawcett J, Rosser AE, Dunnett SB, eds), Oxford: Oxford Univ. Press.
3. (2001b) Stem Cells. In: Brain Damage, Brain Repair (Fawcett J, Rosser AE, Dunnett SB, eds), pp 344-356. Oxford: Oxford Univ. Press.
4. (2006a) In: Neurobiology of Spinal Cord Injury (Kalb RG, Strittmatter SM, eds), pp 169-193. Totowa, New Jersey: Humana Press Inc.
5. <http://www.cdc.gov/health/default.htm>. <http://www.cdc.gov/health/default.htm> . 2006b. Electronic Citation
6. Acheson A, Barker PA, Alderson RF, Miller FD, Murphy RA (1991) Detection of brain-derived neurotrophic factor-like activity in fibroblasts and Schwann cells: inhibition by antibodies to NGF. *Neuron* 7: 265-275.
7. Aebischer P, Guenard V, Brace S (1989a) Peripheral nerve regeneration through blind-ended semipermeable guidance channels: effect of the molecular weight cutoff. *J Neurosci* 9: 3590-3595.
8. Aebischer P, Guenard V, Winn SR, Valentini RF, Galletti PM (1988) Blind-ended semipermeable guidance channels support peripheral nerve regeneration in the absence of a distal nerve stump. *Brain Res* 454: 179-187.
9. Aebischer P, Salessiotis AN, Winn SR (1989b) Basic fibroblast growth factor released from synthetic guidance channels facilitates peripheral nerve regeneration across long nerve gaps. *J Neurosci Res* 23: 282-289.
10. Anselin AD, Fink T, Davey DF (1997) Peripheral nerve regeneration through nerve guides seeded with adult Schwann cells. *Neuropathol Appl Neurobiol* 23: 387-398.
11. Archibald SJ, Krarup C, Shefner J, Li ST, Madison RD (1991) A collagen-based nerve guide conduit for peripheral nerve repair: an electrophysiological study of nerve regeneration in rodents and nonhuman primates. *J Comp Neurol* 306: 685-696.
12. Ard MD, Bunge RP, Bunge MB (1987) Comparison of the Schwann cell surface and Schwann cell extracellular matrix as promoters of neurite growth. *J Neurocytol* 16: 539-555.
13. Aumailley M, Gayraud B (1998) Structure and biological activity of the extracellular matrix. *J Mol Med* 76: 253-265.
14. Bamber NI, Li H, Lu X, Oudega M, Aebischer P, Xu XM (2001) Neurotrophins BDNF and NT-3 promote axonal re-entry into the distal host spinal cord through Schwann cell-seeded mini-channels. *Eur J Neurosci* 13: 257-268.
15. Bandtlow CE, Heumann R, Schwab ME, Thoenen H (1987) Cellular localization of nerve growth factor synthesis by in situ hybridization. *EMBO J* 6: 891-899.
16. Barami K, Diaz FG (2000) Cellular transplantation and spinal cord injury. *Neurosurgery* 47: 691-700.
17. Barbeau H, Rossignol S (1987) Recovery of locomotion after chronic spinalization in the adult cat. *Brain Res* 412: 84-95.

18. Baron-Van Evercooren A, Avellana-Adalid V, Lachapelle F, Liblau R (1997) Schwann cell transplantation and myelin repair of the CNS. *Mult Scler* 3: 157-161.
19. Baron-Van Evercooren A, Gansmuller A, Clerin E, Gumpel M (1991) Hoechst 33342 a suitable fluorescent marker for Schwann cells after transplantation in the mouse spinal cord. *Neurosci Lett* 131: 241-244.
20. Bartsch U (1996) Myelination and axonal regeneration in the central nervous system of mice deficient in the myelin-associated glycoprotein. *J Neurocytol* 25: 303-313.
21. Becker D, Sadowsky CL, McDonald JW (2003) Restoring function after spinal cord injury. *The Neurologist* 9: 1-15.
22. Bernstein JJ, Getz R, Jefferson M, Kelemen M (1985) Astrocytes secrete basal lamina after hemisection of rat spinal cord. *Brain Res* 327: 135-141.
23. Berry M, Hall SM, Rees EL, Yiu P, Sievers J (1987) The role of basal lamina in axon regeneration. In: *Mesenchymal-epithelial Interactions in Neural Development* (Wolff JR, ed), pp 361-383. Springer Verlag.
24. Berry M, Rees EL, Hall S, Yiu P, Sievers J (1988) Optic axons regenerate into sciatic nerve isografts only in presence of Schwann cells. *Brain Res Bull* 20: 223-231.
25. Bethea JR (2000) Spinal cord injury-induced inflammation: a dual-edged sword. *Prog Brain Res* 128: 33-42.
26. Bixby JL, Lilien J, Reichardt LF (1988) Identification of the major proteins that promote neuronal process outgrowth on Schwann cells in vitro. *J Cell Biol* 107: 353-361.
27. Blakemore WF (1977) Remyelination of CNS axons by Schwann Cells transplanted from the sciatic nerve. *Nature (London)* 266: 68-69.
28. Blakemore WF, Franklin RJ (1991) Transplantation of glial cells into the CNS. *Trends Neurosci* 14: 323-327.
29. Blight AR (1992) Macrophages and inflammatory damage in spinal cord injury. *J Neurotrauma* 9 Suppl 1: S83-S91.
30. BMBF Micro-structured bioresorbable guidance channels with glial progenitor cells for nerve regeneration. 2000.
31. BMBF BIOLEIT - Biohybride Regenerationsleitschienen für das zentrale und periphere Nervensystem. 2002.
32. Borgens RB (1999) Electrically mediated regeneration and guidance of adult mammalian spinal axons into polymeric channels. *Neuroscience* 91: 251-264.
33. Borgens RB, Shi RY, Bohnert D (2002) Behavioral recovery from spinal cord injury following delayed application of polyethylene glycol. *J Exp Biol* 205: 1-12.
34. Borkenhagen M, Stoll RC, Neuenschwander P, Suter UW, Aebischer P (1998) In vivo performance of a new biodegradable polyester urethane system used as a nerve guidance channel. *Biomaterials* 19: 2155-2165.
35. Boyd JG, Gordon T (2003) Glial cell line-derived neurotrophic factor and brain-derived neurotrophic factor sustain the axonal regeneration of chronically axotomized motoneurons in vivo. *Exp Neurol* 183: 610-619.

36. Bracken MB, Holford TR (2002) Neurological and functional status 1 year after acute spinal cord injury: estimates of functional recovery in National Acute Spinal Cord Injury Study II from results modeled in National Acute Spinal Cord Injury Study III. *J Neurosurg* 96: 259-266.
37. Bradbury EJ, Khemani S, Von R, King, Priestley JV, McMahon SB (1999) NT-3 promotes growth of lesioned adult rat sensory axons ascending in the dorsal columns of the spinal cord. *Eur J Neurosci* 11: 3873-3883.
38. Bradbury EJ, Moon LD, Popat RJ, King VR, Bennett GS, Patel PN, Fawcett JW, McMahon SB (2002) Chondroitinase ABC promotes functional recovery after spinal cord injury. *Nature* 416: 636-640.
39. Bregman BS, Coumans JV, Dai HN, Kuhn PL, Lynskey J, McAtee M, Sandhu F (2002) Transplants and neurotrophic factors increase regeneration and recovery of function after spinal cord injury. *Prog Brain Res* 137: 257-273.
40. Brockes JP, Fields KL, Raff MC (1979) Studies on cultured rat Schwann cells. I. Establishment of purified populations from cultures of peripheral nerve. *Brain Res* 105-118.
41. Brook GA, Plate D, Franzen R, Martin D, Moonen G, Schoenen J, Schmitt AB, Noth J, Nacimiento W (1998) Spontaneous longitudinally orientated axonal regeneration is associated with the Schwann cell framework within the lesion site following spinal cord compression injury of the rat. *J Neurosci Res* 53: 51-65.
42. Brosamle C, Huber AB, Fiedler M, Skerra A, Schwab ME (2000) Regeneration of lesioned corticospinal tract fibers in the adult rat induced by a recombinant, humanized IN-1 antibody fragment. *J Neurosci* 20: 8061-8068.
43. Brown JC, Timpl R (1995) The collagen superfamily. *Int Arch Allergy Immunol* 107: 484-490.
44. Bunge MB (2002) Bridging the transected or contused adult rat spinal cord with Schwann cell and olfactory ensheathing glia transplants. *Prog Brain Res* 137: 275-282.
45. Bunge MB, Bunge RP, Kleitman N, Dean AC (1989) Role of peripheral nerve extracellular matrix in Schwann cell function and in neurite regeneration. *Dev Neurosci* 11: 348-360.
46. Bunge MB, Kleitman N (1999) Neurotrophins and Neuroprotection Improve Axonal Regeneration into Schwann Cell Transplants Placed in Transected Adult Rat Spinal Cord. In: *CNS Regeneration* pp 631-646. Academic Press.
47. Bunge MB, Pearse DD (2003) Transplantation strategies to promote repair of the injured spinal cord. *Journal of Rehabilitation Research and Development* 40.
48. Bunge RP (1993) Expanding roles for the Schwann cell: ensheathment, myelination, trophism and regeneration. *Curr Opin Neurobiol* 3: 805-809.
49. Bunge RP (1994) The role of Schwann cell in trophic support and regeneration. *J Neurol* 214: S19-S21.
50. Cao Q, Benton RL, Whittemore SR (2002) Stem cell repair of central nervous system injury. *J Neurosci Res* 68: 501-510.
51. Carbonell AL, Boya J (1988) Ultrastructural study on meningeal regeneration and meningo-glial relationships after cerebral stab wound in the adult rat. *Brain Res* 439: 337-344.
52. Cheng H, Cao Y, Olson L (1996) Spinal cord repair in adult paraplegic rats: partial restoration of hind limb function. *Science* 273: 510-513.

53. Cheng H, Liao KK, Liao SF, Chuang TY, Shih YH (2004) Spinal cord repair with acidic fibroblast growth factor as a treatment for a patient with chronic paraplegia. *Spine* 29: E284-E288.
54. Chiu TH (1999) *Hand clin* 15: 667-671.
55. Christie SD, Mendez I (2001) Neural transplantation in spinal cord injury. *Can J Neurol Sci* 28: 6-15.
56. Coumans JV, Lin TT, Dai HN, MacArthur L, McAtee M, Nash C, Bregman BS (2001) Axonal regeneration and functional recovery after complete spinal cord transection in rats by delayed treatment with transplants and neurotrophins. *J Neurosci* 21: 9334-9344.
57. David S, Aguayo AJ (1981) Axonal elongation into peripheral nervous system "bridges" after central nervous system injury in adult rats. *Science* 214: 931-933.
58. Davies SJ, Fitch MT, Memberg SP, Hall AK, Raisman G, Silver J (1997) Regeneration of adult axons in white matter tracts of the central nervous system. *Nature* 390: 680-683.
59. den Dunnen WF, van der LB, Schakenraad JM, Stokroos I, Blaauw E, Bartels H, Pennings AJ, Robinson PH (1996) Poly(DL-lactide-epsilon-caprolactone) nerve guides perform better than autologous nerve grafts. *Microsurgery* 17: 348-357.
60. Dergham P, Ellezam B, Essagian C, Avedissian H, Lubell WD, McKerracher L (2002) Rho signaling pathway targeted to promote spinal cord repair. *J Neurosci* 22: 6570-6577.
61. Dietz V, Boos N (2001) *Klinik der Rückenmarkschädigung: Diagnose - Therapie - Rehabilitation*. Stuttgart: Kohlhammer.
62. Dobkin BH (2003) *The Clinical Science of Neurologic Rehabilitation*. New York: Oxford Univ. Press.
63. Dobkin BH, Havton LA (2004) Basic advances and new avenues in therapy of spinal cord injury. *Annu Rev Med* 55: 255-282.
64. Doolabh VB, Mackinnon S (1999) Transplantation of the peripheral nerve allograft. In: *Composite Tissue Transplantation* (Hewitt CW, Black KS, eds), pp 87-105.
65. Dr. Robin Franklin. *Glial Cell Transplantation*. 2002.
66. Duncan ID, Aguayo AJ, Bunge RP, Wood PM (1981) Transplantation of rat Schwann cells grown in tissue culture into the mouse spinal cord. *J Neurol Sci* 49: 241-252.
67. Duncan MR, Frazier KS, Abramson S, Williams S, Klapper H, Huang X, Grotendorst GR (1999) Connective tissue growth factor mediates transforming growth factor beta-induced collagen synthesis: downregulation by cAMP. *FASEB J* 13: 1774-1786.
68. Dusart I, Schwab ME (1994) Secondary cell death and the inflammatory reaction after dorsal hemisection of the rat spinal cord. *Eur J Neurosci* 6: 712-724.
69. Eckes B, Zigrino P, Kessler D, Holtkotter O, Shephard P, Mauch C, Krieg T (2000) Fibroblast-matrix interactions in wound healing and fibrosis. *Matrix Biol* 19: 325-332.
70. el Masry WS, Short DJ (1997) Current concepts: spinal injuries and rehabilitation. *Curr Opin Neurol* 10: 484-492.
71. Eng LF, Ghimikar RS, Lee YL (2000) Glial fibrillary acidic protein: GFAP-thirty-one years (1969-2000). *Neurochem Res* 25: 1439-1451.

72. Evans GR, Brandt K, Katz S, Chauvin P, Otto L, Bogle M, Wang B, Meszlenyi RK, Lu L, Mikos AG, Patrick CW, Jr. (2002) Bioactive poly(L-lactic acid) conduits seeded with Schwann cells for peripheral nerve regeneration. *Biomaterials* 23: 841-848.
73. Evans PJ, Midha R, MacKinnon SE (1994) The peripheral nerve allograft: a comprehensive review of regeneration and neuroimmunology. *Prog Neurobiol* 43: 187-233.
74. Exner G, Meinecke FW (1997) Trends in the treatment of patients with spinal cord lesions seen within a period of 20 years in German centers. *Spinal Cord* 35: 415-419.
75. Fabre T, Schappacher M, Bareille R, Dupuy B, Soum A, Bertrand-Barat J, Baquey C (2001) Study of a (trimethylenecarbonate-co-epsilon-caprolactone) polymer--part 2: in vitro cytocompatibility analysis and in vivo ED1 cell response of a new nerve guide. *Biomaterials* 22: 2951-2958.
76. Faulkner JR, Herrmann JE, Woo MJ, Tansey KE, Doan NB, Sofroniew MV (2004) Reactive Astrocytes Protect Tissue and Preserve Function after Spinal Cord Injury. *J Neurosci* 24: 2143-2155.
77. Fawcett J (1998) From experimental models to human application. *Spinal Cord* 36: 811-817.
78. Fawcett JW, Asher RA (1999) The glial scar and central nervous system repair. *Brain Res Bull* 49: 377-391.
79. Feringa ER, Kowalski TF, Vahlsing HL (1980) Basal lamina formation at the site of spinal cord transection. *Ann Neurol* 8: 148-154.
80. Fernandez E, Mannino S, Tufo T, Pallini R, Lauretti L, Albanese A, Denaro L (2006) The adult "paraplegic" rat: treatment with cell grafting. *Surgical Neurology* 223-237.
81. Fields RD, Le Beau JM, Longo FM, Ellisman MH (1989) Nerve regeneration through artificial tubular implants. *Prog Neurobiol* 33: 87-134.
82. Filbin MT (1995) Myelin-associated glycoprotein: a role in myelination and the inhibition of axonal regeneration? *Curr Opin Neurobiol* 5: 588-595.
83. Fine EG, Valentini RF, Aebischer P (2000) Nerve Regeneration. In: *Principles of Tissue Engineering* pp 785-798.
84. Fitch MT, Silver J (1997) Activated macrophages and the blood-brain barrier: inflammation after CNS injury leads to increases in putative inhibitory molecules. *Exp Neurol* 148: 587-603.
85. Fitch MT, Silver J (1999) Beyond the glial scar. Cellular and molecular mechanisms by which glial cells contribute to CNS regenerative failure. In: *In CNS regeneration: basic science and clinical advances* (Tuszynski M, Kordower JH, eds), pp 55-88. Academic Press.
86. Fouad K, Dietz V, Schwab ME (2001) Improving axonal growth and functional recovery after experimental spinal cord injury by neutralizing myelin associated inhibitors. *Brain Res Brain Res Rev* 36: 204-212.
87. Fouad K, Schnell L, Bunge MB, Schwab ME, Liebscher T, Pearse DD (2005) Combining Schwann cell bridges and olfactory-ensheathing glia grafts with chondroitinase promotes locomotor recovery after complete transection of the spinal cord. *J Neurosci* 25: 1169-1178.
88. Fournier AE, Strittmatter SM (2001) Repulsive factors and axon regeneration in the CNS. *Curr Opin Neurobiol* 11: 89-94.
89. Fournier AE, Takizawa BT, Strittmatter SM (2003a) Rho kinase inhibition enhances axonal regeneration in the injured CNS. *J Neurosci* 23: 1416-1423.

90. Fournier E, Passirani C, Montero-Menei CN, Benoit JP (2003b) Biocompatibility of implantable synthetic polymeric drug carriers: focus on brain compatibility. *Biomaterials* 24: 3311-3331.
91. Franklin RJ (1991) Approaches to the design of anti-fibrotic drugs.
92. Franklin RJ (2003) Remyelination by transplanted olfactory ensheathing cells. *Anat Rec* 271B: 71-76.
93. Franklin RJ, Blakemore WF (1993) Requirements for Schwann cell migration within CNS environments: a viewpoint. *Int J Dev Neurosci* 11: 641-649.
94. Franzen R, Martin D, Dalozze A, Moonen G, Schoenen J (1999) Grafts of meningeal fibroblasts in adult rat spinal cord lesion promote axonal regrowth. *Neuroreport* 10: 1551-1556.
95. Franzen R, Schoenen J, Leprince P, Joosten EA, Moonen G (1998) Effects of macrophage transplantation in the injured adult spinal cord: A combined immunocytochemical and biochemical study. *J Neurosci Res* 51: 316-327.
96. Friedman JA, Windebank AJ, Moore MJ, Spinner RJ, Currier BL, Yaszemski MJ (2002) Biodegradable polymer grafts for surgical repair of the injured spinal cord. *Neurosurgery* 51: 742-751.
97. Fry EJ (2001) Central nervous system regeneration: mission impossible? *Clin Exp Pharmacol Physiol* 28: 253-258.
98. Garcia-Alias G, Lopez-Vales R, Fores J, Navarro X, Verdu E (2004) Acute transplantation of olfactory ensheathing cells or Schwann cells promotes recovery after spinal cord injury in the rat. *J Neurosci Res* 75: 632-641.
99. George, Griffin (1994) Delayed macrophage responses and myelin clearance in CNS. *Exp Neurol* 129: 225-236.
100. Ghirnikar RS, Lee YL, Eng LF (2001) Spinal Cord Injury: Hope for a Cure. *Indian J Pharm Sci* 63: 349-363.
101. Giardino R, Fini M, Nicoli AN, Giavaresi G, Rocca M (1999) Polylactide bioabsorbable polymers for guided tissue regeneration. *J Trauma* 47: 303-308.
102. Glück T (1880) Über Neoplastik auf dem Wege der Transplantation. *Arch Klin Chir* 26: 606-616.
103. GrandPre T, Strittmatter SM (2001) Nogo: a molecular determinant of axonal growth and regeneration. *Neuroscientist* 7: 377-386.
104. Grill R, Murai K, Blesch A, Gage FH, Tuszynski MH (1997) Cellular delivery of neurotrophin-3 promotes corticospinal axonal growth and partial functional recovery after spinal cord injury. *J Neurosci* 17: 5560-5572.
105. Grimpe B, Silver J (2002) The extracellular matrix in axon regeneration. *Prog Brain Res* 137: 333-349.
106. Guenard V, Kleitman N, Morrissey TK, Bunge RP, Aebischer P (1992) Syngeneic Schwann cells derived from adult nerves seeded in semipermeable guidance channels enhance peripheral nerve regeneration. *J Neurosci* 12: 3310-3320.
107. Guenard V, Xu X, Bunge MB (1993) The use of Schwann cell transplantation to foster central nervous system repair. *Seminars in The Neurosciences* 5: 401-411.



108. Guest J, Eleraky MA, Apostolides PJ (2002) Traumatic central cord syndrome: results of surgical management. *J Neurosurg* 97: 25-32.
109. Guest JD, Hesse D, Schnell L, Schwab ME, Bunge MB, Bunge RP (1997a) Influence of IN-1 antibody and acidic FGF-fibrin glue on the response of injured corticospinal tract axons to human Schwann cell grafts. *J Neurosci Res* 50: 888-905.
110. Guest JD, Rao A, Olson L, Bunge MB, Bunge RP (1997b) The ability of human Schwann cell grafts to promote regeneration in the transected nude rat spinal cord. *Exp Neurol* 148: 502-522.
111. Gunnarsson T, Fehlings MG (2003) Acute neurosurgical management of traumatic brain injury and spinal cord injury. *Curr Opin Neurol* 16: 717-723.
112. Guth L, Albuquerque EX, Deshpande SS, Barrett CP, Donati EJ, Warnick JE (1980) Ineffectiveness of enzyme therapy on regeneration in the transected spinal cord of the rat. *J Neurosurg* 52: 73-86.
113. Hadley M (1997) *Exp Neurol* 146: 380-387.
114. Hadley M (2002) Pharmacological therapy after acute cervical spinal cord injury. *Neurosurgery* 50: S63-S72.
115. Hadlock T, Sundback C, Hunter D, Cheney M, Vacanti JP (2000) A polymer foam conduit seeded with Schwann cells promotes guided peripheral nerve regeneration. *Tissue Eng* 6: 119-127.
116. Hales NJ, Beattie JF (1993) Novel inhibitors of prolyl 4-hydroxylase. The intriguing structure-activity relationships seen with 2,2'-bipyridine and its 5,5'-dicarboxylic acid derivatives. *J Med Chem* 36: 3853-3858.
117. Halfter W, Liverani D, Vigny M, Monard D (1990) Deposition of extracellular matrix along the pathways of migrating fibroblasts. *Cell Tissue Res* 262: 467-481.
118. Hanenberg H, Batish SD, Pollok KE, Vieten L, Verlander PC, Leurs C, Cooper RJ, Gottsche K, Haneline L, Clapp DW, Lobitz S, Williams DA, Auerbach AD (2002) Phenotypic correction of primary Fanconi anemia T cells with retroviral vectors as a diagnostic tool. *Exp Hematol* 410-420.
119. Harkey HL, III, White EA, Tibbs RE, Jr., Haines DE (2003) A clinician's view of spinal cord injury. *Anat Rec* 271B: 41-48.
120. Heck N, Garwood J, Schutte K, Fawcett J, Faissner A (2003) Astrocytes in culture express fibrillar collagen. *Glia* 41: 382-392.
121. Hempstead BL, Salzer JL (2002) Neurobiology. A glial spin on neurotrophins. *Science* 298: 1184-1186.
122. Hermanns, S. Stimulation axonaler Regeneration im durchtrennten Rückenmark der adulten Ratte. 2001.
123. Hermanns, S. Meeting Vancouver. 2004. Personal Communication
124. Hermanns S, Klapka N, Gasis M, Müller HW (2005) The collagenous wound healing scar in the injured central nervous system and its role in impeding axonal regeneration. In: *Brain Repair* (electronic book) (Bähr M, ed), Eureka.com.
125. Hermanns S, Klapka N, Müller HW (2001a) The collagenous lesion scar--an obstacle for axonal regeneration in brain and spinal cord injury. *Restor Neurol Neurosci* 19: 139-148.

126. Hermanns S, Muller HW (2001) Preservation and detection of lesion-induced collagenous scar in the CNS depend on the method of tissue processing. *Brain Res Brain Res Protoc* 7: 162-167.
127. Hermanns S, Reiprich P, Muller HW (2001b) A reliable method to reduce collagen scar formation in the lesioned rat spinal cord. *J Neurosci Methods* 110: 141-146.
128. Hill CE, Moon LD, Wood P, Bunge MB (2006) Labeled Schwann Cell Transplantation: Cell Loss, Host Schwann Cell Replacement and Strategies to enhance survival. *Glia* 338.
129. Houle JD, Ziegler MK (1994) Bridging a complete transection lesion of adult rat spinal cord with growth factor-treated nitrocellulose implants. *J Neural Transplant Plast* 5: 115-124.
130. Howe DG, McCarthy KD (1998) A dicistronic retroviral vector and culture model for analysis of neuron-Schwann cell interactions. *J Neurosci Methods* 83: 133-142.
131. Huber AB, Schwab ME (2000) Nogo-A, a potent inhibitor of neurite outgrowth and regeneration. *Biol Chem* 381: 407-419.
132. Hugenholtz H (2003) Methylprednisolone for acute spinal cord injury: not a standard of care. *CMAJ* 168: 1145-1146.
133. Hulsebosch CE (2002) Recent advances in pathophysiology and treatment of spinal cord injury. *Adv Physiol Educ* 26: 238-255.
134. Hunt D, Coffin RS, Anderson PN (2002) The Nogo receptor, its ligands and axonal regeneration in the spinal cord; a review. *J Neurocytol* 31: 93-120.
135. Hurlbert RJ (2000) Methylprednisolone for acute spinal cord injury: an inappropriate standard of care. *J Neurosurg* 93: 1-7.
136. Iannotti C, Li H, Yan P, Lu X, Wirthlin L, Xu XM (2003) Glial cell line-derived neurotrophic factor-enriched bridging transplants promote propriospinal axonal regeneration and enhance myelination after spinal cord injury. *Exp Neurol* 183: 379-393.
137. Jain A, Kim YT, McKeon RJ, Bellamkonda RB (2005) In situ gelling hydrogels for conformal repair of spinal cord defects and local delivery of BDNF after spinal cord injury. *Biomaterials* 497-504.
138. Johnsen, Lise, Larsen, Helen, Sorensen, Heidi, and Sorensen, Kristoffer W. *Guidance Signals in Nerve Regeneration*. 2003.
139. Jones DG, Anderson ER, Galvin KA (2003) Spinal cord regeneration: moving tentatively towards new perspectives. *NeuroRehabilitation* 18: 339-351.
140. Jones KJ (2003) Olfactory ensheathing cells: Therapeutic potential in spinal cord injury and other neurological disorders. *Anat Rec* 271B: 39-40.
141. Jones LL, Oudega M, Bunge MB, Tuszynski MH (2001) Neurotrophic factors, cellular bridges and gene therapy for spinal cord injury. *J Physiol* 533: 83-89.
142. Joosten EA, Bar PR, Gispens WH (1995) Collagen implants and cortico-spinal axonal growth after mid-thoracic spinal cord lesion in the adult rat. *J Neurosci Res* 41: 481-490.
143. Kakulas BA (1999a) A review of the neuropathology of human spinal cord injury with emphasis on special features. *J Spinal Cord Med* 22: 119-124.
144. Kakulas BA (1999b) The applied neuropathology of human spinal cord injury. *Spinal Cord* 37: 79-88.

145. Keyvan-Fouladi N, Raisman G, Li Y (2003) Functional repair of the corticospinal tract by delayed transplantation of olfactory ensheathing cells in adult rats. *J Neurosci* 23: 9428-9434.
146. Keyvan-Fouladi N, Raisman G, Li Y (2005) Delayed repair of corticospinal tract lesions as an assay for the effectiveness of transplantation of Schwann cells. *Glia* 51: 306-311.
147. Khan T, Dauzvardis M, Sayers S (1991) Carbon filament implants promote axonal growth across the transected rat spinal cord. *Brain Res* 541: 139-145.
148. Kim BS, Yoo JJ, Atala A (2004) Peripheral nerve regeneration using acellular nerve grafts. *J Biomed Mater Res A* 68: 201-209.
149. Kim DH, Connolly SE, Kline DG, Voorhies RM, Smith A, Powell M, Yoes T, Daniloff JK (1994) Labeled Schwann cell transplants versus sural nerve grafts in nerve repair. *J Neurosurg* 80: 254-260.
150. Klapka, N. Axonale Regeneration und funktionelle Erholung nach Läsion im Rückenmark der adulten Ratte. 2003.
151. Klapka N, Hermanns S, Müller HW (2002) Interactions between Glia and Extracellular Matrix and their Role for Axonal Growth. *Glia Interfaces in the Nervous System* 139-151.
152. Klapka N, Hermanns S, Straten G, Masannek C, Duis S, Hamers FP, Müller D, Zuschratter W, Müller HW (2005) Suppression of fibrous scarring in spinal cord injury of rat promotes long-distance regeneration of corticospinal tract axons, rescue of primary motoneurons in somatosensory cortex and significant functional recovery. *Eur J Neurosci* 22: 3047-3058.
153. Klapka N, Muller HW (2006) Collagen Matrix in Spinal Cord Injury. *Journal of Neurotrauma* 23: 422-436.
154. Kleitman N (2001) Under one roof: the Miami Project to Cure Paralysis model for spinal cord injury research. *Neuroscientist* 7: 192-201.
155. Kleitman N, Wood P, Johnson MI, Bunge RP (1988) Schwann cell surfaces but not extracellular matrix organized by Schwann cells support neurite outgrowth from embryonic rat retina. *J Neurosci* 8: 653-663.
156. Krekoski CA, Neubauer D, Zuo J, Muir D (2001) Axonal regeneration into acellular nerve grafts is enhanced by degradation of chondroitin sulfate proteoglycan. *J Neurosci* 21: 6206-6213.
157. Kromer LF, Cornbrooks CJ (1987) Identification of trophic factors and transplanted cellular environments that promote CNS axonal regeneration. *Ann N Y Acad Sci* 495: 207-224.
158. Kuhlengel KR, Bunge MB, Bunge RP (1990a) Implantation of cultured sensory neurons and Schwann cells into lesioned neonatal rat spinal cord. I. Methods for preparing implants from dissociated cells. *J Comp Neurol* 293: 63-73.
159. Kuhlengel KR, Bunge MB, Bunge RP, Burton H (1990b) Implantation of cultured sensory neurons and Schwann cells into lesioned neonatal rat spinal cord. II. Implant characteristics and examination of corticospinal tract growth. *J Comp Neurol* 293: 74-91.
160. Kwon BK, Borisoff JF, Tetzlaff W (2002a) Molecular targets for therapeutic intervention after spinal cord injury. *Mol Interv* 2: 244-258.
161. Kwon BK, Oxland TR, Tetzlaff W (2002b) Animal models used in spinal cord regeneration research. *Spine* 27: 1504-1510.

162. Lakatos A, Barnett SC, Franklin RJ (2003) Olfactory ensheathing cells induce less host astrocyte response and chondroitin sulphate proteoglycan expression than schwann cells following transplantation into adult CNS white matter. *Exp Neurol* 184: 237-246.
163. Lakatos A, Franklin RJ (2002) Transplant mediated repair of the central nervous system: an imminent solution? *Curr Opin Neurol* 15: 701-705.
164. Lakatos A, Franklin RJ, Barnett SC (2000) Olfactory ensheathing cells and Schwann cells differ in their in vitro interactions with astrocytes. *Glia* 32: 214-225.
165. Lassner, Franz. Experimentelle Untersuchungen zu den Ersatzverfahren der autologen Nerven-Transplantation. 1444.
166. Lee SK, Wolfe SW (2000) Peripheral nerve injury and repair. *J Am Acad Orthop Surg* 243-252.
167. Leme RJ, Chadi G (2001) Distant microglial and astroglial activation secondary to experimental spinal cord lesion. *Arq Neuropsiquiatr* 59: 483-492.
168. Leskovaara A, Moriarty LJ, Turek JJ, Schoenlein IA, Borgens RB (2000) The macrophage in acute neural injury: changes in cell numbers over time and levels of cytokine production in mammalian central and peripheral nervous systems. *J Exp Biol* 203 Pt 12: 1783-1795.
169. Levi AD, Dancausse H, Li X, Duncan S, Horkey L, Oliviera M (2002) Peripheral nerve grafts promoting central nervous system regeneration after spinal cord injury in the primate. *J Neurosurg* 96: 197-205.
170. Levi AD, Guenard V, Aebischer P, Bunge RP (1994) The functional characteristics of Schwann cells cultured from human peripheral nerve after transplantation into a gap within the rat sciatic nerve. *J Neurosci* 14: 1309-1319.
171. Li S, Strittmatter SM (2003) Delayed systemic Nogo-66 receptor antagonist promotes recovery from spinal cord injury. *J Neurosci* 23: 4219-4227.
172. Li Y, Raisman G (1994) Schwann cells induce sprouting in motor and sensory axons in the adult rat spinal cord. *J Neurosci* 14: 4050-4063.
173. Li Y, Sauve Y, Li D, Lund RD, Raisman G (2003) Transplanted olfactory ensheathing cells promote regeneration of cut adult rat optic nerve axons. *J Neurosci* 23: 7783-7788.
174. Liesi P, Kaakkola S, Dahl D, Vaeheri A (1984) Laminin is induced in astrocytes of adult brain by injury. *EMBO J* 3: 683-686.
175. Liesi P, Kauppila T (2002) Induction of type IV collagen and other basement-membrane-associated proteins after spinal cord injury of the adult rat may participate in formation of the glial scar. *Exp Neurol* 173: 31-45.
176. Lietz M, Ullrich A, Schulte-Eversum C, Oberhoffner S, Fricke C, Müller HW, Schlosshauer B (2005) Physical and biological performance of a novel block copolymer nerve guide. *Biotechnol Bioeng*.
177. Liu BP, Fournier AE, GrandPre T, Strittmatter SM (2002) Myelin-associated glycoprotein as a functional ligand for Nogo-66 receptor. *Science* 297: 1190-1193.
178. Ljungberg C, Johansson-Ruden G, Bostrom KJ, Novikov L, Wiberg M (1999) Neuronal survival using a resorbable synthetic conduit as an alternative to primary nerve repair. *Microsurgery* 19: 259-264.
179. Loeb GE, Peck RA, Moore W, Hood K (2001) BION (TM) system for distributed neural prosthetic interfaces. *Med Eng Phys* 23: 9-18.

180. Lundborg G, Drott J, Wallman L, Reimer M, Kanje M (1998) Regeneration of axons from central neurons into microchips at the level of the spinal cord. *Neuroreport* 9: 861-864.
181. Maquet V, Martin D, Malgrange B, Franzen R, Schoenen J, Moonen G, Jerome R (2000) Peripheral nerve regeneration using bioresorbable macroporous polylactide scaffolds. *J Biomed Mater Res* 52: 639-651.
182. Maquet V, Martin D, Scholtes F, Franzen R, Schoenen J, Moonen G, Jer mR (2001) Poly(D,L-lactide) foams modified by poly(ethylene oxide)-block-poly(D,L-lactide) copolymers and a-FGF: in vitro and in vivo evaluation for spinal cord regeneration. *Biomaterials* 22: 1137-1146.
183. Martin D, Robe P, Franzen R, Delree P, Schoenen J, Stevenaert A, Moonen G (1996) Effects of Schwann cell transplantation in a contusion model of rat spinal cord injury. *J Neurosci Res* 45: 588-597.
184. Martin D, Schoenen J, Delree P, Rigo JM, Rogister B, Leprince P, Moonen G (1993) Syngeneic grafting of adult rat DRG-derived Schwann cells to the injured spinal cord. *Brain Res Bull* 30: 507-514.
185. Masanneck, C. Statistische Datenerhebung SCI. 2003. Personal Communication
186. Masanneck, C., Müller, D., Heyden, A., Hermanns, S., Kury, P., and Müller, H. W. Suppression of Fibrous Scar Formation after Spinal Cord Injury affects Inhibitory Proteoglycan Deposition. Program No.415.10.2003 Abstract Viewer/Itinerary Planner. 2003. Society for Neuroscience, Washington DC.
187. Matinian LA, Andreasian AS (1973) Enzyme therapy in organic lesions of the spinal cord. In: *Akademia Nauk Armenian SSR (English translation 1976, 156pp, University of California, L.A., Brain Information Service.*
188. McDonald JW, Liu XZ, Qu Y, Liu S, Mickey SK, Turetsky D, . (1999) Transplanted embryonic stem cells survive, differentiate and promote recovery in injured rat spinal cord. *Nat Med* 5: 1410-1412.
189. McKerracher L (2001) Spinal cord repair: strategies to promote axon regeneration. *Neurobiol Dis* 8: 11-18.
190. McKerracher L, Winton MJ (2002) Nogo on the go. *Neuron* 36: 345-348.
191. Meek MF, den Dunnen WF, Schakenraad JM, Robinson PH (1999) Long-term evaluation of functional nerve recovery after reconstruction with a thin-walled biodegradable poly (DL-lactide-epsilon-caprolactone) nerve guide, using walking track analysis and electrostimulation tests. *Microsurgery* 19: 247-253.
192. Meijs MFL, Timmers L, Pearse DD, Tresco PA, Bates ML, Joosten EA, Bunge MB, Oudega M (2004) Basic Fibroblast Growth Factor promotes neuronal survival but not behavioral recovery in the transected and Schwann cell implanted rat thoracic spinal cord. *Journal of Neurotrauma* 21: 1415-1430.
193. Mey J, Morassutti J, Brook G, Liu RH, Zhang YP, Koopmans G, McCaffery P (2005) Retinoic acid synthesis by a population of NG2-positive cells in the injured spinal cord. *Eur J Neurosci* 21: 1555-1568.
194. Mezey E, Key S, Vogelsang G, Szalayova I, Lange GD, Crain B (2003) Transplanted bone marrow generates new neurons in human brains. *Proc Natl Acad Sci U S A* 100: 1364-1369.

195. Miller AD, Garcia JV, von Suhr N, Lynch CM, Wilson C, Eiden MV (1991) Construction and properties of retrovirus packaging cells based on gibbon ape leukemia virus. *J Virol* 2220-2224.
196. Mirsky R, Jessen KR (1999) The neurobiology of Schwann cells. *Brain Pathol* 9: 293-311.
197. Monje PV, Bunge MB, Wood P (2006) Cyclic AMP synergeistically enhances neuregulin-dependent ERK and Akt activation and cell cycle progression in Schwann cells. *Glia* 649-659.
198. Montgomery CT, Robson JA (1993) Implants of cultured Schwann cells support axonal growth in the central nervous system of adult rats. *Exp Neurol* 122: 107-124.
199. Montgomery CT, Tenaglia EA, Robson JA (1996) Axonal growth into tubes implanted within lesions in the spinal cords of adult rats. *Exp Neurol* 137: 277-290.
200. Moon LD, Brecknell JE, Franklin RJ, Dunnett SB, Fawcett JW (2000) Robust regeneration of CNS axons through a track depleted of CNS glia. *Exp Neurol* 161: 49-66.
201. Morrissey TK, Kleitman N, Bunge RP (1991) Isolation and functional characterization of Schwann cells derived from adult peripheral nerve. *J Neurosci* 11: 2433-2442.
202. Mueller M, Leonhard C, Wacker K, Ringelstein EB, Okabe M, Hickey WF, Kiefer R (2003) Macrophage response to peripheral nerve injury: the quantitative contribution of resident and hematogenous macrophages. *Lab Invest* 83: 175-185.
203. Mulcahey MJ, Betz RR, Kozin SH, Smith BT, Hutchinson D, Lutz C (2004) Implantation of the Freehand System during initial rehabilitation using minimally invasive techniques. *Spinal Cord* 42: 146-155.
204. Murray M, Fischer I (2001) Transplantation and gene therapy: combined approaches for repair of spinal cord injury. *Neuroscientist* 7: 28-41.
205. Murray M, Kim D, Liu Y, Tobias C, Tessler A, Fischer I (2002) Transplantation of genetically modified cells contributes to repair and recovery from spinal injury. *Brain Res Brain Res Rev* 40: 292-300.
206. Nacimiento W, Noth J (1997) Zelluläre Pathomechanismen und experimentelle Therapien nach Rückenmarkstrauma. *Nervenheilkunde* 16: 1-11.
207. Nicholas MK, Arnason BGW (1992) Immunologic responses in central nervous system transplantation. *seminars in The Neurosciences* 4: 273-283.
208. Nicoli AN, Fini M, Rocca M, Giavaresi G, Giardino R (2000) Guided regeneration with resorbable conduits in experimental peripheral nerve injuries. *Int Orthop* 24: 121-125.
209. Novikov LN, Novikova LN, Mosahebi A, Wiberg M, Terenghi G, Kellerth JO (2002) A novel biodegradable implant for neuronal rescue and regeneration after spinal cord injury. *Biomaterials* 23: 3369-3376.
210. Novikova, L. N., Mosahebi, A., Wiberg, M., Terenghi, G., Kellerth, J. O., and Novikov, L. Alginate hydrogel and matrigel as potential cell carriers for neurotransplantation. [www.interscience.wiley.com](http://www.interscience.wiley.com) DOI: 10.1002/jbm.a.30603. 2005.
211. Novikova LN, Novikov LN, Kellerth JO (2003) Biopolymers and biodegradable smart implants for tissue regeneration after spinal cord injury. *Curr Opin Neurol* 16: 711-715.
212. Ohta M, Suzuki Y, Noda T (2004) Bone marrow stromal cells infused into the cerebrospinal fluid promote functional recovery of the injured rat spinal cord with reduced cavity formation. *Exp Neurol* 187: 266-278.

213. Oudega M, Gautier SE, Chapon P, Fragoso M, Bates ML, Parel JM, Bunge MB (2001) Axonal regeneration into Schwann cell grafts within resorbable poly(alpha-hydroxyacid) guidance channels in the adult rat spinal cord. *Biomaterials* 22: 1125-1136.
214. Oudega M, Moon LD, Almeida Leme RJ (2005) Schwann cells for spinal cord repair. *Braz J Med Biol Res* 38: 825-835.
215. Pachence JM, Kohn J (2000) Biodegradable Polymers. In: *Principles in Tissue Engineering* pp 263-277. Academic Press.
216. Paino CL, Bunge MB (1991) Induction of axon growth into Schwann cell implants grafted into lesioned adult rat spinal cord. *Exp Neurol* 114: 254-257.
217. Paino CL, Fernandez-Valle C, Bates ML, Bunge MB (1994) Regrowth of axons in lesioned adult rat spinal cord: promotion by implants of cultured Schwann cells. *J Neurocytol* 23: 433-452.
218. Pasterkamp RJ, Giger RJ, Ruitenber MJ, Holmaat AJ, DeWit J, DeWinter F, Verhaagen J (1999) Expression of the gene encoding the chemorepellent semaphorin III is induced in the fibroblast component of the neural scar tissue formed following injuries of adult but not neonatal CNS. *Mol Cell Neurosci* 13: 143-166.
219. Pekny M, Nilsson M (2005) Astrocyte activation and reactive gliosis. *Glia* 50: 427-434.
220. Perry (1987) *J Exp Med* 165: 1218-1223.
221. Perry (1992) *Curr Op Neurobiol* 2: 679-682.
222. Pinzon A, Calancie B, Oudega M, Noga BR (2001) Conduction of impulses by axons regenerated in a Schwann cell graft in the transected adult rat thoracic spinal cord. *J Neurosci Res* 64: 533-541.
223. Plant GW, Bates ML, Bunge MB (2001) Inhibitory proteoglycan immunoreactivity is higher at the caudal than the rostral Schwann cell graft-transected spinal cord interface. *Mol Cell Neurosci* 17: 471-487.
224. Plant GW, Chirila TV, Harvey AR (1998) Implantation of collagen IV/poly(2-hydroxyethyl methacrylate) hydrogels containing Schwann cells into the lesioned rat optic tract. *Cell Transplant* 7: 381-391.
225. Plant GW, Harvey AR, Chirila TV (1995) Axonal growth within poly (2-hydroxyethyl methacrylate) sponges infiltrated with Schwann cells and implanted into the lesioned rat optic tract. *Brain Res* 671: 119-130.
226. Plant GW, Ramon-Cueto A, Bunge MB (2000) Transplantation of Schwann cells and ensheathing glia to improve regeneration in adult spinal cord. pp 529-561.
227. Porter S, Clark MB, Glaser L, Bunge RP (1986) Schwann cells stimulated to proliferate in the absence of neurons retain full functional capability. *J Neurosci* 3070-3078.
228. Prewitt CM, Niesman IR, Kane CJ, Houle JD (1997) Activated macrophage/microglial cells can promote the regeneration of sensory axons into the injured spinal cord. *Exp Neurol* 148: 433-443.
229. Qiu J, Cai D, Filbin MT (2000) Glial inhibition of nerve regeneration in the mature mammalian CNS. *Glia* 29: 166-174.
230. Radojicic M, Reier PJ, Steward O, Keirstead HS (2005) Septations in chronic spinal cord injury cavities contain axons. *Exp Neurol*.

231. Raff MC, Hornby-Smith A, Brackes JP (1978) Cyclic AMP as a mitogenic signal for cultured rat Schwann cells. *Nature* 273 (5664): 672-673.
232. Raisman G (1997) Use of Schwann cells to induce repair of adult CNS tracts. *Rev Neurol (Paris)* 153: 521-525.
233. Raivich G, Kreutzberg GW (2000) Inflammatory Response Following Nerve Injury. pp 287-313.
234. Ramer LM, Au E, Richter MW, Liu J, Tetzlaff W, Roskams AJ (2004) Peripheral olfactory ensheathing cells reduce scar and cavity formation and promote regeneration after spinal cord injury. *J Comp Neurol* 473: 1-15.
235. Ramer MS, Harper GP, Bradbury EJ (2000) Progress in spinal cord research - a refined strategy for the International Spinal Research Trust. *Spinal Cord* 38: 449-472.
236. Ramon y Cajal S (1928) *Degeneration and Regeneration of the nervous system*. New York: Hafner.
237. Ramon-Cueto A, Cordero MI, Santos-Benito FF, Avila J (2000) Functional recovery of paraplegic rats and motor axon regeneration in their spinal cords by olfactory ensheathing glia. *Neuron* 25: 425-435.
238. Ramon-Cueto A, Plant GW, Avila J, Bunge MB (1998) Long-distance axonal regeneration in the transected adult rat spinal cord is promoted by olfactory ensheathing glia transplants. *J Neurosci* 18: 3803-3815.
239. Rapalino O, Lazarov-Spiegler O, Agranov G, Velan GJ, Yoles E, Fraidakis M (1998) Implantation of stimulated homologous macrophages results in partial recovery of paraplegic rats. *Nat Med* 4: 814-821.
240. Reier PJ (2004) Cellular transplantation strategies for spinal cord injury and translational neurobiology. *NeuroRx* 1: 424-451.
241. Reier PJ, Guth L (1983) The astrocytic scar as an impediment to regeneration in the central nervous system. *Spinal Cord Reconstruction*.
242. Reinkensmeyer D, Lum P, Winters J (2002) Emerging technologies for improving access to movement therapy following neurologic injury. In: *Emerging and Accessible Telecommunications, Information and Healthcare Technologies* (Winters J, Robinson C, Simpson R, Vanderheiden G, eds), pp 123-128. New York: IEEE Press.
243. Ribotta M, Gaviria M, Menet V, Privat A (2002) Strategies for regeneration and repair in spinal cord traumatic injury. *Prog Brain Res* 137: 191-212.
244. Richardson PM, Issa VMK, Aguayo AJ (1984) Regeneration of long spinal axons in the rat. *J Neurocytol* 13: 165-182.
245. Rodriguez FJ, Verdu E, Ceballos D, Navarro X (2000) Nerve guides seeded with autologous schwann cells improve nerve regeneration. *Exp Neurol* 161: 571-584.
246. Rosen JM, Padilla JA, Nguyen KD, Padilla MA, Sabelman EE, Pham HN (1990) Artificial nerve graft using collagen as an extracellular matrix for nerve repair compared with sutured autograft in a rat model. *Ann Plast Surg* 25: 375-387.
247. Rosenzweig ES, McDonald JW (2004) Rodent models for treatment of spinal cord injury: research trends and progress toward useful repair. *Curr Opin Neurol* 17: 121-131.



248. Sagen J, Bunge MB, Kleitman N (2000) Transplantation Strategies for Treatment of Spinal Cord Dysfunction and Injury. In: Principles in Tissue Engineering pp 799-820. Academic Press.
249. Sandvig A, Berry M, Barrett LB, Butt A, Logan A (2004) Myelin-, reactive glia-, and scar-derived CNS axon growth inhibitors: expression, receptor signaling, and correlation with axon regeneration. *Glia* 46: 225-251.
250. Santos-Benito FF, Ramon-Cueto A (2003) Olfactory ensheathing glia transplantation: a therapy to promote repair in the mammalian central nervous system. *Anat Rec* 271B: 77-85.
251. Sayer FT, Kronvall E, Nilsson OG (2006) Methylprednisolone treatment in acute spinal cord injury: the myth challenged through a structured analysis of published literature. *The Spine Journal* 335-343.
252. Schaller E, Lassner F, Becker M, Walter GF, Berger A (1991) Regeneration of autologous and allogenic nerve grafts in a rat genetic model: preliminary report. *J Reconstr Microsurg* 7: 9-12.
253. Schaumburg (1992) Disorders of peripheral nerves. Philadelphia: F.A. Davies.
254. Scherer SS, Salzer JL (2001) Axon-Schwann Cell interactions during peripheral nerve degeneration and regeneration. In: Glial cell development (Jessen KR, Richardson WD, eds), pp 299-330.
255. Schlosshauer, B. Biohybrid Nerve Guides: Material Characteristics, Conduit Microstructure, Cell interactions and in vivo models. 2003.
256. Schlosshauer B, Muller E, Schroder B, Planck H, Muller HW (2003) Rat Schwann cells in bioresorbable nerve guides to promote and accelerate axonal regeneration. *Brain Res* 963: 321-326.
257. Schnell L, Schwab ME (1990) Axonal regeneration in the rat spinal cord produced by an antibody against myelin-associated neurite growth inhibitors. *Nature* 343: 269-272.
258. Schwab JM, Brechtel K, Mueller CA, Kaps HP, Meyermann R, Schluesener HJ (2004) Akute Rückenmarkverletzung: Experimentelle Strategien als Basis zukünftiger Behandlungen. *Deutsches Ärzteblatt* 101: B1183-B1195.
259. Schwab ME, Bartholdi D (1996) Degeneration and regeneration of axons in the lesioned spinal cord. *Physiol Rev* 76: 319-370.
260. Schwab ME, Brosamle C (1997) Regeneration of lesioned corticospinal tract fibers in the adult rat spinal cord under experimental conditions. *Spinal Cord* 35: 469-473.
261. Scremin A, Kurta L, Gentili A (2000) Increasing muscle mass in spinal cord injured persons with a functional electrical stimulation exercise program. *Arch Phys Med Rehabil* 80: 1531-1536.
262. Sekhon LH, Fehlings MG (2001) Epidemiology, demographics, and pathophysiology of acute spinal cord injury. *Spine* 26: S2-12.
263. Silver J, Miller JH (2004) Regeneration beyond the glial scar. *Nat Rev Neurosci* 5: 146-156.
264. Sinis N, Schaller HE, Schulte-Eversum C, Doser M, Dietz K, Rösner H, Müller HW, Haerle M (2005) Nerve regeneration across a 2cm gap in the rat median nerve using a resorbable nerve conduit filled with Schwann cells. *J Neurosurg* 103: 1067-1076.
265. So KF, Yip HK (2000) The Use of Peripheral Nerve Transplants to Enhance Axonal Regeneration in CNS Neurons. pp 505-527.

266. Stichel CC (1997) The role of microenvironment in axonal regeneration. In: *Advances in Anatomy, Embryology and Cell Biology* 137 pp VII-77. Springer.
267. Stichel CC, Hermanns S, Luhmann HJ, Lausberg F, Niermann H, D'Urso D, Servos G, Hartwig HG, Müller HW (1999a) Inhibition of collagen IV deposition promotes regeneration of injured CNS axons. *Eur J Neurosci* 11: 632-646.
268. Stichel CC, Müller HW (1994) Relationship between injury-induced astrogliosis, laminin expression and axonal sprouting in the adult rat brain. *J Neurocytol* 23: 615-630.
269. Stichel CC, Müller HW (1998a) Experimental strategies to promote axonal regeneration after traumatic central nervous system injury. *Prog Neurobiol* 56: 119-148.
270. Stichel CC, Müller HW (1998b) The CNS lesion scar: new vistas on an old regeneration barrier. *Cell Tissue Res* 294: 1-9.
271. Stichel CC, Müller HW (1998) Die Läsionsnarbe - ein unüberwindbares Hindernis für regenerierende Axone ? *Neuroforum* 236-242.
272. Stichel CC, Niermann H, D'Urso D, Lausberg F, Hermanns S, Müller HW (1999b) Basal membrane-depleted scar in lesioned CNS: characteristics and relationships with regenerating axons. *Neuroscience* 93: 321-333.
273. Stoll G, Jander S, Myers RR (2002) Degeneration and regeneration of the peripheral nervous system: from Augustus Waller's observations to neuroinflammation. *J Peripher Nerv Syst* 7: 13-27.
274. Stoll G, Müller HW (1999) Nerve injury, axonal degeneration and neural regeneration: basic insights. *Brain Pathol* 9: 313-325.
275. Sufan W, Suzuki Y, Tanihara M, Ohnishi K, Suzuki K, Endo K, Nishimura Y (2001) Sciatic nerve regeneration through alginate with tubulation or nontubulation repair in cat. *J Neurotrauma* 18: 329-338.
276. Suzuki Y, Kitaura M, Wu S (2002) Electrophysiological and horseradish peroxidase-tracing studies of nerve regeneration through alginate-filled gap in adult rat spinal cord. *Neurosci Lett* 318: 124.
277. Takami T, Oudega M, Bates ML, Wood PM, Kleitman N, Bunge MB (2002) Schwann cell but not olfactory ensheathing glia transplants improve hindlimb locomotor performance in the moderately contused adult rat thoracic spinal cord. *J Neurosci* 22: 6670-6681.
278. Talac R, Friedman JA, Moore MJ, Lu L, Jabbari E, Windebank AJ, Currier BL, Yaszemski MJ (2004) Animal models of spinal cord injury for evaluation of tissue engineering treatment strategies. *Biomaterials* 25: 1505-1510.
279. Tang Y (1995) *Microsurgery* 16: 133-137.
280. Tello F (1911) La influencia del neurotropismo en la regeneracion de los centros nerviosos. *Trab Lab Invest Biol* 9: 123-159.
281. Teng YD, Lavik EB, Qu X, Park KI, Ourednik J, Zurakowski D, Langer R, Snyder EY (2002) Functional recovery following traumatic spinal cord injury mediated by a unique polymer scaffold seeded with neural stem cells. *Proc Natl Acad Sci U S A* 99: 3024-3029.
282. Tresco PA (2000) Tissue engineering strategies for nervous system repair. *Prog Brain Res* 128: 349-363.

283. Tsai EC, Dalton PD, Shoichet MS, Tator CH (2006) Matrix inclusion within synthetic hydrogel guidance channels improves specific supraspinal and local axonal regeneration after complete spinal cord transection. *Biomaterials* 519-533.
284. Tuszynski M (1999) Neurotrophic Factors. In: *CNS Regeneration* pp 109-158. Academic Press.
285. Tuszynski MH, Weidner N, McCormack M, Miller I, Powell H, Conner J (1998) Grafts of genetically modified Schwann cells to the spinal cord: survival, axon growth, and myelination. *Cell Transplant* 7: 187-196.
286. Vellman PW, Hawkes AP, Lammertse DP (2003) Administration of corticosteroids for acute spinal cord injury: the current practice of trauma medical directors and emergency medical system physician advisors. *Spine* 28: 941-947.
287. Venstrom KA, Reichardt LF (1993) Extracellular matrix. 2: Role of extracellular matrix molecules and their receptors in the nervous system. *FASEB J* 7: 996-1003.
288. Walter I, Fleischmann M, Klein D, Muller M, Salmons B, Gunzburg WH, Renner M, Gelbman W (2000) Rapid and sensitive detection of enhanced green fluorescent protein expression in paraffin sections by confocal laser scanning microscopy. *Histochem J* 32: 99-103.
289. Wang KC, Kopprivica VUK, Kim JA, Sivasankaran R, Guo Y, Neve RL, He Z (2002) Oligodendrocyte-myelin glycoprotein is a Nogo receptor ligand that inhibits neurite outgrowth. *Nature* 417: 941-944.
290. Wang S, Wan AC, Xu X, Gao S, Mao HQ, Leong KW, Yu H (2001) A new nerve guide conduit material composed of a biodegradable poly(phosphoester). *Biomaterials* 22: 1157-1169.
291. Wekerle H, Meyermann R (1986) Cellular immune reactivity within the CNS. *TINS*.
292. Woerly S (2000) Restorative surgery of the central nervous system by means of tissue engineering using NeuroGel implants. *Neurosurg Rev* 23: 59-77.
293. [www.bio.davidson.edu](http://www.bio.davidson.edu). Recent Advances in Spinal Cord Injury Research. 2003.
294. Xu XM, Chen A, Guenard V, Kleitman N, Bunge MB (1997) Bridging Schwann cell transplants promote axonal regeneration from both the rostral and caudal stumps of transected adult rat spinal cord. *J Neurocytol* 26: 1-16.
295. Xu XM, Guenard V, Kleitman N, Aebischer P, Bunge MB (1995a) A combination of BDNF and NT-3 promotes supraspinal axonal regeneration into Schwann cell grafts in adult rat thoracic spinal cord. *Exp Neurol* 134: 261-272.
296. Xu XM, Guenard V, Kleitman N, Bunge MB (1995b) Axonal regeneration into Schwann cell-seeded guidance channels grafted into transected adult rat spinal cord. *J Comp Neurol* 351: 145-160.
297. Xu XM, Zhang SX, Li H, Aebischer P, Bunge MB (1999) Regrowth of axons into the distal spinal cord through a Schwann-cell-seeded mini-channel implanted into hemisectioned adult rat spinal cord. *Eur J Neurosci* 11: 1723-1740.
298. Yick LW, Cheung PT, So KF, Wu W (2003) Axonal regeneration of Clarke's neurons beyond the spinal cord injury scar after treatment with chondroitinase ABC. *Exp Neurol* 182: 160-168.
299. Young, Wise. Bases for Hope in Spinal Cord Injury Research. 1995. Internet Communication
300. Young, Wise. Experimental Therapies of Spinal Cord Injury. 2002.

#### Internet Communication

301. Young, Wise. Spinal Cord Injury Levels and Classification. <http://carecure.rutgers.edu/Spinewire/Articles/SpinalLevels/SpinalLevels.html> , 1-9. 2006. CareCure Community; SW. M. Keck Center for Collaborative Neuroscience, Rutgers University, Piscataway, NJ.
302. Yu X, Bellamkonda RV (2003) Tissue-engineered scaffolds are effective alternatives to autografts for bridging peripheral nerve gaps. *Tissue Eng* 9: 421-430.
303. Yurchenco PD, O'Rear JJ (1994) Basal lamina assembly. *Curr Opin Cell Biol* 6: 674-681.
304. Yurchenco PD, Schittny JC (1990) Molecular architecture of basement membranes. *FASEB* 4: 1577-1590.
305. Zhang N, Yan H, Wen X (2005) Tissue-engineering approaches for axonal guidance. *Brain Res Brain Res Rev* 49: 48-64.

# DANKSAGUNG

Tja, nun ist es endlich so weit...

Es gilt noch Dank zu sagen an...

- ... Daniela Müller und Marcia Gasis für das Anlernen einer laborunerfahrenen Medizinerin.
- ... Friedemann Pohlig und Simone Duis für die Unmöglichkeit, im Labor schlechte Laune zu haben und für die Hilfe bei der Tierpflege natürlich.
- ... Veronica Estrada für Ruhe im Sturm, die immer hilfsbereite Hand, ein kürzungsfreudiges Auge und vieles mehr.
- ... Jessica Opatz für das „Wohlfühlen in feindlichen Gefilden“.
- ... Dr. Frank Bosse für Rat und Tat bei allem, was mit Zellen zu tun hat und überhaupt.
- ... Sabine Hamm dafür, dass ich mich bei ihr ausbreiten durfte, solange ich wollte.
- ... die gastroenterologische Abteilung in der TVA für die freundliche Bereitstellung des Brutschrankes und der Mikrowelle.
- ... Dr. Nektarios Sinis für Pizza, Spaß und operative Tricks.
- ... Dr. Christian Teschner für Rat und Tat bei der Korrektur der Arbeit sowie für das ein oder andere Telefonat.
- ... Dr. Susanne Hermanns für Begeisterung, immer gute Laune, tolle Ideen, Anmerkungen und Unter-die-Arme Greifen, wenn es nötig war...
- ... Dr. Nicole Brazda (geb. Klapka) für die hervorragende und engagierte Betreuung in allen Phasen dieser Arbeit.
- ... Prof. Dr. Guido Reifenberger für die Mitbetreuung dieser Arbeit.
- ... Prof. Dr. Hans-Werner Müller dafür, dass er mich für das Thema begeistert hat und für die Möglichkeit, diese Arbeit erstellen zu dürfen.

Mein ganz besonderer Dank gilt meinen Eltern Hans und Roswitha Schulte-Eversum, die in allen Lebenslagen immer für mich da sind und mir mit Rat und Tat beistehen sowie meinem Freund Dr. Martin Wiebel, der mich durch alle Höhen und Tiefen nicht nur während der Anfertigung dieser Arbeit begleitet hat.

# CURRICULUM VITAE

## Persönliche Daten

Vor- und Zuname: Simone Caterina Schulte-Eversum  
Anschrift / Kontakt: Raental 53; 42289 Wuppertal  
Geburtsdatum/-ort: 11.04.1978 / Bonn  
Familienstand: ledig  
Staatsangehörigkeit: deutsch

## Schulbildung

1984-1988 St. Nikolaus Grundschule, Dormagen-Stürzelberg  
1988-1997 Bettina-von-Arnim Gymnasium, Dormagen  
davon 12 Monate (1994/95) Manatee Highschool, Bradenton, Florida, USA  
1997 Abitur, Abschlussnote „sehr gut“

## Hochschulstudium

10/1997 Aufnahme des Studiums der Humanmedizin an der Heinrich Heine Universität, Düsseldorf  
08/1999 Physikum, Note „gut“  
08/2000 Erstes Staatsexamen, Note „befriedigend“  
09/2001 – 08/2002 Erasmus an der Université de Nantes, Frankreich  
08/2003 Zweites Staatsexamen, Note „gut“  
04/2004 – 04/2005 Praktisches Jahr an der HHU Düsseldorf und der Université de Marseille, Frankreich  
06/2005 Drittes Staatsexamen, Note „gut“

## Anstellungen

10/2005 – 03/2007 Assistenzärztin in der Klinik für Unfall-, Hand- und Wiederherstellungschirurgie, Sana-Klinikum Remscheid, Chefarzt: Prof. Ruf  
seit 04/2007 Assistenzärztin in der Chirurgischen Klinik des Petrus-Krankenhauses Wuppertal, Chefarzt: Dr. Damanakis

## SUMMARY AND PERSPECTIVES

The implantation of guidance channels becomes more and more important in spinal cord injury research. Guidance channels are supposed to serve as scaffolds to facilitate nerve regrowth by guiding the regrowing fibres. Lesion cavities can be overcome, the rare peripheral nerve material can be spared. In CNS implantation studies, the application of guidance channels alone, however, did not present good results. As today it is widely accepted that the application of only one of the diverse regeneration promoting strategies following SCI does not lead to functionally relevant long-distance axonal regeneration along former pathways, combination approaches seem crucial.

The objective of the current study was the establishment of a combination model bridging a partial cut and aspiration lesion in rat spinal cord tissue. A novel biodegradable polymer guidance channel filled with a Matrigel® / Schwann cell mixture was implanted to bridge the newly formed gap. The AST developed in our laboratory was additionally administered at both host tissue/tube interface areas to suppress fibrous scarring and thus facilitate re-entrance of regeneration axons into the host tissue.

The implanted eGFP labelled Schwann cells survive the transplantation. Schwann cells enhance axonal regeneration, whereby fibres appear to be in close proximity to transplanted SCs. Fibres were seen to enter the guidance channels. Fibre re-entrance into the host tissue has not been proven, though. It can be stated that a “cap-like” collagen IV immunopositive scar develops around the implanted channels. Schwann cell implantation does not seem to influence the scar development. The AST as applied in this study probably is insufficient to create a Collagen IV-free time window facilitating axonal regeneration. Tracing studies have not been successful yet. The exact time range for polymer degradation can only be speculated on. At 3 months, changes in morphology are visible, at 6 months, however, there is still tube material found within spinal cord tissue.

In future studies, application of the AST has to be modified and proven to be efficient in order to be on better ground for evaluation of regenerating axons in MG/SC and AST groups. A prolonged application form of BPY-DCA to retain the chelator at the lesion site would be interesting. Only a double-staining for PAM/Coll IV would confirm regeneration facilitation by reduction of the fibrous scar. The establishment of a PAM/eGFP double-staining is inevitable to verify a suspected co-localization of regenerating fibres with implanted Schwann cells. Immunostainings for neurotransmitters or tracing studies are necessary to identify the fibres' origin and to visualize potentially host tissue re-entering fibres.

## ZUSAMMENFASSUNG

Die Implantation von Leitkanälen zur Verbesserung der Nervenregeneration in der Rückenmarksforschung gewinnt zunehmend an Wichtigkeit. Die nachwachsenden Nervenfasern sollen auf diese Weise, von Leitkanälen geführt, gerichtet aussprossen. Nervenläsionen können so überbrückt und rares peripheres Nervenmaterial eingespart werden. In den bisherigen ZNS Regenerationsstudien zeigte die alleinige Nutzung von Leitkanälen keine kongruenten Ergebnisse. Gleiches gilt für die singuläre Anwendung anderer regenerationsfördernder Therapien. Es hat den Anschein, dass eine Kombination verschiedener Strategien zur Promotion regenerativen Nervenwachstums im ZNS eine ausschlaggebende Rolle spielt.

Das Ziel dieser Arbeit war die Etablierung eines neuen Kombinationsmodells. Das verwendete Rattenmodell sah eine, sowohl schnitt- als auch aspirationsinduzierte, Form der Rückenmarksläsion mit nachfolgender Läsionsüberbrückung mittels eines Leitkanals vor. Die Leitschiene besteht aus einem neuartigen, biodegradierbaren Material und ist mit einer Mischung aus Matrigel® und Schwannzellen gefüllt. Die in der Leitschiene vorhandenen Microporen dienen sowohl zur Orientierung der regenerierenden Axone als auch zur Sicherung der Zellernährung, und hemmen zusätzlich die Migration unerwünschter Zellen aus der Umgebung in den Leitkanal. Die im Leitkanal implantierten Schwannzellen können ebenfalls als Leitstrukturen dienen. Sie orientieren sich in Längsrichtung und bilden Büngnersche Bänder. Zusätzlich sezernieren sie kontinuierlich neurotrophe Faktoren, die das Faserwachstum stimulieren. Die in unserem Labor verwendete Behandlung zur Hemmung der Narbenbildung wurde an beide Läsionsgrenzen eingebracht, um das Einsprossen der Schwannzellen in die Rückenmarkstümpfe zu ermöglichen. Die implantierten und mit eGFP markierten Schwannzellen überleben die Transplantation und fördern axonale Regeneration, wobei sich eine Nervenfaserneubildung in direkter Nachbarschaft zu den implantierten Schwannzellen zeigt. Die Fasern wachsen in die Leitschiene ein. Auswachsen jedoch konnte bisher nicht beobachtet werden. Um die implantierten Leitschienen bildet sich eine „kappenartige“ Collagen IV positive Narbe. Implantierte Schwannzellen scheinen keinen Einfluß auf die Vernarbung zu haben. Das applizierte AST erscheint insuffizient zur Schaffung eines adäquaten Zeitfensters, welches eine Nervenfaserverregeneration über die Leitschiene hinaus zuließe. Die Degradation der Polymer-Leitschiene im Rückenmark wurde über 6 Monate mikroskopisch verfolgt. Drei Monaten post Implantation sind morphologische Veränderungen sichtbar, und auch nach sechs Monaten können noch Polymerreste im Rattenrückenmark nachgewiesen werden.

Die vorliegende Studie zeigt die positiven Wachstumseigenschaften der verwendeten Nervenleitschienen sowie der implantierten Schwannzellen und unterstreicht die Notwendigkeit kombinierter Therapieansätze zur Behandlung traumatischer ZNS-Läsionen unter Berücksichtigung der Hemmung fibröser Narbenbildung.